Risk Assessment of RNP10 and RVSM in the South Atlantic Flight Identification Regions

2551 Riva Road
Annapolis, MD
21401-7465
U.S.A.

ARINC Proprietary

RISK ASSESSMENT OF RNP10 AND RVSM

IN THE

SOUTH ATLANTIC FLIGHT IDENTIFICATION REGIONS

Prepared for
SAT Group
In cooperation with
Aena, IATA, and Indra

7 May 2001

Prepared by

Geert Moek, National Aerospace Laboratory NLR
Edward Lutz, ARINC Incorporated
William Mosberg, ARINC Incorporated

Executive Summary

This report assesses the current and projected risk of collision in the EUR/SAM Corridor between FL290 and FL410 after the implementation of Required Navigation Performance (RNP) 10/50 NM in the airspace and after the implementation of Reduced Vertical Separation Minima (RVSM) on a modified route system to include an additional eastern route. The EUR/SAM Corridor lies in the South Atlantic airspace between the Canary Islands and Brazil. As shown in the figure below, the existing route network is composed of three nearly parallel north-south routes with minimum lateral separation of 100 NM carrying approximately 60 flights a day.

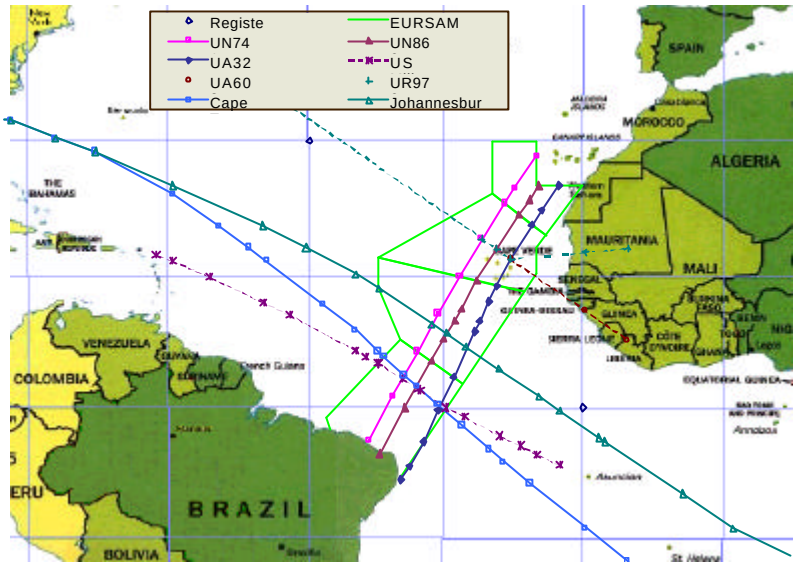

Existing route network and risk assessment area

The proposed route structure for the short term and medium term is shown in the figure below. The short-term modifications include the splitting of UA32 into two new routes, UN873 and UN857 with 50 NM spacing and includes an interim change of the partial implementation of RVSM on UN741 between flight levels FL330 and FL370. The medium term change is the proposed new route to the west, also with RNP10/50 NM spacing and full implementation of RVSM. These medium-term changes have not been addressed by this report.

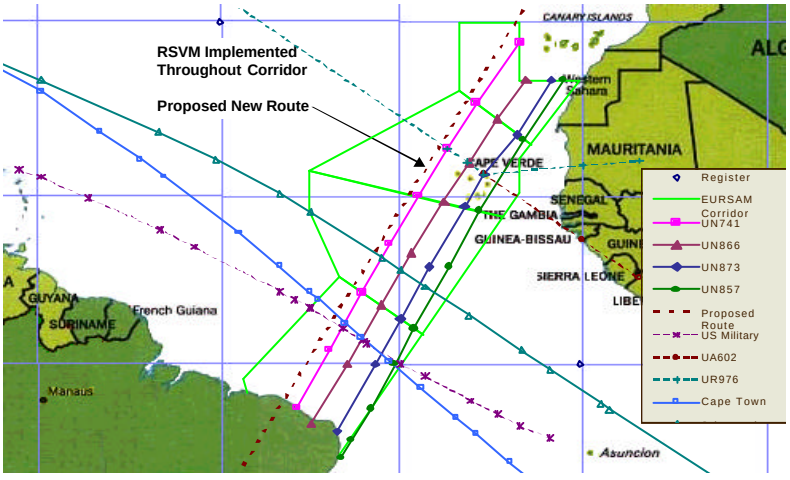

Future route network and risk assessment area

The safety assessments presented in this analysis are based on the well-known Reich collision risk models (CRM), with parameters calculated from data collected in the current system. The model outputs for the current situation were projected over a planning horizon of ten years, assuming traffic growth rates of 5.1% and 8% per year. The estimates of the lateral and vertical risk due to all causes are compared with a Target Level of Safety (TLS) of 5×10^{-9} accidents per flight hour. At the current level of traffic in the EUR/SAM Corridor , this TLS corresponds to one collision approximately every 2000 years. In addition, an estimate of the technical portion alone of the vertical risk is compared with a separate TLS for the technical vertical collision risk of 2.5×10^{-9} accidents per flight hour.INCRUSTAR

Fourteen months of data, representing over 25,000 flights, were examined to determine the types of aircraft in the airspace, the average flight characteristics of the typical aircraft, and the passing frequencies of these aircraft. The data indicated that the average aircraft within this route system was flying at 475 knots and was roughly the size of an A340. The data also showed that any given flight had a 25% chance of being within 80 NM of an aircraft flying on an adjacent track at the same altitude, a 14% chance of being within 80 NM of an aircraft flying on the same track at an adjacent altitude, and had a 0.3% chance of being within 80 NM of an aircraft crossing its track at an adjacent altitude. These values, along with probability of lateral and vertical overlap based on the predicted lateral navigation and vertical height keeping performance, are the main parameters for determining the risk of a collision.

In this analysis, a concerted effort was made to use the available data to provide the values required to exercise the collision risk models. Due to the incomplete nature of some data and the non-availability of other data, it was necessary to provide conservative estimates for some of the collision risk model parameters. Without complete data for the aircraft flight levels, the amount of crossing traffic in the region, and information on how aircraft may deviate in the lateral and vertical directions, it was not possible to develop a full understanding of how well actual operations conformed to established airspace standards. The resulting collision risk estimates are on the conservative side and could probably be improved by more complete reporting of navigation and height keeping errors, traffic data flight levels and crossing traffic data.

The estimate of the traffic growth to be used over the next ten years in the Corridor was specified as 8 percent at the SAT/9 Meeting. This has added an extra 25 percent to the risk estimates in the out years and has not been realized in the current traffic measurements. In addition to the 8% growth rate, the ICAO Global value for growth of 5.1% per year was also used to calculate the out years. This value is much more representative of the current traffic growth experienced in the airspace.

The lateral collision risk with a growth rate of 5.1% per year over the time period 2000 to 2010 is displayed below, both without RNP10/50 NM on the current tracks and with RNP10/50 NM on the proposed track system. The implementation of RNP10/50 NM has a significant impact on the computed level of safety because an aircraft is almost 4 times *more* likely to deviate 50 NM from its course than to deviate by 100 NM. The dip in the projection at year 2002 included the effect of the estimated 15% reduction in lateral occupancy from the implementation of RVSM in the Corridor. The expected benefit to the lateral risk from having more levels with fewer aircraft on each level as experienced in the NAT is shown by the estimates of lateral risk for the future. For

a 50/50 distribution of traffic from old UA32 to new routes UN873 and UN857, the lateral risk from implementation of RNP10/50NM and current traffic levels is well within the TLS of 5 x 10^{-9} accidents per flight hour except for the year 2009. For this reason, it is important to follow through with a program of data collection to validate the assumptions used in the collision risk analyses.

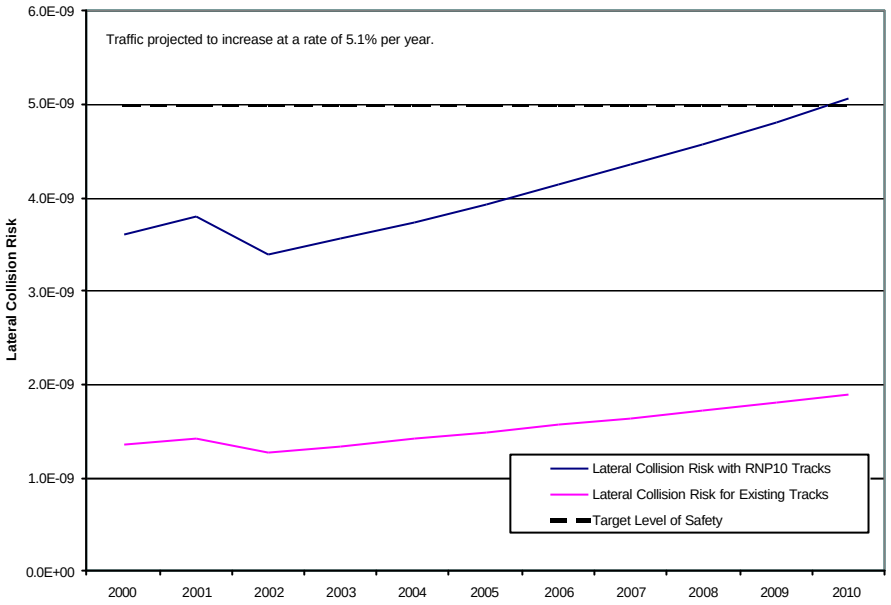

Lateral Collision Risk Through 2010

The vertical collision risk is assessed using two different models, one for the technical vertical risk and the second for the vertical risk due to all causes, which includes the technical vertical risk. An estimate of the technical portion alone is compared with a separate TLS for the technical vertical collision risk of 2.5×10^{-9} accidents per flight hour. The technical vertical collision risk is displayed below over the time period 2000 to 2010, for both the existing route structure and the modified routes with RVSM. The implementation of RVSM with 1000-foot separation has a significant impact on the computed level of safety because an aircraft is 100 times *more* likely to deviate 1000 feet in altitude than to deviate by 2000 feet. Nonetheless, the technical vertical risk projected out to 2010 under RVSM is below the TLS of 2.5 x 10^{-9} through the year 2010.

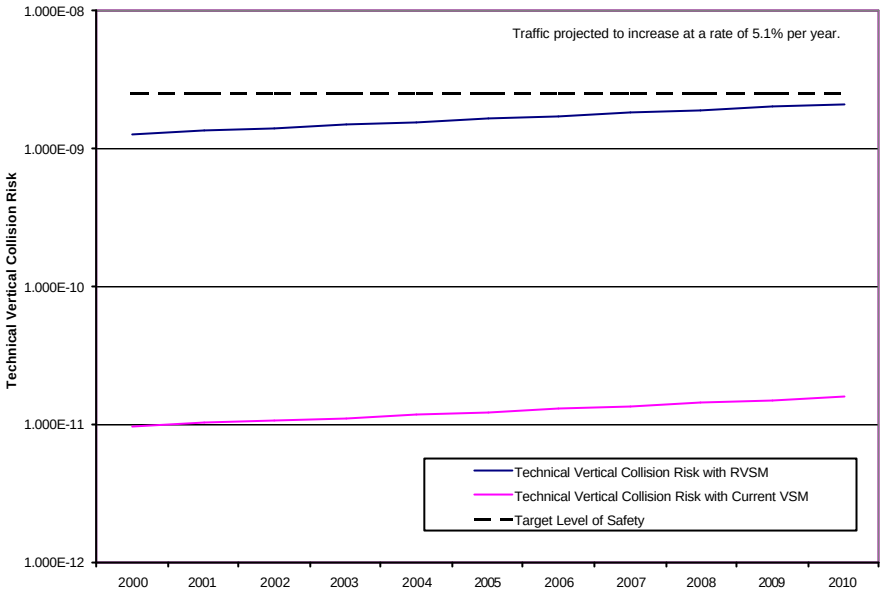

Technical Vertical Risk Through 2010

With little available data on large height-keeping deviations due to nontechnical causes, the maximum allowable values of the vertical risk factors computed for certain types of deviations are: $a^{lc} = 3.33 \times 10^{-6}$ levels crossed per flight hour and $a^{wl} = 1.00 \times 10^{-7}$ events of aircraft leveling off at a wrong level per flight hour. These values make up the other portion of the total vertical risk of 5 x 10^{-9} accidents per flight hour that is over and above the technical vertical risk and should not be exceeded in order to assure that RVSM operations remain within the TLS. Assuming 60 flights a day, with an average flight time of 3.5 hours, the above error rates can be related back to the EUR/SAM Corridor to find that the Corridor can tolerate about 31 seconds *per year* of aircraft leveling off at a wrong level, or about 4 flight levels crossed at 20 kts without clearance *per year*, without exceeding the TLS.

This risk assessment concludes with the following recommendations:

- It is recommended that additional data collections be mounted and/or appropriate monitoring procedures developed in the entire EUR/SAM Corridor FIR/UIRs in conjunction with the implementation of any of the proposed separation minima. This could include a program, similar to the NAT program, using radar data at Canaries and Recife ACCs to capture and document information on AAD and lateral deviation events in order to improve the estimation of overlap probabilities.
- It is recommended that accurate flight progress data for a minimum of (2) days per month, e.g. the 4th and 15th, be made available from all FIR/UIRs to facilitate the verification of traffic flows, distribution, and passing frequencies used in this analysis. This data collection effort should be put in place along with the implementation of the new separation standards.
- It is recommended that the crossing traffic occupancy be recomputed when sufficient data for all crossing routes becomes available (minimum two to three months of daily crossing traffic data from all FIRs).
- It is recommended that the Collision Risk Assessment be updated with the new data from the previous recommendations and reviewed prior to the implementation of RVSM.

Table of Contents

1 Introduction

The EUR/SAM Corridor refers to the airspace over the South Atlantic (SAT) between the Canary Islands and the Northeast coast of Brazil. The daily number of flights amounts to approximately 60 with most traffic being concentrated in an eight-hour period between 22.00 and 06.00 hours (Canaries local time). The current route network comprises three (nearly) parallel routes with minimum lateral separation of 100 NM. In order to improve the efficiency of the system, two short-term changes are being examined. The first one concerns the implementation of RNP10 whereas the second one concerns the implementation of RVSM between FL290 and FL410. The current implementation dates are the 6th September 2001 and 24th January 2002, respectively. The RVSM implementation date matches the implementation of RVSM in European airspace. The RNP10 implementation involves some re-alignment of the current most easterly route and the addition of a new route in the east. An additional system change foreseen for the medium term concerns the addition of a new route west of the current most westerly route. The minimum separation between all but two of the routes will then become 50 NM. On the longer term, some random routes are expected to be implemented.

As set out in the *Manual on Airspace Planning Methodology* (Ref. 1), reductions in separation minima should be supported by safety assessments demonstrating that the resulting systems are acceptably safe. In this context, *ICAO Annex 11* suggests that it be shown that the resulting system meets a Target Level of Safety (TLS) of 5×10^{-9} per dimension (Ref. 2). Based on discussions within the SAT Task Force, Aena has taken the responsibility to carry out the pertinent safety assessments as described in this report by granting a contract to ARINC Incorporated.

The safety assessments are based on suitable versions of the well-known Reich collision risk model (Refs. 3 – 5). Parameters of the model have been estimated from data collected in the current system. This involved some projection of the current situation into that over a planning horizon of ten years. The estimates of the lateral and vertical risk have been compared with a TLS of 5×10^{-9} per dimension where these TLSs apply to the pertinent risks due to all causes. In addition, and associated with the global nature of aircraft height keeping, an estimate of technical vertical risk was compared with a technical TLS of 2.5×10^{-9}.

The description of the safety assessments begins with a fairly detailed description of the airspace concerned in Section 2. Section 3 presents the lateral collision risk assessment. Following that, Sections 4 and 5 report on the assessments of the vertical collision risk due to technical causes and due to all causes respectively. Each of these three sections successively discusses the type of model, model parameter estimation and risk estimates. Overall conclusions and recommendations for implementation are presented in Section 6.

2 Airspace Description

This section describes the current and proposed route network and traffic flow characteristics, available ATS services, the aircraft population, and the data sources used in the study.

2.1 Route Network and Traffic Flows

Figure 2.1 shows the existing route network within the EUR/SAM Corridor together with the horizontal boundaries of the area to be considered for the risk assessment. This area is based on the proposed RNP10 airspace as defined in Reference 6. It involves the flight level band FL290 – FL410, both prior to and after the planned implementation of RVSM on 24th January 2002 (Ref. 7). The route network is situated within the Canaries UIR, SAL Oceanic UIR/UTA, Dakar Oceanic UIR and Recife FIR. Table 2.1 lists the Waypoint Position Reporting (WPR) points for each route and Table 2.2 provides some additional geographical details[1]. The typical flying time between WPR points is approximately 35 to 40 minutes. Note that the majority of the reporting points are at the boundaries between two adjacent FIR/UIRs. WPRs are utilised in Sections 3.4 and 4.4 to estimate the occupancy parameters of the (lateral and vertical) collision risk models.

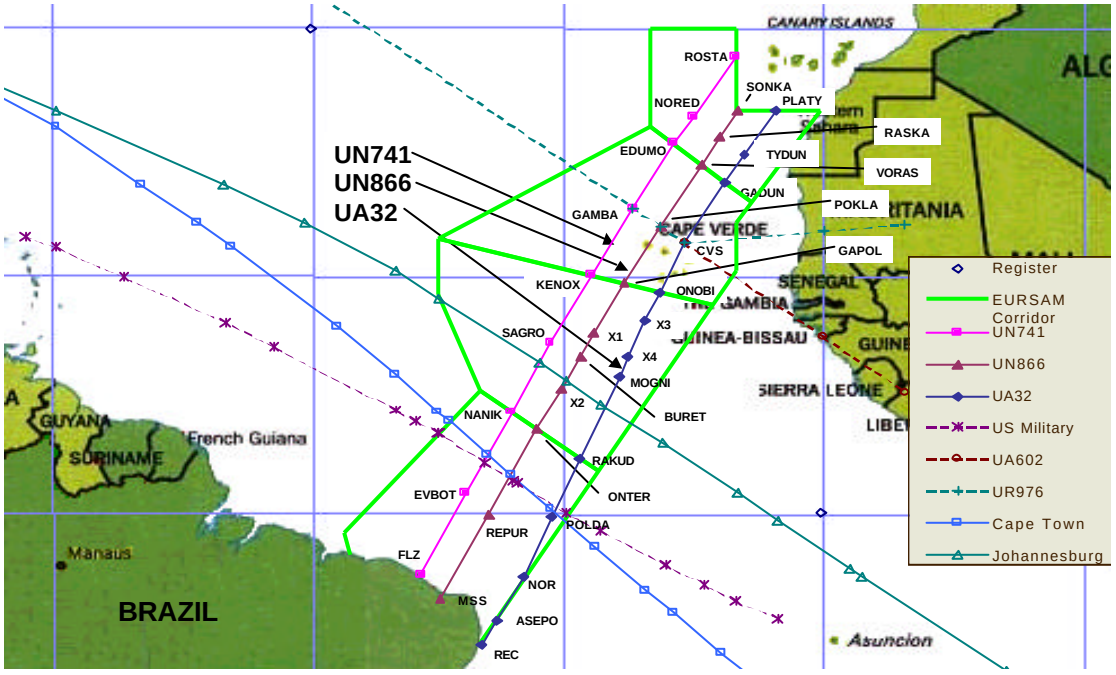

Figure 2-1. Existing Route Network and Risk Assessment Area

[1] Source: Atlas South Atlantic Crossing 57C, 20 Apr 00

Table 2-1. Waypoint Position Reporting Points on the Different Routes of the Current Route Network

FIR/UIR	Route		
	UN741	UN866	UA32
CANARIES	ROSTA NORED EDUMO	SONKA RASCA VORAS	PLATY NORGA GADUN
SAL OCEANIC	EDUMO GAMBA KENOX	VORAS POKLA GAPOL	GADUN CVS ONOBI
DAKAR OCEANIC	KENOX SAGRO NANIK	GAPOL X1 BURET X2 ONTER	ONOBI X3 X4 MOGNI RAKUD
RECIFE	NANIK EVBOT FLZ (Fortaleza)	ONTER REPUR MSS (Mossoro)	RAKUD POLDA NOR (Noronha) ASEPO REC (Recife)

Table 2-2. Additional Geographical Details of Waypoint Position Reporting Points of the Current Route Network

Route	Waypoint Position Reporting point	Latitude (°N)	Longitude (°W)	Distance to next WPR point (NM)
	ROSTA	28 15.4	020 00.0	254
	NORED	24 38.3	022 28.2	120
	EDUMO	22 55.0	023 36.0	275
	GAMBA	18 57.1	026 03.7	285
	KENOX	14 46.8	028 29.6	287
	SAGRO	10 35.0	030 51.8	288
	NANIK	06 20.5	033 10.3	343
	EVBOT	01 16.9	035 52.1	342
	FLZ (Fortaleza)	-03 46.3	038 32.9	

Route	Waypoint Position Reporting point	Latitude (°N)	Longitude (°W)	Distance to next WPR point (NM)
UN866	SONKA	25 00.0	019 48.7	114
	RASCA	23 21.7	020 53.1	120
	VORAS	21 38.0	021 59.0	268
	POKLA	17 47.5	024 25.0	244
	GAPOL	14 16.8	026 32.6	213
	X1	11 11.5	028 19.6	97
	BURET	09 45.0	029 05.0	135
	X2	07 48.2	030 14.2	176
	ONTER	05 14.1	031 39.5	356
	REPUR	00 01.0	034 30.9	355
	MSS (Mossoro)	-05 11.8	037 21.9	
UA32	PLATY	25 00.0	017 37.6	196
	NORGA	22 13.5	019 29.9	120
	GADUN	20 30.6	020 36.7	263
	CVS	16 44.2	022 57.1	201
	ONOBI	13 41.5	024 26.6	144
	X3	11 53.3	025 17.9	144
	X4	09 42.5	026 18.9	75
	MOGNI	08 33.5	026 50.7	338
	RAKUD	03 24.6	029 11.0	239
	POLDA	-00 14.0	030 49.1	238
	NOR (Noronha)	-03 51.9	032 26.9	190
	ASEPO	-06 37.1	034 02.5	105
	REC (Recife)	-08 08.2	034 55.6	

Figure 2.2 shows the proposed new route network based on the implementation of RNP10. It comprises the route UN741 as before. Route UN866 now connects APASO on the northern boundary of the Canaries FIR with Mossoro in the Recife FIR. The third parallel route consists of the new UN873 route between NATAL and CVS plus the part between CVS and LIMAL. This can be considered as a re-alignment of the existing UA32 route between Fernando de Noronha and CVS which under the RNP10 implementation will continued to be used up to FL280 as UB623. The fourth, new parallel route is the UN857 between Fernando de Noronha and BIPET. Tables 2.3 and 2.4 list again the WPR-points for each route and some additional geographical details[2].

[2] Source: Task-force of the SAT Group, new ATS route network for the South Atlantic area

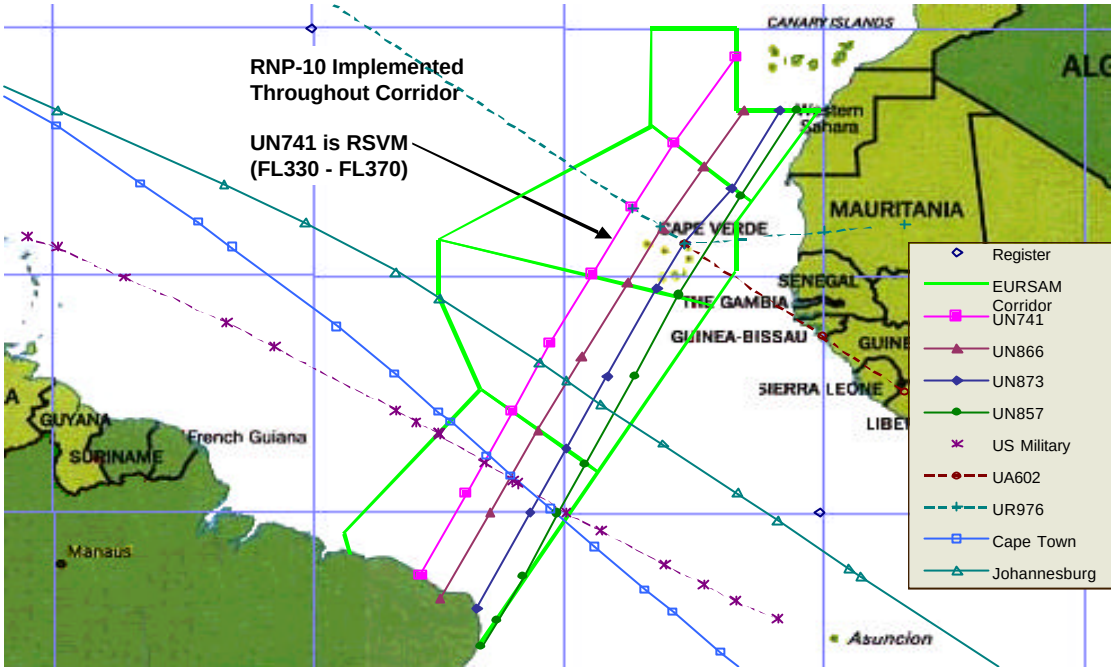

Figure 2-2. Proposed RNP10 RNAV Route Network and Risk Assessment Area

Table 2-3. Waypoint Position Reporting Points for the Proposed New RNP10 RNAV Route Network

FIR/UIR	Route			
	UN741	UN866	UN873	UN857
CANARIES	ROSTA EDUMO	APASO TENPA	LIMAL (PLATY) IPERIA (GADUN) CVS	BIPET GUNET
SAL OCEANIC	EDUMO GAMBA KENOX	TENPA BOMSA AMDOL	CVS POMAT	GUNET X-UA602 BOTNO
DAKAR OCEANIC	KENOX SAGRO NANIK	AMDOL NELTO DEKON	POMAT SAGMA TASIL	BOTNO DELAX ERETU
RECIFE	NANIK EVBOT FLZ (Fortaleza)	DEKON SETEL MSS (Mossoro)	TASIL BUNIL NATAL	ERETU IPIMA NOR (Noronha) ASEPO REC (Recife)

Table 2-4. Additional geographical details of Waypoint Position Reporting Points for the Proposed New RNP10 RNAV Route Network[3]

Route	Waypoint Position Reporting point	Latitude (°N)	Longitude (°W)
UN741	ROSTA	28 15.4	020 00.0
	EDUMO	22 55.0	023 36.0
	GAMBA	18 57.1	026 03.7
	KENOX	14 46.8	028 29.6
	SAGRO	10 35.0	030 51.8
	NANIK	06 20.5	033 10.3
	EVBOT	01 16.9	035 52.1
	FLZ (Fortaleza)	-03 46.3	038 32.9
UN866	APASO	25 00.0	019 29.8
	TENPA	21 31.4	021 50.9
	BOMSA (x)	17 43.3	024 17.1
	AMDOL	14 20.6	026 19.6
	NELTO	09 45.0	029 00.6
	DEKON	05 11.2	031 35.5
	SETEL	00 00.0	034 28.5
	MSS (Mossoro)	-05 11.8	037 21.9
UN873/ UN858	LIMAL (PLATY)	25 00.0	017 22.0
	IPERA (GADUN)	20 10.1	020 12.1
	CVS	16 44.2	022 57.1
	POMAT	13 52.6	024 35.8
	SAGMA (x)	08 33.5	027 32.6
	TASIL	04 00.3	029 59.3
	BUNIL	00 00.0	032 06.6
	NATAL	-05 54.5	035 14.8
UN857	BIPET	25 00.0	016 21.5
	GUNET	19 41.0	019 40.9
	x-UR976		
	x-UA602		
	BOTNO	13 31.3	023 19.0
	DELAX	08 33.0	025 56.1
	ERETU	03 07.5	028 48.0
	IPIMA	00 00.0	030 25.9
	NOR (Noronha)	-03 51.9	032 26.9
	ASEPO[4]	-06 37.1	034 02.5
	REC (Recife)[5]	-08 08.2	034 55.6

[3] Note that there are occasional minor differences between latitude and longitude values given in Table 2.2 and 2.4
[4] Source: Atlas South Atlantic Crossing 57C, 20 Apr 00
[5] Source: Atlas South Atlantic Crossing 57C, 20 Apr 00

Figure 2.3 shows an additional candidate route, defined by the points IRKID (N33 55.5, W018 04.2) and Barreiras (S12 04.8, W045 00.4), to be implemented in the new RNP10 airspace in the medium term after the implementation of RVSM throughout the Corridor in January of 2002.

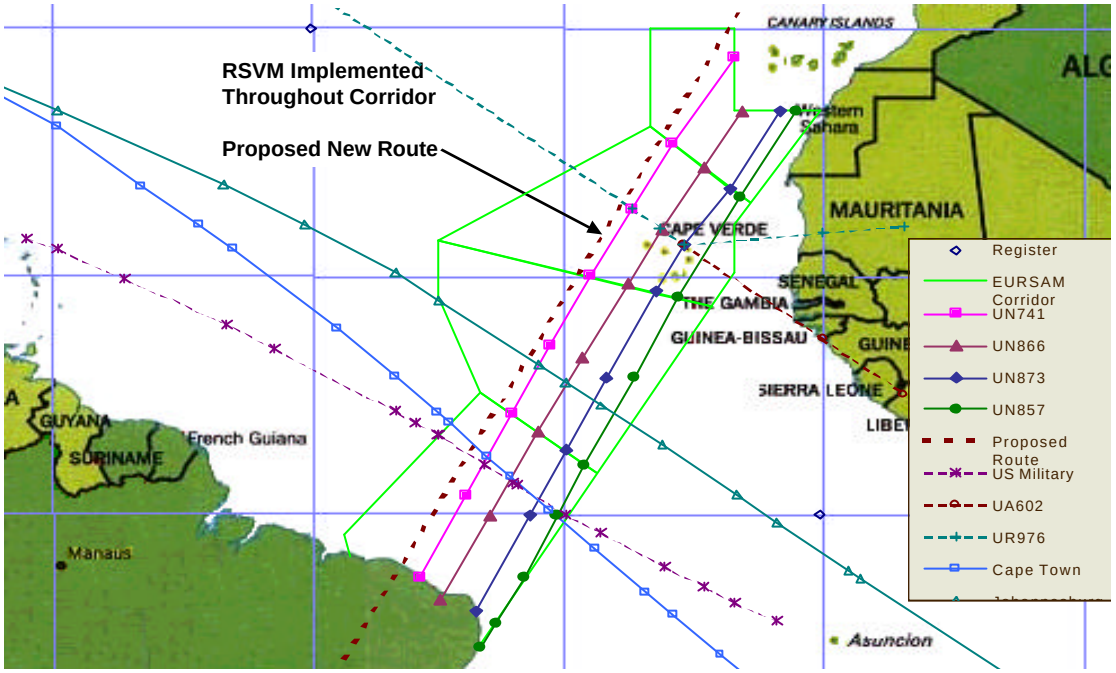

Figure 2-3. Additional Medium Term Candidate for Inclusion within the RNP10 RNAV Route Network

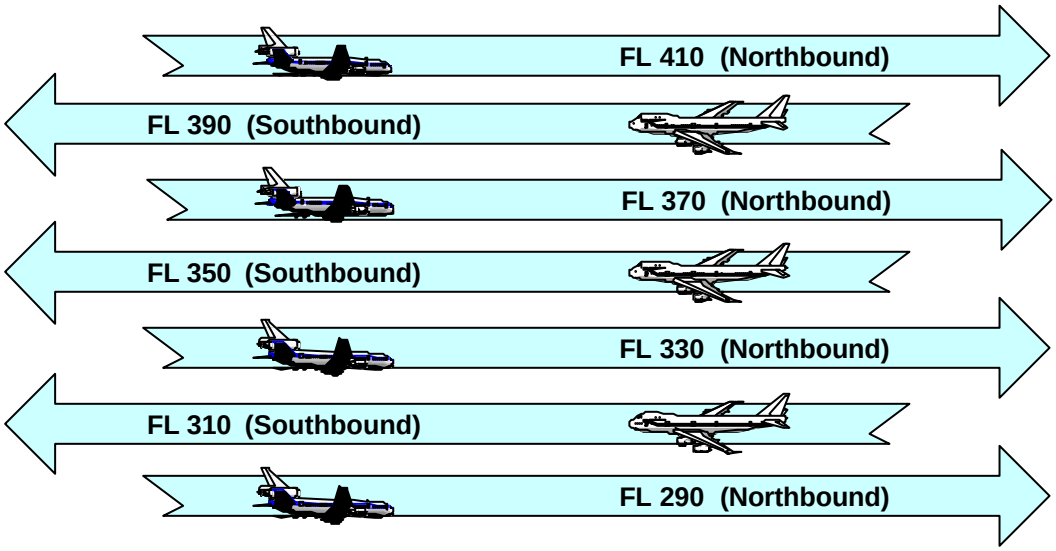

Figure 2-4. Flight Level Allocation Scheme in Use in CANARIES UIR, SAL OCEANIC UIR, DAKAR OCEANIC UIR and Recife FIR

[6] Note that there are occasional minor differences between latitude and longitude values given in Table 2.2 and 2.4

The magnetic track direction varies around 45º for northbound traffic and 225º for southbound traffic. Based on ICAO Annex 2, the flight level allocation within the four FIR/UIRs is as shown in Figure 2.4. This is opposite to what is used north of the Canaries TMA. In fact, the transition between the two schedules takes place under radar control in the Canaries TMA. This also includes route and/or level changes to accommodate flights for which the preferred route/level was not initially available. As a result, it can be assumed that the aircraft on the routes in the four FIR/UIRs making up the RNP10 airspace are in straight and level flight. This applies to both northbound and southbound traffic. Some step climbs do occur under the procedural control of the SAL ACC.

Figures 2.1 to 2.3 show that the parallel route system is crossed by a number of routes. Route UR 976 is defined by the waypoints YF, CVS, and ULTEM. Route UA602 continues east from CVS in the direction defined by ULTEM and CVS. An U.S. military route between the Caribbean and Ascension has been tentatively identified, as have proposed routes from Atlanta to Cape Town and from Atlanta to Johannesburg. Aircraft on these routes are separated vertically from aircraft on the parallel route system. There is some military traffic in the Recife FIR, crossing on random routes subject to clearance.

2.2 ATS Services and Procedures

The airspace in the RNP10 area of the South Atlantic EUR/SAM Corridor is subject to procedural control with pilot voice waypoint position reporting. While VHF voice communications are available over approximately the same areas where DME coverage is available, the primary means of communication is HF voice. In the Dakar Oceanic UIR, only HF voice communication is available. Appropriately equipped aircraft can also use SATCOM and HF Data Link (HFDL) throughout the South Atlantic EUR/SAM Corridor.

There are two DME stations inside the proposed RNP10 airspace, namely CVS, Amilcar Cabral, and NOR, Noronha. Their ranges are limited by the RF horizon to about 200 NM. Table 2.5 lists some DME stations to the north and south of the proposed RNP10 airspace. Figure 2.5 shows the approximate DME (and VHF voice) coverage.

Table 2-5. Adjacent DME Stations

DME station	
TFN	Tenerife
TFS	Tenerife Sur
HR	Hierro
GDV	Grand Canaria
LAY	Laayoune
DKH	Dakhla
PE	Nouadhibou
FLZ	Fortaleza
MSS	Mossoro
REC	Recife

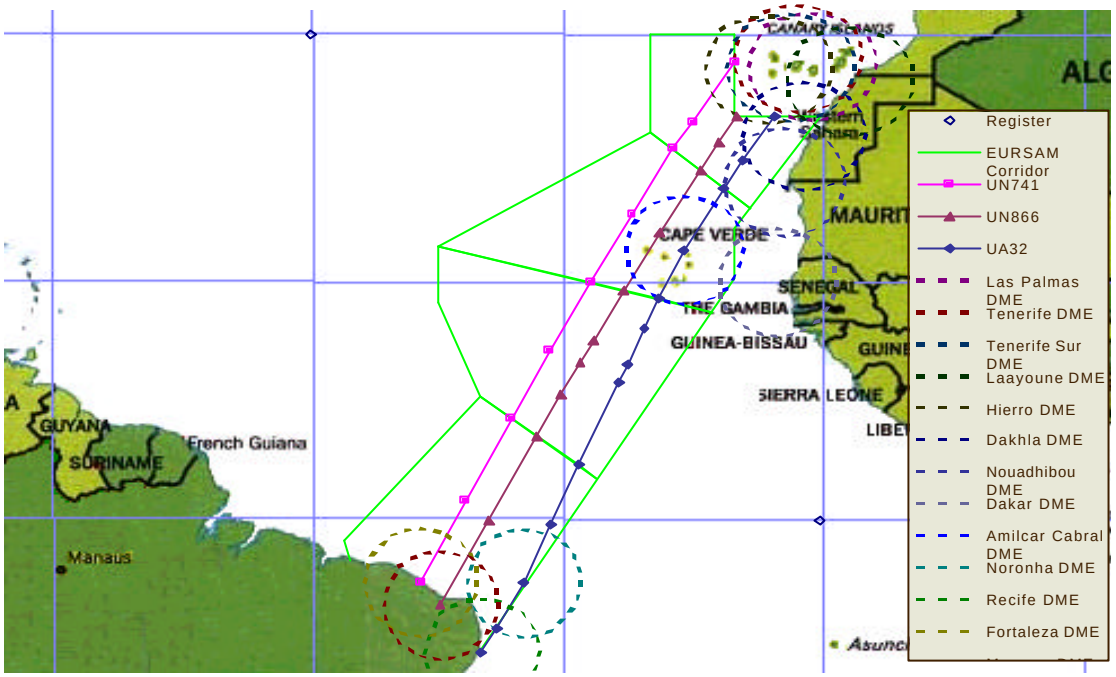

Figure 2-5. Coverage area of DME stations

For those aircraft so equipped, the DMEs provide a means of updating the INS NAV solution with a radio DME position input which may be critical to maintaining RNP10 performance.

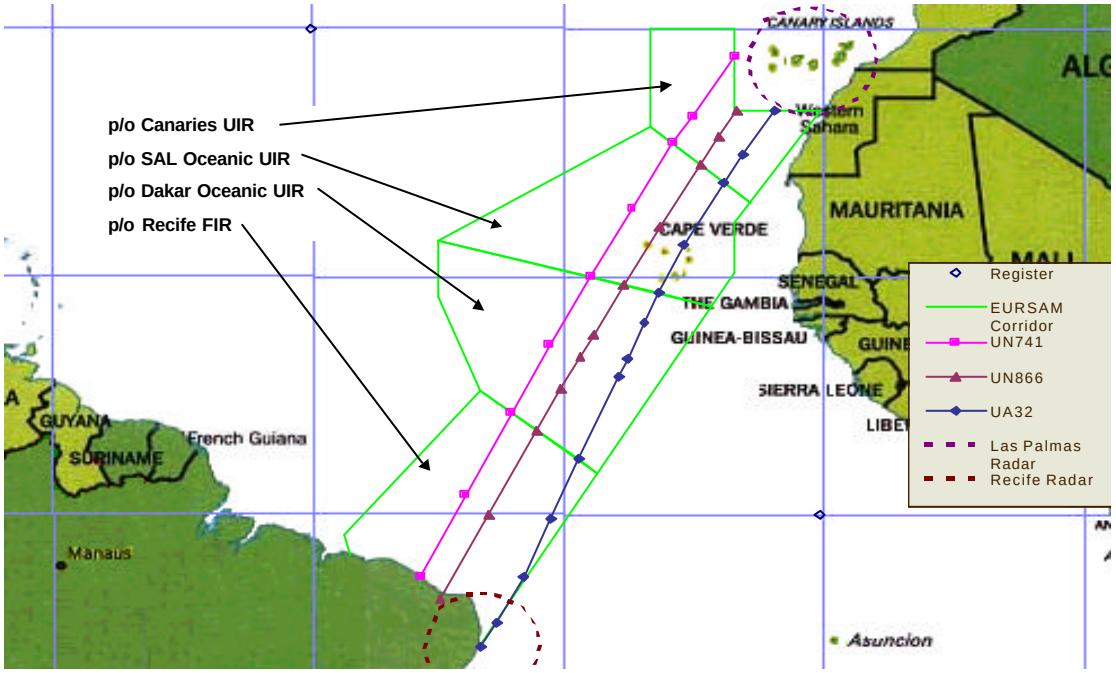

Figure 2-6. Coverage Area of Las Palmas and Recife Radar

Although radar surveillance is not available for the parallel route system in the four FIR/UIRs, it is available in the adjacent Canaries TMA and on the coast of Brazil. Radar range is also limited by the RF horizon. These radars do provide an opportunity to monitor the lateral and vertical deviations of aircraft flying in the Corridor. Figure 2.6 shows the respective radar coverage areas.

Controllers use the Mach Number Technique on a flight-by-flight basis to maintain the spacing between trailing aircraft in the same track. This does not, however, result in the MNT being applied uniformly or consistently to using a specific Mach Number on specific tracks, but rather it is dependent on the speed of the leading aircraft on the track.

ACAS II must be carried and operated from 1 January 2000 as specified in Reference 12. In the case of any significant ACAS event, pilots and controllers should complete an ACAS resolution Advisory (RA) report.

2.3 Aircraft Population

The aircraft population has been obtained from the Canaries flight information database system (see Section 2.4). Table 2.6 shows the most common aircraft types and numbers of flights per type for waypoint reports over EDUMO, VORAS, and GADUN, at altitudes between FL 290 and FL 410, from August 1999 to September 2000.

Table 2-6. Aircraft Population and Number of Flights per aircraft type

Aircraft	Count	% AC	Length [ft]	Width [ft]	Height [ft]	Cruising Speed [kts]
Average			**193.12**	**174.45**	**55.43**	**538.3**
B767-300	4483	17.64%	180.25	156.08	52.00	530
MD11	4451	17.51%	202.17	169.83	57.92	588
A340	4115	16.19%	194.83	197.83	54.75	495
B747-400	3051	12.00%	231.83	211.42	63.67	565
B747-200	1647	6.48%	231.83	195.67	63.42	555
A310	1338	5.26%	153.08	144.00	51.83	484
B777-200	1273	5.01%	209.08	199.92	60.75	555
B767-200	1164	4.58%	159.17	156.08	52.00	530
B757-200	1113	4.38%	155.25	124.83	44.50	530
A330	576	2.27%	208.83	197.83	54.92	495
B747	492	1.94%	231.83	195.67	63.42	555
DC10	471	1.85%	182.25	155.33	58.08	600
A320	223	0.88%	123.00	111.00	38.00	472
B767	155	0.61%	159.17	156.08	52.00	530
F900	97	0.38%	66.33	63.42	24.75	360
E145	59	0.23%	98.00	65.75	22.17	
CL60	58	0.23%	68.00	64.00	21.00	

Aircraft	Count	% AC	Length [ft]	Width [ft]	Height [ft]	Cruising Speed [kts]
B737-300	43	0.17%	109.58	94.75	36.50	495
B747-100	41	0.16%	231.83	195.67	63.42	555
GLF4	37	0.15%	88.33	77.83	24.42	459
B707-300	35	0.14%	152.08	145.75	42.42	521
IL76	35	0.14%	152.00	166.00	49.00	432
MD80	35	0.14%	147.67	107.67	29.50	504
A124	34	0.13%	228.50	240.50	42.17	466
FA50	33	0.13%	60.75	61.83	22.08	360
L101	32	0.13%	177.00	155.00	55.00	
B747-300	31	0.12%	231.83	195.67	63.42	565
H25B	30	0.12%	51.00	47.00	17.00	
B777	27	0.11%	209.00	199.00	60.00	555
LJ55	19	0.07%	55.00	44.00	15.00	

The data sample included 25420 flights by 85 aircraft types within the flight level band (FL290 – FL410). The population is dominated by large airframes such as the A340, MD11, B763 and the B744 as illustrated by the average dimensions shown in Figure 2.7. These four types make up about 63% of the total number of flights. Another 26% are made up by the A310, B742, B752, B762 and the B772. Note that the average number of flights is about 60 flights per day.

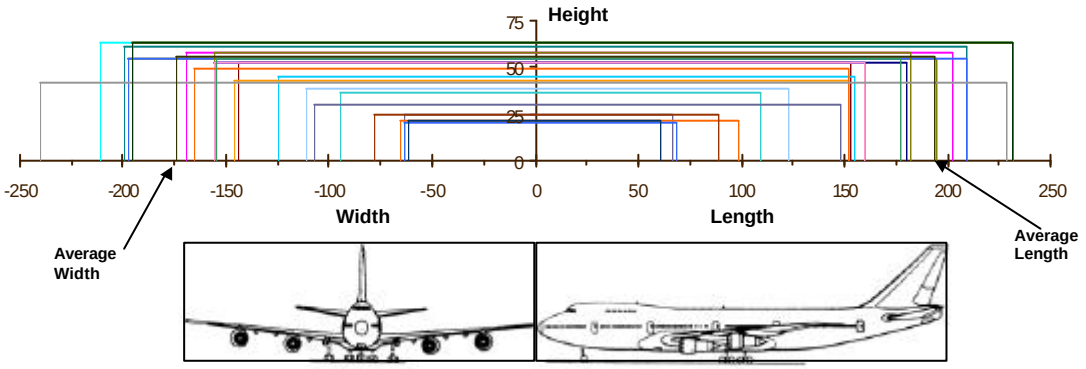

Figure 2-7. The Aircraft Dimensions Used in the Model are a Weighted Average of the Airframes Using the South Atlantic Track System

2.4 Data Sources

Several sources of data are needed for the estimation of the parameters of the lateral and vertical collision risk models.

Flight progress data from the Canaries, SAL and Recife ACCs have been made available for the project. Flight progress data from the Canaries ACC is stored in a large computer database. It consists of initial flight plan data updated by the controllers with pilot position reports. Occasionally, it can happen that due to workload constraints controllers, although obviously

updating their personal flight progress information, do not enter the information into the database system. As a consequence, the altitude information from the database is not always correct. The flight data from SAL consists of initial flight plan data, fully updated with pilot position reports. This was used as a crosscheck on the flight data from the Canaries database. Finally, the flight data from the Recife ACC consists of fully updated flight progress information as well.

The primary data source consisted of 25791 waypoint position reports from the Canaries ACC database for EDUMO, VORAS and GADUN, covering the time period 30JUL99 to 25SEP00. Only 25420 of these flights reported altitudes within the flight level band (FL290 – FL410). Secondary data sources include:

- Reports for all waypoints in the Canaries FIR, August 1999 to July 2000 (the CD could not be read completely).
- Reports for all waypoints in the SAL FIR, 2 days June and 2 days July 2000, 283 flights.
- Reports for all waypoints in the Recife FIR, 2 days each, February to August 2000, 776 flights. Reports for crossing traffic entering and departing the Recife FIR during August and September 2000, 93 flights.

The flight progress data included flight ID, registration, aircraft type, route and altitude information, date and time of waypoint crossing and aircraft navigation equipment. All complete flight records in the primary data set were used to estimate lateral and vertical occupancies in the current system and to identify the aircraft population. The latter has been used to estimate average aircraft dimensions and has also contributed to the determination of probability distributions of lateral and vertical navigation deviations.

An incident reporting system has been in operation at Aena for several years. The database includes data on airproxies, procedural problems and aircraft navigation system failures. There is likely to be an issue of some underreporting as events tend to be reported only when they really posed a problem to the controller or pilot or to the system's safety. Nonetheless, the incident database was queried to obtain data on large lateral and vertical deviations.

Radar data are available at the Canaries ACC. Radar data are stored for at least six months. Radar data can, in principle, be used to determine a distribution of deviations from track. However, in practice, there are a couple of problems. These concern the fact that the actual area of interest (proposed RNP10 airspace) is not covered by radar; the tracks recorded by radar may already have been influenced by aircraft position updates using ground beacons; and the large amount of data to be processed. It was agreed that the possibility of developing suitable filters would be investigated. It was also agreed that a procedure would be developed that would require controllers to record any lateral deviations seen on their screens larger than 5 NM in magnitude. The procedure would become applicable on 1st August 2000. The value of 5 NM was chosen to avoid an unnecessarily large amount of records to be made. In this context, it should be noted that the airspace covered by the Canaries radar is RNP5 airspace, meaning that the aircraft population should be within 5 NM of the assigned track at least 95% of time. Although this data is not directly applicable to the proposed RNP10 airspace, it might have been possible to scale it up so that it could have been used to provide deviation probabilities.

Height monitoring data from the North Atlantic and/or European RVSM height-monitoring programs were used for the benefit of the vertical risk assessment.

Because the primary data source was sufficiently large and complete, with the exception of flight levels, it lent itself both to internal consistency checking and to a detailed analysis of the traffic. By sorting this data by time, flight ID, departure point, etc., investigators were able to identify and correct obvious typographical errors and duplicate reports. Inconsistencies in the traffic analysis also identified typographical errors or missing information.

In order to use the primary data set, the direction (NB/SB) of each flight was derived from the departure/destination information *within that data set*. Applying this algorithm to 14865 paired waypoint reports from the secondary Canaries data set and independently determining direction by comparing the times of the paired reports found this approach correct 98.86% of the time. Where pairs were found, this approach proved *wrong* only 0.08% of the time. However, 1.06% of the reports could not be paired, indicating data errors or "East-West" or local traffic.

With a reliable estimate of direction, the investigators examined the reported altitude and determined that approximately 30% were showing the wrong altitude for the direction of the flight. The waypoint reports in the primary data set have the altitude distribution shown in Figure 2.8.

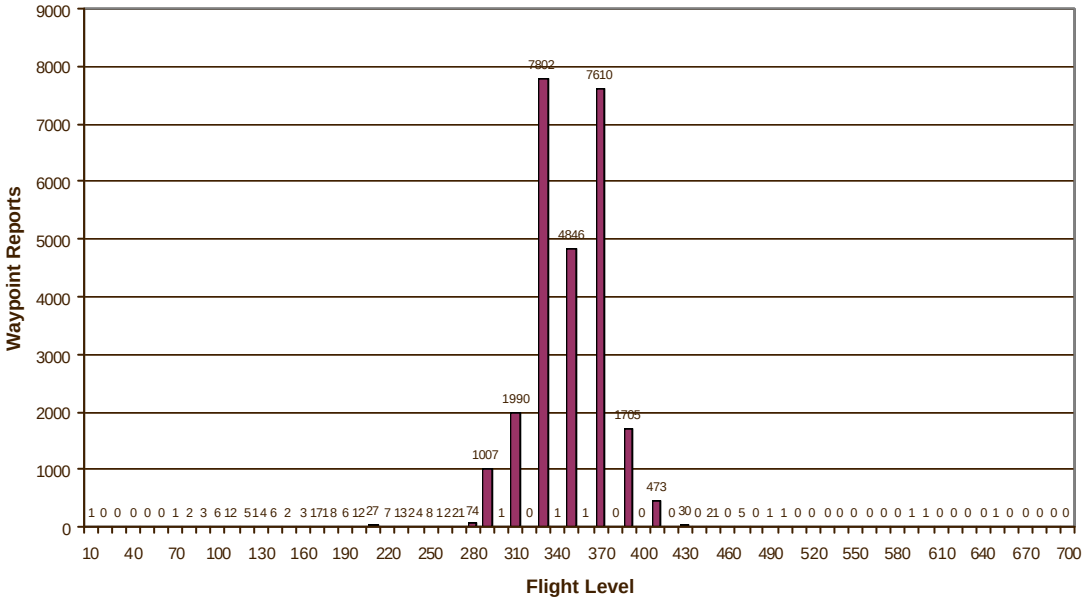

Figure 2-8. Reported Flight Levels at EDUMO, VORAS, and GADUN

This investigation is only concerned with aircraft in the flight level band indicated in Figure 2.4; so aircraft reporting altitudes less than FL 290 and greater than FL 410 were discarded from the data set before further analyses were performed.

The altitude data in the primary data set is known to include uncorrected flight plan inputs. This is confirmed by the "uncorrected" portion of Figure 2.9, which shows that about 1/3 of the

reported altitudes do not match the vertical route structure described in Figure 2.4. Using the uncorrected altitude data to compute vertical occupancy indicated there would be about 500 opposing pairs per year, (which obviously do not occur). The altitude data in the primary data set was "corrected" by assuming:

- All aircraft conformed to the vertical route structure.
- No aircraft entered or left the vertical route structure.
- The reported altitudes were "close" to the actual altitudes.
- Unless the flight was arriving or departing an airport with an ICAO identifier starting with "G", the reported altitudes were "less" than the actual altitudes.

Altitudes corrected using this approach were compared to altitudes for matching flights in the SAL data set and found to match about 84% of the time. While this result is not significantly better than what one would expect from randomly reassigning aircraft to flight levels, it is (a) repeatable and (b) significantly better than the 65% correlation before applying the corrections. The resulting distribution, shown in the "corrected" portion of Figure 2.9, conforms to the vertical route structure and was used to compute occupancy. This approach to correcting the flight levels masks any aircraft that may not have been conforming to the vertical route structure.

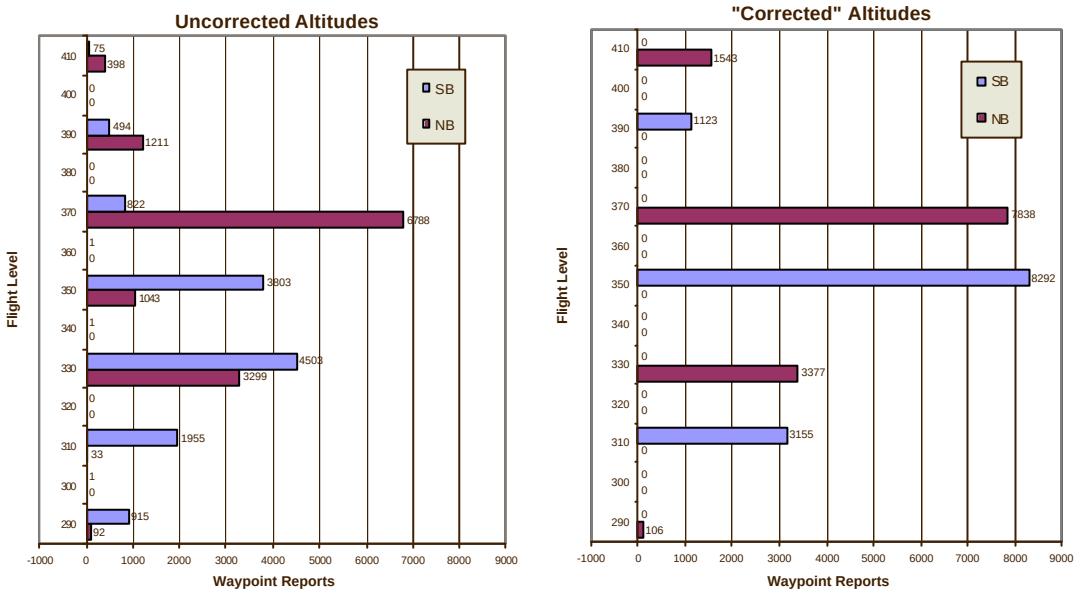

Figure 2-9. Reported versus Corrected Flight Levels at EDUMO, VORAS, and GADUN

The primary data set also supported analysis of the temporal distribution of the number of flights. Figure 2.10 shows the combined number of northbound and southbound flights per day from the primary data set in the vertical route structure. Since the daily flight count shows a strong 7-day periodicity, the figure includes a 28-day rolling average of the number of flights per day. The overall average traffic is 60.2 flights per day with a standard deviation of 6.55 flights per day. It is noted from the analysis of this data sample that the increase in traffic over the 14-month period is barely perceptible.

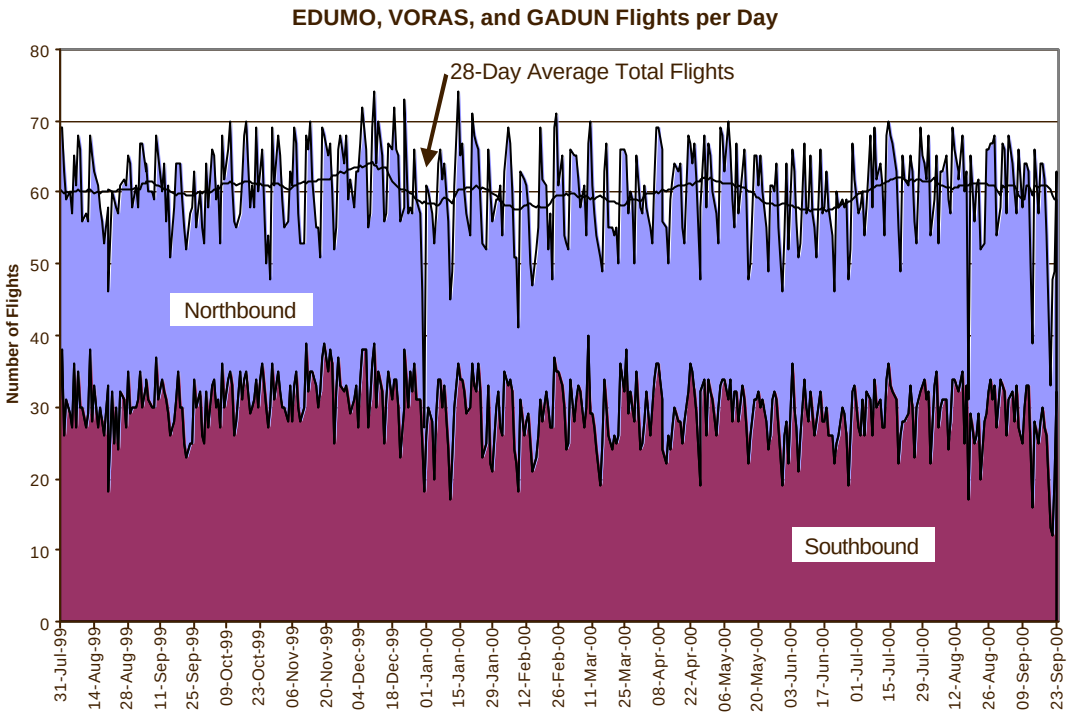

Figure 2-10. Number of Flights per Day

In light of the obvious 7-day periodicity, Figure 2.11 shows the distribution of the same traffic over the days of the week. As expected, the minimum occurs in the middle of the week.

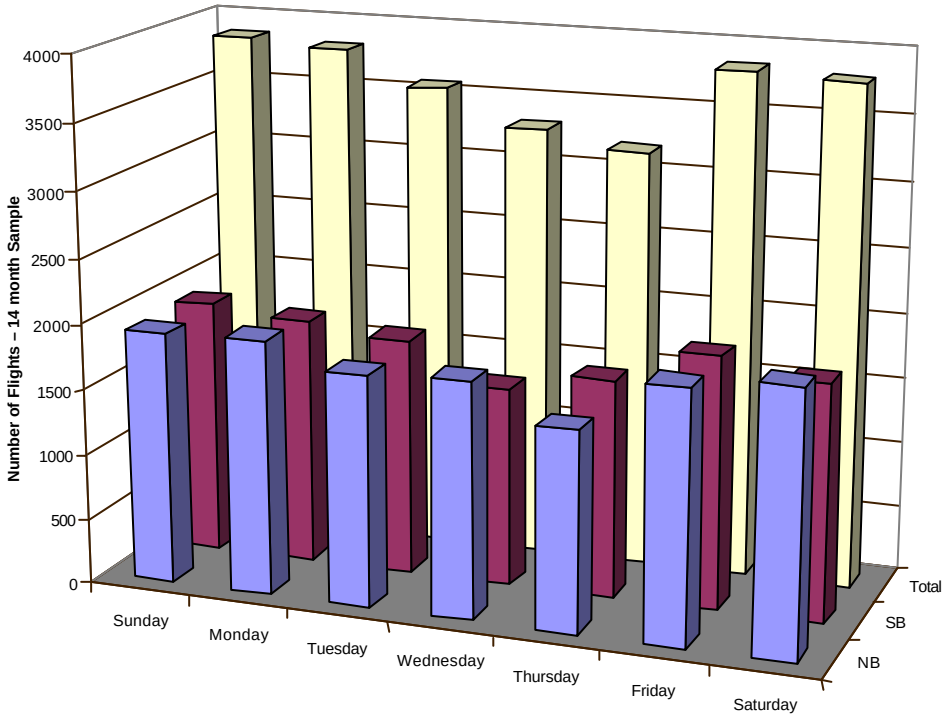

Figure 2-11. Number of Flights per Day of the Week

Figure 2.12 shows the distribution of the same set of flight reports within a 24-hour day. It is immediately apparent that, while there are peaks and quiescent periods within the day, the traffic is not as concentrated as in the North Atlantic.

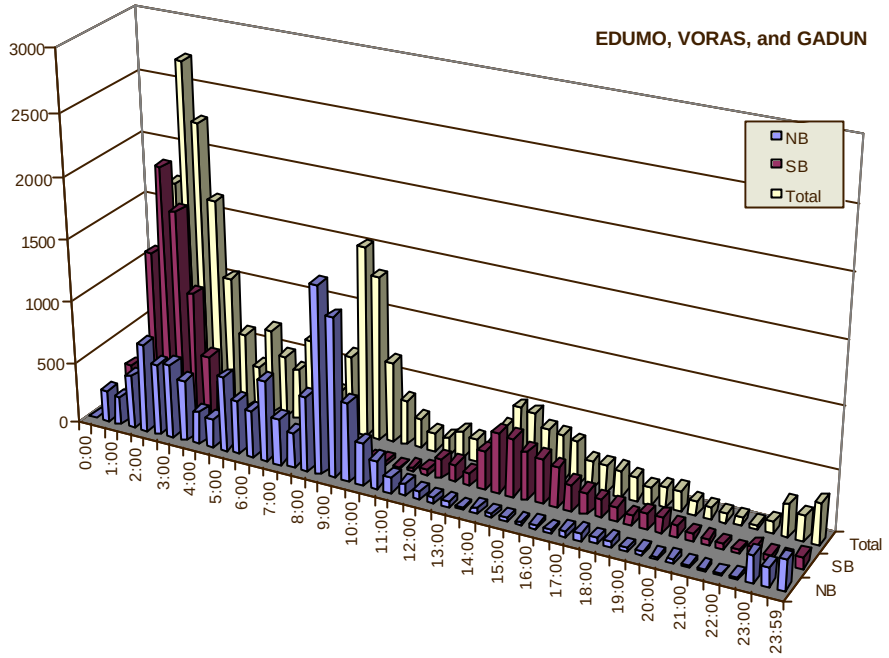

Figure 2-12. Number of Flights per half -hour crossing EDUMO, VORAS, and GADUN

It is less obvious that the traffic at any point in the route system can be extrapolated from the distributions measured at any one plane. This is accomplished by moving the north and southbound distributions measured at one plane along the (circular) time axis in opposite directions and multiplying this time shift by the average aircraft speed. Start with the distributions for EDUMO, VORAS, and GADUN shown in Figure 2.12. Shift the northbound distribution *back* in time by 3.5 hours and the southbound distribution *forward* in time by 3.5 hours. The resulting plot, shown in Figure 2.13, aligns the peaks of the north and southbound distributions. The 3.5-hour time shift is equivalent to moving the measurement plane about 1660 nautical miles south. This indicates that the highest traffic concentration in the route system occurs in the southernmost segment of the route system (1660 nautical miles south of EDUMO, VORAS, and GADUN and under Recife control) between 0500 and 0700.

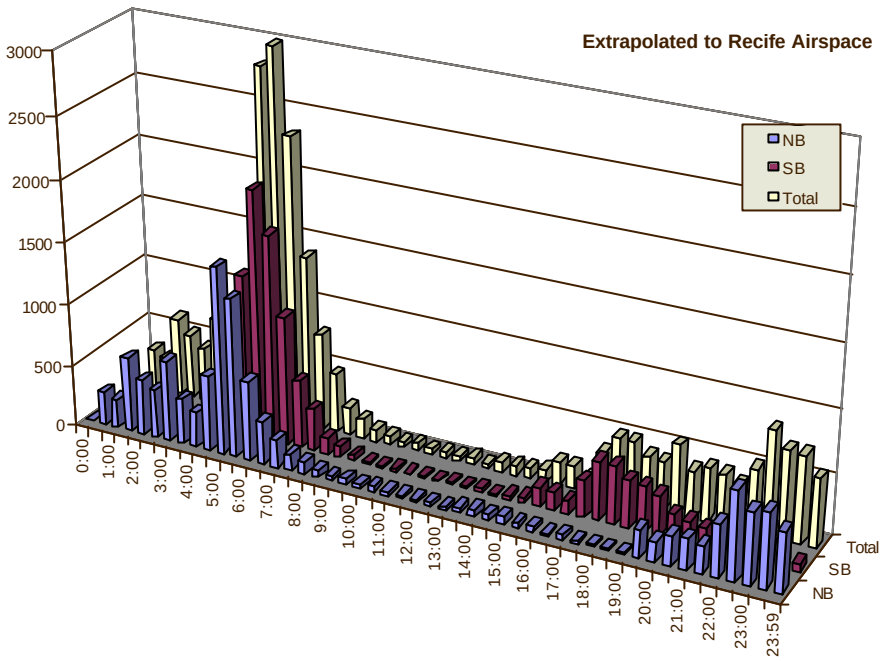

Figure 2-13. Extrapolated Number of Flights per Half Hour in Recife Airspace

3 Lateral Collision Risk Assessment

3.1 Introduction

Guidance material on a spacing of 50 NM between parallel tracks or RNAV route center lines in a procedural RNP10 environment is given in Section 3 of Attachment B to Annex 11 (Ref. 2). The basis underlying this spacing is a safety assessment with a lateral collision risk model applied to the North Pacific (NOPAC) parallel route system. It has been recognized (Ref. 9) that this safety assessment is not readily available and it has been proposed, therefore, to include it as an Appendix to *the Manual on Airspace Planning Methodology* (Ref. 1). Although this has not yet been achieved to date, and although Reference 9 suggests that the safety assessment is documented in Section 10 of Reference 10, it is actually given in an Appendix to the PAC SUPP Amendment Proposal in 1998 (Ref. 11). The type of model used is that described in Reference 12; model parameter values are typical for the NOPAC. Note that the spacing between adjacent NOPAC routes was reduced from 100 NM to 50 NM on 23rd April 1998, cf. chapter 6.0 of *Middle East/Asia (Mid/Asia) Regional Supplementary Procedures* of Reference 8.

Thus, the appropriate type of model for the assessment of the lateral collision risk for the parallel route system in the proposed RNP10 airspace of the SAT is examined in Section 3.2. Next, a description of how the various parameters of the collision risk model can be estimated is presented in Sections 3.3 – 3.8. Finally, Section 3.9 presents estimates of lateral collision risk for the current levels of traffic as well as traffic levels projected forward to the year 2010. The risk estimates are then compared with a TLS of 5×10^{-9} for the lateral risk due to all causes. No formal distinction is made between technical and operational lateral risk.

3.2 Lateral Collision Risk Model

The lateral collision risk to be modelled is that due to the loss of lateral separation between aircraft on adjacent parallel tracks, flying at the same altitude (flight level).

Modeling this type of collision risk started with the development of the Reich model for the North Atlantic (NAT) region (Refs. 3 – 5). This has since been used as the basis for a number of applications in the NAT, Europe, Canaries and the NOPAC (Refs. 13 – 18, 10). A suitable variant has also been developed for the collision risk due to the loss of vertical separation, see Section 4.

The lateral collision risk model used for the NOPAC reads as follows (Refs. 10 - 12):

$$N_{ay} = 10^7 P_y(S_y) P_z(0) \frac{l_x}{\tilde{S}_x} \left[E_y(same) \left\{ \frac{\overline{|\Delta V|}}{2l_x} + \frac{\overline{|\dot{y}|}}{2l_y} + \frac{\overline{|\dot{z}|}}{2l_z} \right\} + E_y(opp) \left\{ \frac{2\overline{|V|}}{2l_x} + \frac{\overline{|\dot{y}|}}{2l_y} + \frac{\overline{|\dot{z}|}}{2l_z} \right\} \right] \tag{3.1}$$

In equation (3.1), the symbol N_{ay} represents the expected number of aircraft accidents per 10^7 flight hours. Today, it is more common to drop the factor 10^7 in the right-hand side of equation

(3.1) and to let N_{ay} represent the expected number of aircraft accidents per flight hour. The two parts within the square brackets in the right-hand side of equation (3.1) refer to same and opposite direction traffic at the same flight level of adjacent parallel tracks respectively. $E_y(same)$ and $E_y(opp)$ are referred to as same and opposite direction lateral occupancy. It should be noted that one collision between two aircraft is counted as two aircraft accidents. The pertinent factor of two is included in the occupancy parameters.

The parameters used in the right-hand side of equation (3.1) are defined in Reference 12 as follows:

Table 3-1. Definition of Parameters of the Lateral Collision Risk Model of Equation (3.1)

Parameter	Description
S_y	The lateral separation standard
$P_y(S_y)$	The probability of lateral overlap of aircraft nominally flying on laterally adjacent paths
$P_z(0)$	The probability of vertical overlap of aircraft nominally flying at the same flight level
l_x	The average length of an aircraft
l_y	The average width of an aircraft
l_z	The average height of an aircraft
$\tilde{S}_x$	A parameter used in the calculation of E_y values
$E_y(same)$	The average number of same direction aircraft flying on laterally adjacent tracks at the same flight level within segments of length $2\tilde{S}_x$ centered on the typical aircraft
$E_y(opp)$	The average number of opposite direction aircraft flying on laterally adjacent tracks at the same flight level within segments of length $2\tilde{S}_x$ centered on the typical aircraft
$\overline{\lvert\Delta V\rvert}$	The average relative along-track speed of two aircraft flying at the same flight level in the same direction
$\overline{\lvert V\rvert}$	The average ground speed of an aircraft
$\overline{\lvert\dot{y}\rvert}$	The average relative cross-track speed between aircraft which have lost S_y NM of separation
$\overline{\lvert\dot{z}\rvert}$	The average relative vertical speed of aircraft flying at the same flight level

Obviously, a collision can only occur when there is overlap between two aircraft in all three dimensions simultaneously. The probabilities of overlap in the lateral and vertical dimensions are denoted by $P_y(S_y)$ and $P_z(0)$ respectively, where the argument S_y of $P_y(S_y)$ indicates that the nominal separation between aircraft on adjacent parallel tracks is S_y and the argument "0" of $P_z(0)$ indicates that the nominal vertical separation between the aircraft is zero, i.e. they are

flying at the same altitude. The combinations $\frac{l_x}{\tilde{S}_x} E_y(same)$ and $\frac{l_x}{\tilde{S}_x} E_y(opp)$ relate to the probability of longitudinal overlap of aircraft on adjacent parallel tracks and at the same altitude (cf. Section 3.4). All the probabilities can be interpreted as proportions of flight time in the airspace during which overlap in the pertinent dimension occurs. As the Target Level of Safety (TLS) is expressed as the expected number of accidents in the airspace per flight hour, the joint overlap probability needs to be converted into the number of events involving joint overlap in the three dimensions. This is achieved by means of the expressions within accolades. Each of the terms within the accolades represents the reciprocal of the average duration of an overlap in one of the dimensions, e.g. $\frac{\overline{|\Delta V|}}{2l_x}$ is the reciprocal of the average duration of an overlap in the longitudinal direction for same direction traffic. Note that the average duration of a longitudinal overlap is different between same and opposite direction traffic. The three terms then represent the three different ways in which a collision can originate, i.e. head/tail (or head/head for opposite direction traffic), sideways or from above/below.

The model above is based on the following explicit assumptions, see Appendix B of Reference 12 for more details:

1. All tracks are parallel with a constant spacing S_y;
2. All collisions occur between aircraft normally[1] on adjacent tracks;
3. The entry times into the track system are uncorrelated;
4. The lateral deviations of aircraft on adjacent tracks are uncorrelated;
5. The lateral speed of an aircraft is not correlated with its lateral deviation;
6. There is no corrective action by pilots or ATC when aircraft are about to collide; and
7. In the collision risk model, the aircraft are replaced by rectangular boxes.

Two factors are particularly important with regard to the type of model, namely whether, or not, the airspace is procedural and the nature of the events making up the lateral collision risk. The former is represented by assumption 6 above. In general, this assumption considerably simplifies the modeling process, as reliably modeling intervention is difficult. As set out in Section 2.2, the proposed RNP10 airspace is subject to procedural control and the model of equation (3.1) is therefore valid. The validity of the assumptions 2 to 5 inclusive are further examined in the sections on model parameter estimation.

With regard to the nature of the events making up the lateral collision risk, it is important to note that the model of equation (3.1) effectively assumes that this nature is completely random (i.e., without any systematic effects) throughout the airspace. This is sometimes referred to as the "snapshot" principle (Refs. 13 and 14). Its practical meaning is that any location within the system can be used to collect a representative data sample on the performance of the system such as occupancy and lateral deviations. The validity of this assumption is discussed in Section 3.3 ff. on model parameter estimation.

[1] May also occur on non-adjacent tracks if the probability of overlap is significantly large

If it would not be possible to confirm the validity of the snapshot principle, it would be necessary to extend the model of equation (3.1) by developing models for individual types of events and subsequently combining these into an overall model. Some examples of this approach are the NAT weighted errors model of Reference 14 and the lateral risk models presented in Reference 18 and Appendix 8 to Reference 1.

In summary, the type of model given by equation (3.1) was used for the assessment of the lateral collision risk for the parallel routes within the proposed RNP10 airspace, but with three modifications. Firstly, there is no opposite direction traffic at the same flight level of adjacent tracks due to the flight level orientation scheme in use (cf. Figure 2.4). Secondly, as sketched in Figure 3.1, the track spacing between the routes UN741 and UN866 is maintained at 100NM, i.e. twice the minimum lateral separation minimum of $S_y = 50\,\text{NM}$. Thirdly, the possible interaction between aircraft on the non-adjacent tracks UN866 and UN857, also separated by 100 NM, was incorporated. Thus, the lateral collision risk model used for the EUR/SAM traffic flow in the SAT becomes:

$$N_{ay} = \left\{P_y(S_y)E_y(same) + P_y(2S_y)E_y^{*}(same) + P_y(2S_y)E_y^{**}(same)\right\}\times P_z(0)\frac{l_x}{\tilde{S}_x}\left\{\frac{\overline{|\Delta V|}}{2l_x} + \frac{\overline{|\dot{y}|}}{2l_y} + \frac{\overline{|\dot{z}|}}{2l_z}\right\}. \tag{3.2}$$

This CRM has three same direction occupancy parameters, namely $E_y(same)$ for the three right-most tracks separated by S_y, $E_y^{*}(same)$ for the two left-most tracks separated by $2\times S_y$, and $E_y^{**}(same)$ for the tracks UN866 and UN857 also separated by $2\times S_y$. Similarly, the model has two probabilities of lateral overlap, $P_y(S_y)$ and $P_y(2S_y)$. When the latter is sufficiently small in relation to $P_y(S_y)$, the effect on lateral collision risk of aircraft on all tracks separated by twice the separation standard S_y is negligible.

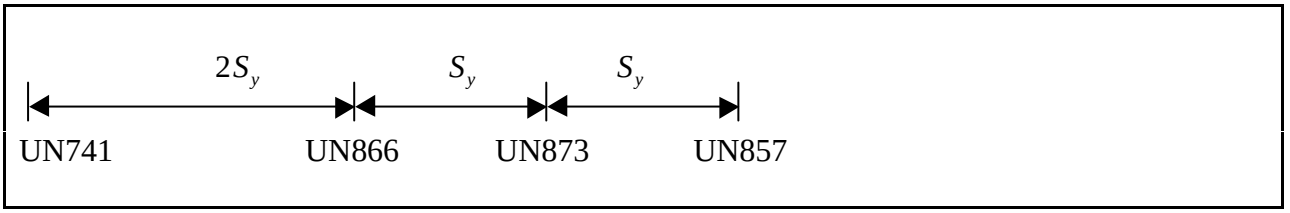

Figure 3-1. Proposed Track System

3.3 The Probability of Lateral Overlap

The probability of lateral overlap of aircraft nominally flying at adjacent flight paths separated by S_y is denoted by $P_y(S_y)$. It is defined by

$$P_y(S_y) = \int_{-l_y}^{l_y} f^{y_{12}}(y)dy \tag{3.3}$$

where $f^{y_{12}}(y)$ denotes the probability density of the lateral distance y_{12} between two aircraft with lateral navigation deviations y_1 and y_2, nominally separated by S_y, i.e.

$$y_{12} = S_y + y_1 - y_2 \tag{3.4}$$

and

$$f^{y_{12}}(y) = \int_{-\infty}^{\infty} f^Y(y_1) f^Y(S_y + y_1 - y) dy_1 . \tag{3.5}$$

Note that equation (3.5) assumes that the lateral deviations of the two aircraft are independent and have the same probability density, $f^Y(y_1)$, say. As defined in Table 3.1, l_y denotes the average aircraft width. Substitution of equation (3.5) into equation (3.3) gives

$$P_y(S_y) = \int_{-l_y}^{l_y} \int_{-\infty}^{\infty} f^Y(y_1) f^Y(S_y + y_1 - y) dy_1 dy . \tag{3.6}$$

In practice, $P_y(S_y)$ may be able to be approximated by

$$P_y(S_y) \approx 2 l_y \int_{-\infty}^{\infty} f^Y(y_1) f^Y(S_y + y_1) dy_1 \tag{3.7}$$

or

$$P_y(S_y) \approx 2 l_y f^{y_{12}}(0) . \tag{3.8}$$

It follows from the equations above that the probability density $f^Y(y_1)$ of the lateral navigation deviations of aircraft can be used to calculate the probability of lateral overlap $P_y(S_y)$. This probability density or distribution depends first of all on the navigation capability of the aircraft as specified by the RNP type of the airspace. But this does not completely determine the density $f^Y(y_1)$ as, in particular, there may exist some rare, non-nominal navigation errors which are not covered by the RNP type and whose potential occurrence may have a significant effect on the collision risk in the airspace. Hence, the nature of the lateral navigation errors and its impact on the modeling of their probability distribution needs to be addressed.

There are two basic approaches to the modeling of the probability distribution of the lateral navigation errors that might be called on an “overall basis” and on an “individual basis”.

Modeling of the lateral navigation errors on an overall basis means that it is assumed that all lateral errors or deviations follow the same probability distribution. This distribution may then be

determined on the basis of a sample of data describing lateral deviations of aircraft from their tracks. A fairly large data sample is needed to be able to model the lateral deviation data confidently. In particular, it is important to avoid underestimating the tail of the distribution, i.e. the probability of "large" or "gross" errors, as the lateral risk estimate is sensitive to that part of the distribution. In practice, a mixture of two individual distributions is often used, where one distribution describes the core performance and the other the tail or "gross" deviation performance. To make the mixture distribution conservative, the tail distribution is often taken as a double exponential distribution. (The double exponential distribution is known for its relatively thick tail.) As stated in Reference 11, a double double exponential distribution was used for the NOPAC lateral collision risk analysis.

The approach to the modeling of the lateral navigation performance on an individual basis means that for each individual type of navigation error, an appropriate probability distribution of the lateral deviations associated with the error is determined first. Subsequently, an overall distribution of lateral deviations from track is established by taking a weighted mixture of the individual deviation distributions. The weighting factors are determined by the frequencies with which the different types of errors occur. Following this approach, it may be possible to approximate or bound the resulting mixture distribution by some simpler distribution without adversely affecting the credibility of the estimate of the probability of lateral overlap. This approach has been used for the lateral collision risk assessment in the NAT (Refs. 14 and 19).

The two approaches are not completely independent in the sense that choosing a mixture distribution representing good and gross performance within the "overall basis approach" may be interpreted as a special case of the "individual basis approach." The reason to consider it as of the former type is that there may be somewhat less emphasis on a detailed modeling of the mechanisms causing the errors. Reverse, approximating the probability distribution resulting from the "individual basis approach" by some simpler distribution makes the approach less individual and more overall.

Which approach to follow in a particular application is to a certain extent dependent on what data are available. Aena's incident reporting system has been scrutinized for the occurrence of the types of lateral navigation errors listed in Table 3.2; but no lateral navigation errors were found for any of the above error classes. However, this does not necessarily imply that such errors did not occur in reality. As mentioned in Section 2.4, there is a serious possibility of the number of errors being underreported as the errors tend to be reported only when it is perceived that a safety issue is involved. From a risk analysis point of view, however, any occurrence is important because a safety issue could have been involved had circumstances been different. Also, experience with other airspaces suggests that lateral separation related anomalies do occur in practice. In the absence of these data, it does not seem to make much sense to attempt to apply the modeling approach on an individual basis.

Table 3-2. Definition of Lateral Navigation Error Types

Error class	Description	Example
A	Committed by aircraft not certified for RNP10 operation	
B	ATC system loop error	Pilot misunderstanding of clearance message; ATC issuing incorrect clearance
C1	Equipment control error encompassing incorrect operation of fully functional FMS or navigation system	Pilot incorrectly operating navigation equipment
C2	Incorrect transcription of ATC clearance or re-clearance into the FMS	
C3	Wrong information faithfully transcribed into the FMS	Flight plan followed rather than ATC clearance; Original clearance followed instead of re-clearance
D[1]	Other with failure notified to ATC in time for action	
E[1]	Other with failure notified to ATC too late for action	
F[1]	Other with failure not notified or received by ATC	

Note: [1] Errors in classes D, E and F are primarily due to equipment failure

Consider, therefore, the overall basis approach. First, this requires the type of probability density to be specified. When a distinction is made between nominal and non-nominal performance, or between normal deviations and gross deviations, the overall probability density may be taken as a mixture of two component densities, i.e.

$$f^{Y}(y_1) = (1-a) \times f^{Y}_{norm}(y_1) + a \times f^{Y}_{gross}(y_1) \tag{3.9}$$

Next, the two component densities are to be specified. The first density within the mixture may be specified on the basis of the RNP type of the airspace. Recall that the RNP type specifies the proportion (5%) of deviations larger in magnitude than the RNP value, but not the type (shape) of the distribution. (The type of distribution has some effect on the relative frequency of occurrence of deviations larger than the RNP value, but this effect is less than that of the distribution of the gross deviations.) A useful family of probability distributions is that of the Generalized Laplace distributions sometimes also referred to as power exponential distributions. This family is characterized by three parameters, a location parameter (the mean value), a scale

parameter and a shape parameter. All members of the family are symmetric about the mean value. Within the family, the shape parameter determines the type of the distribution. Two well-known probability distributions that are included are the gaussian and the double exponential distributions. As the double exponential is more conservative with regard to the occurrence of deviations larger than the RNP value, the density $f^Y_{norm}(y_1)$ was taken as a zero mean double exponential distribution with the scale parameter determined by the RNP value, i.e.

$$f^Y_{norm}(y_1) = \frac{1}{2a_1}\exp - \left|\frac{y_1}{a_1}\right| \tag{3.10}$$

with

$$\int_{-10}^{10} f^Y_{norm}(y_1)\,dy_1 = 0.95 \tag{3.11}$$

It follows from equations (3.10) and (3.11) that the scale parameter a_1 is given by

$$a_1 = -\frac{10}{{}^e\log 0.05}, \tag{3.12}$$

i.e. $a_1 = 3.338$ NM. This corresponds with a standard deviation value of

$$s_1 = a_1\sqrt{2} = 4.721 \text{ NM} \tag{3.13}$$

As was stated above, to make the overall density $f^Y(y_1)$ conservative, the tail density is also taken as double exponential with unknown scale parameter a_2, i.e.

$$f^Y_{gross}(y_1) = \frac{1}{2a_2}\exp - \left|\frac{y_1}{a_2}\right|. \tag{3.14}$$

Combining the above equations leads to the following double double exponential distribution for the lateral deviations:

$$f^Y(y_1) = (1-a)\times\frac{1}{2\times 3.338}\exp - \left|\frac{y_1}{3.338}\right| + a\times\frac{1}{2a_2}\exp - \left|\frac{y_1}{a_2}\right|. \tag{3.15}$$

Note that it still contains two unknown parameters, a and a_2, which remain to be determined.

As remarked in Reference 9, double double exponential densities have been used for many years to model lateral navigation errors (see also References 10 - 12). A feature of the model, in

addition to it being conservative due to its relatively thick tail, is that the probability of lateral overlap $P_y(S_y)$ can be evaluated analytically, viz.

$$P_y(S_y) \approx 2\,l_y\left[\left(\frac{1-a}{2a_1}\right)^2\left(a_1+S_y\right)\exp-\left|\frac{S_y}{a_1}\right|+\left(\frac{a}{2a_2}\right)^2\left(a_2+S_y\right)\exp-\left|\frac{S_y}{a_2}\right|+\right.$$

$$\left.\frac{a(1-a)}{2}\left\{\left(\frac{\exp-\left|\frac{S_y}{a_1}\right|+\exp-\left|\frac{S_y}{a_2}\right|}{a_1+a_2}\right)+\left(\frac{\exp-\left|\frac{S_y}{a_1}\right|-\exp-\left|\frac{S_y}{a_2}\right|}{a_1-a_2}\right)\right\}\right] \tag{3.16}$$

The expression for $P_y(S_y)$ consists of three parts, of which the first part may be referred to as core-core interaction, the second as tail-tail interaction and the third as core-tail interaction. It holds that the second term is negligibly small for sufficiently small values of a and the dependence of $P_y(S_y)$ on a can then be examined on the basis of only the first and third parts.

The probability of lateral overlap due to just the RNP10 navigation performance $(S_y = 50NM)$, i.e. $a_1 = 3.338$ and $a = 0$, with $l_y = 0.02871$ NM is equal to 2.1466×10^{-8}.

Given the lack of data on gross lateral navigation errors, it has been attempted to produce a conservative estimate of $P_y(S_y)$. It is based on first determining a conservative estimate of a and then examining $P_y(S_y)$ as a function of the scale parameter a_2 of the gross deviation probability density $f^{Y}_{gross}(y_1)$.

A derivation for the estimate of the weighting factor a is presented in Appendix A. The resulting value is $a = 1.346\times10^{-4}$. By comparison, the upper bounds for a derived in References 9 and 11 for the NOPAC system are 1.87×10^{-4} and 2.37×10^{-4} respectively. It should be realized, however, that the SAT and NOPAC systems are not identical and the values can only be compared when the differences between the two systems are taken into account. Nonetheless, the values are of the same order of magnitude.

The remaining parameter to be fixed is the scale parameter a_2 of the tail density within the mixture density. The analyses of References 9 to 11 suggest that the probability of lateral overlap $P_y(S_y)$ as a function of a_2 may be approximated by an expression that attains a maximum for $a_2 = S_y$ when a is sufficiently small. For the current assessment, $P_y(S_y)$ defined by equation (3.16) has been evaluated for $S_y = 50NM$ as a function of a and a_2 on the domain $[1.00\times10^{-5}, 1.00\times10^{-3}]$ for a and [20,75] for a_2. Figure 3.2 shows the resulting surface. It can

be seen that for each value of a, $P_y(S_y)$ as a function of a_2 is a nearly flat curve. The practical meaning of this is that the value of the lateral overlap probability is not sensitive to the value of the scale parameter a_2 on the domain under consideration. This can also be verified from Figure 3.3, which shows the lateral overlap probability as a function of the track separation S_y for various values of the tail density scale parameter a_2. An analysis of the numerical data underlying Figure 3.2 showed that there was a slight maximum at $a_2 = S_y = 50$ for each value of a. Figure 3.4 shows the lateral overlap probability as a function of the track separation S_y for various values of the weighting factor a. The diagram shows that the lateral overlap probability is more sensitive to the weighting factor a than it is to the scale factor a_2. The sensitivity of $P_y(S_y)$ to a at a track separation of $S_y = 50$ is moderate. Nonetheless, the diagram once again demonstrates the importance of obtaining sufficient data for the estimation of a.

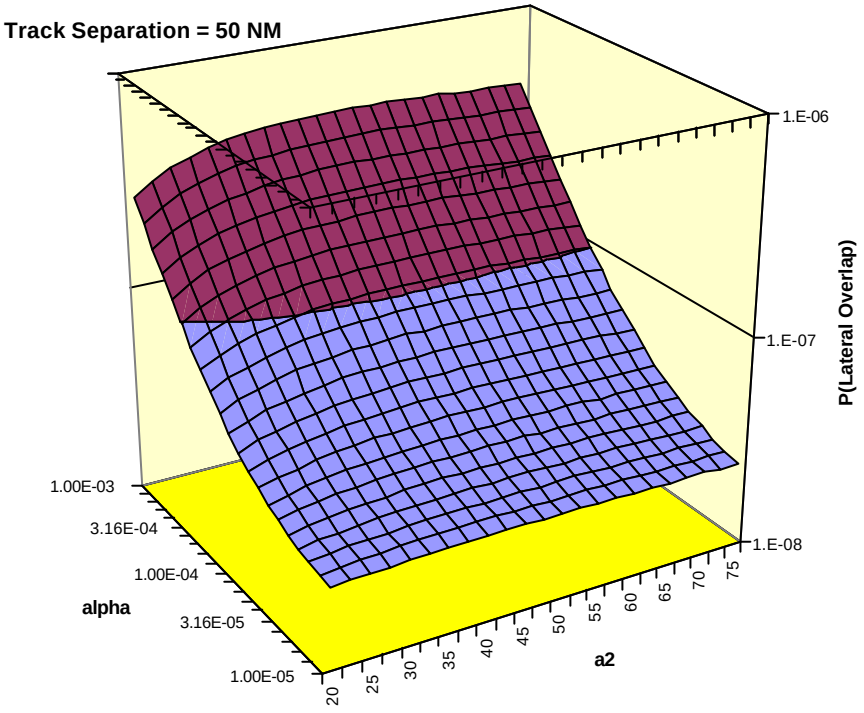

INCRUSTARINCRUSTARINCRUSTARINCRUSTAR**Figure 3-2. The lateral overlap probability $P_y(S_y)$ as a function of a and a_2 ($a_1 = 3.338NM$)**

In a more heuristic sense, these figures show that the probability of lateral overlap $P_y(S_y)$ varies far more as the track spacing S_y is reduced below 50 NM than it does as the track spacing is reduced from 100 NM to 50 NM. This follows from the initial assumption of RNP10 performance based on the experience in the NAT and the projection of the Double Double Exponential probability mixture distribution for lateral deviations presented in Appendix A..

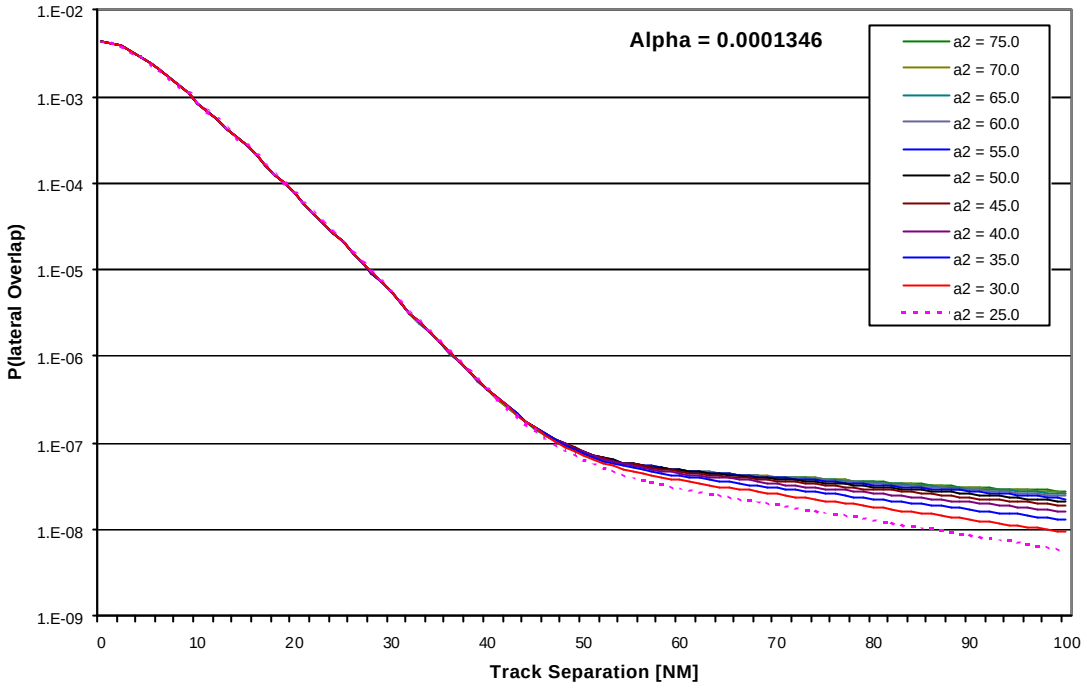

Figure 3-3. The Lateral Overlap Probability $P_y(S_y)$ as a Function of Track Separation for Different Values of the Scale Parameter a_2 ($a_1 = 3.338NM$)

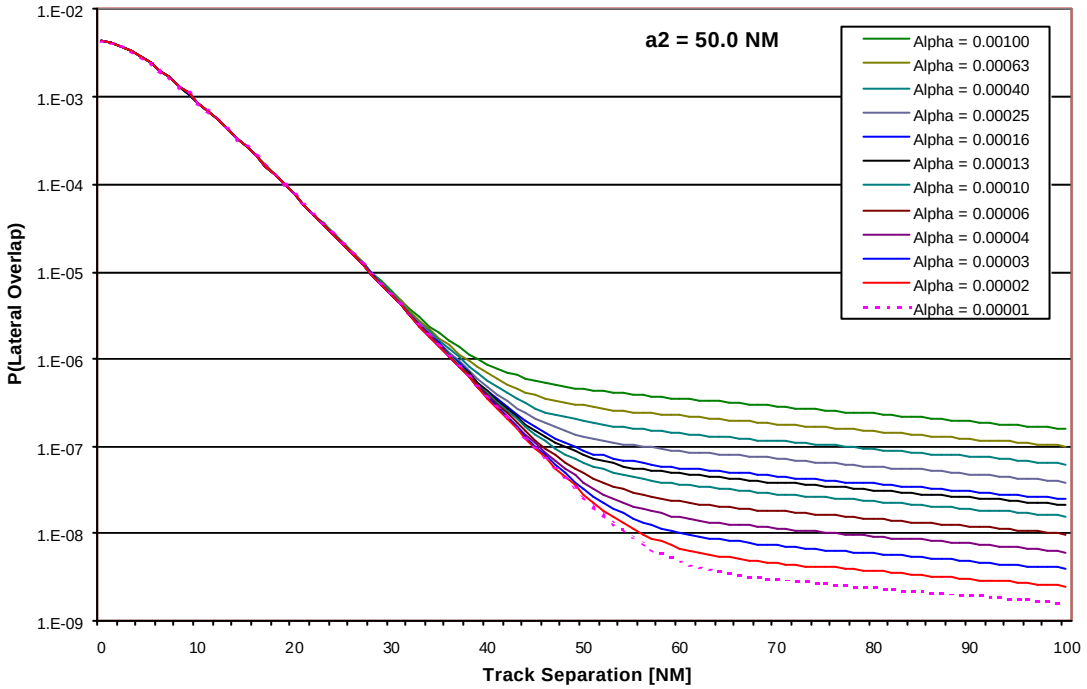

Figure 3-4. The Lateral Overlap Probability $P_y(S_y)$ as a Function of Track Separation for Different Values of the Weighting Factor a ($a_1 = 3.338NM$)

In summary, the probability density of the lateral navigation deviations in the RNP10 airspace to be implemented in the SAT is modeled by a double double exponential probability density with the following parameter values:

$$a = 1.346 \times 10^{-4}$$
$$a_1 = 3.338 \qquad (3.17)$$
$$a_2 = 50$$

Based on this model, the probability of lateral overlap was calculated and is shown in Table 3.3. By comparison, the maximum tolerable lateral overlap probabilities derived in References 9 and 11 for the NOPAC were $P_y(S_y) = 9.66 \times 10^{-8}$ and $P_y(S_y) = 1.23 \times 10^{-7}$, respectively. The difference between the two values is due to different assumed traffic growth factors for the NOPAC. They are quite comparable to the estimate of $P_y(S_y)$ obtained here for the SAT.

Table 3.3 also shows the probability of lateral overlap for aircraft separated by twice the lateral separation standard. As this value is about 27% of $P_y(S_y)$, its contribution to the lateral collision risk (cf. Equation (3.2)) cannot be ignored a priori.

Table 3-3. Estimates of lateral overlap probability for the SAT based on equations (3.9), (3.10), (3.14) and (3.17)

Probability of lateral overlap for $S_y = 50NM$	
$P_y(S_y)$	$P_y(2 \times S_y)$
7.858×10^{-8}	2.101×10^{-8}

3.4 Lateral Occupancy

Paragraph 1.1 of Appendix C of Reference 12 defines "same direction, single separation standard lateral occupancy" for a parallel track system as the average number of aircraft which are, in relation to the typical aircraft:

a) flying in the same direction as it;
b) nominally flying on tracks one lateral separation standard away from it;
c) nominally at the same flight level as it; and
d) within a longitudinal segment centered on it.

Part (b) of the above definition has been expanded to include tracks that are 'one or two lateral separation standards away' for two reasons:

- The track system includes adjacent tracks that are *two* lateral separation standards apart.
- There is a significant collision risk arising from the probability of overlap between non-adjacent tracks that are *two* lateral separation standards apart.

A similar set of criteria can be used to define opposite direction occupancy. The length of the longitudinal segment, $2\tilde{S}_x$, is fairly arbitrary but appears elsewhere in the risk model. The sensitivity of the lateral collision risk to $\tilde{S}_x$ is discussed further in Addendum 1 to this report.

Paragraph 2.3 of the same reference states that for a particular system the lateral occupancy E_y is related to two other quantities T_y and H by

$$E_y = \frac{2T_y}{H} \tag{3.18}$$

where

T_y: The total proximity time generated in the system, i.e. the t

H: The total number of flying hours generated in the system during the period considered.

Lateral occupancy is an estimate of the probability of aircraft pairs being in longitudinal overlap in the system and, at the same time, converts numbers of collisions into numbers of accidents through the factor of 2 in the numerator of equation (3.18). With regard to the definition of occupancy above and equation (3.18), it is believed that equation (3.18) (without the factor of 2) is in fact more in agreement with the definition of probabilities as proportions of time in the original Reich model. Under certain assumptions, equation (3.18) may be converted into the form of the definition.

Occupancy is sometimes confused with the volume of traffic, but these two parameters are not directly related. Occupancy is a calculated value that depends upon the *actual* distribution of flights within the Corridor and may be interpreted as the probability that a given aircraft has another aircraft within a range of $\tilde{S}_x$. (Since occupancy can theoretically take on values greater than one, it may also be interpreted as the probable number of aircraft within a range $\tilde{S}_x$ of a given aircraft.) For example, if the traffic level is 60 flights per day and the lateral occupancy is 0.25, then (an average of) 15 of those flights satisfy the four conditions listed at the beginning of this section. This seems like a high percentage until you revisit Figure 2.12 and realize that all of the flights depart at roughly the same time. Imagine a multi-route airspace with 100 aircraft in it. If those 100 aircraft all travel close together in a group, then the occupancy is fairly high. (Conversely, if they were spread out over a long stretch of the routes, the occupancy would be fairly low.) If you take 100 more aircraft, traveling in an identical group, and place that group on the routes behind (but not overlapping) the first group of 100 aircraft, you have doubled the traffic but the occupancy (and hence the risk) *remains the same.* On the other hand, if you take *one* aircraft and set it down in the *middle* of the group of 100 aircraft, you have increased both the traffic and the occupancy (and again the risk) by 1%. This latter, more conservative, approach has been adopted when estimating the impact of traffic growth on occupancy - and risk. The presumption is that the passengers buying the tickets on those additional flights will still want to depart at the same general time.

Appendix B discusses some methods that may be used for the estimation of lateral occupancy. Occupancy for the current track system has been calculated by means of the "direct estimation from time at waypoint passing" method. It was verified that the relationship between $\tilde{S}_x$ and occupancy was linear. Lateral collision risk, therefore, was calculated on the basis of $\tilde{S}_x = 80NM$. Some results for $\tilde{S}_x = 80NM$ are summarized in Table 3.4.

Table 3-4. Lateral Occupancy for Existing Track System and Some Associated Quantities Based on Traffic Flow Data for the Period of Time from August 1999 to September 2000.

Quantity	Estimate
Lateral occupancy $E_y(same)$ for existing track system with $\tilde{S}_x = 80NM$	0.2562
Number of flights on UN741	8526
Number of flights on UN866	5167
Number of flights on UA32	11740
Number of flights on UN741, UN866 and UA32	25433
Number of proximate events for tracks UN741 and UN866	1721
Number of proximate events for tracks UN866 and UA32	1537
Number of proximate events for UN741, UN866 and UA32	3258

For the proposed new track system (recall Figure 3.1), two occupancy values play a major part, namely one for the two most westerly routes UN741 and UN866, separated by twice the separation minimum S_y, and one for the routes UN866, UN873 and UN857 separated by the separation minimum. In addition, the occupancy for the routes UN866 and UN857, separated by twice the separation minimum, contributes to the collision risk. An overall occupancy value may be defined by assuming that all the four tracks in the new system would be separated by the separation minimum S_y. It has been assumed for the calculations that the additional route in the east has no impact on the traffic load on the two western most routes UN741 and UN866. It has also been assumed that the traffic on the existing route UA32 will be distributed over the new routes UN873 and UN857 in the proportions f and $1-f$, respectively, the nominal situation being an equal split. Under this convention, the case $f = 0$ is equivalent to the existing track system; see Figure 3.5. The impact of the traffic redistribution on lateral occupancy has been analyzed as described in Appendix B.

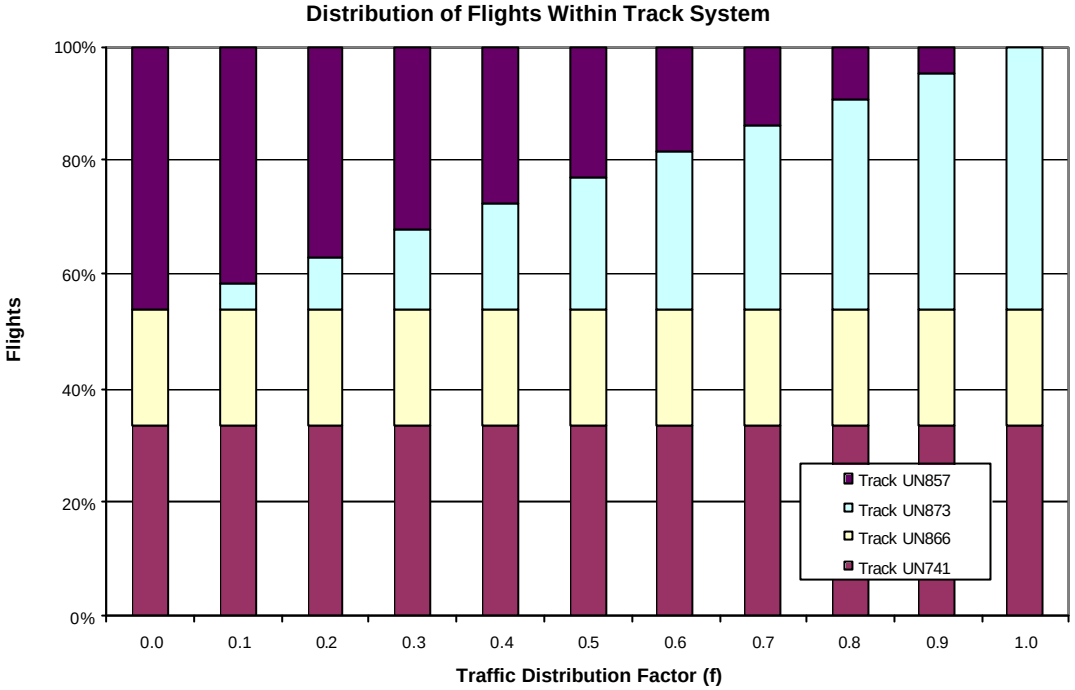

Figure 3-5. Effect of the Traffic Distribution Factor (f) on the per track traffic load.

A number of assumptions have had to be made in Appendix B, particularly concerning the redistribution of the traffic within the new track system. It is important that these assumptions be verified after the implementation of the new structure to confirm the validity of the projections.

Using current traffic flows, some lateral occupancy results are shown in Table 3.5. It can be seen that the combined lateral occupancy for the routes UN866 and UN873 & UN873 and UN857 is small when the proportion of traffic f on the middle of these three routes is small. Over the range of traffic distribution factors considered, this lateral occupancy varies by a factor of approximately four. There is a peak in *this* occupancy for $f = 0.7$. The location of the peak depends on the ratio of the traffic flows on the existing routes UA32 and UN866, see appendix B. Because the separation between routes UN866 and UN857 is the same as the separation between routes UN741 and UN866 ($2S_y$), the lateral occupancy between routes UN866 and UN857 is also included in Table 3.5 and the computation of the overall occupancy. Over the range of traffic distribution factors considered, the *overall* lateral occupancy varies by a factor of approximately 1.3, with a peak at $f = 0.5$. Note also that when *any* of the traffic on the original route UA32 is assigned to route UN873, the overall lateral occupancy is larger than the lateral occupancy in the existing track structure. This is caused by the route UN873 traffic flow interacting with the traffic flows on two adjacent routes, one on the left of it (UN866) and one on the right (UN857).

Table 3-5. Lateral Occupancy Estimates for Proposed Track System Based on Current Traffic Levels

Traffic distribution factor *f*	Lateral occupancy between UN866 and UN873 & UN873 and UN857	Lateral occupancy between UN866 and UN857	Lateral occupancy between UN741 and UN866	Overall lateral occupancy
0.0	0.0000	0.1209	0.1353	0.2562
0.1	0.0368	0.1088	0.1353	0.2809
0.2	0.0681	0.0967	0.1353	0.3001
0.3	0.0939	0.0846	0.1353	0.3139
0.4	0.1143	0.0725	0.1353	0.3221
0.5	0.1291	0.0604	0.1353	0.3249
0.6	0.1384	0.0483	0.1353	0.3221
0.7	0.1423	0.0363	0.1353	0.3139
0.8	0.1406	0.0242	0.1353	0.3001
0.9	0.1335	0.0121	0.1353	0.2809
1.0	0.1209	0.0000	0.1353	0.2562

Another factor that was taken into account is the effect of traffic growth on lateral occupancy. It holds that occupancy is approximately proportional to traffic flow rate. Assuming a planning horizon of 10 years and an annual traffic growth rate of 5.1% gives an overall traffic growth factor of 1.64. It was also assumed that the introduction of RVSM in 2002 would result in an across-the-board 15% reduction in occupancy that reduces the overall traffic growth factor to 1.40. Application of this factor to the estimates in Table 3.5 results in the numbers shown in Table 3.6a. The results given in Table 3.5 and Table 3.6a are summarized in Figure 3.6a.

Table 3-6a. Lateral Occupancy Estimates for Proposed Track System Based on Traffic Levels Projected Over a Ten Year Planning Horizon at 5.1% per year growth

Traffic distribution factor *f*	Lateral occupancy between UN866 and UN873 & UN873 and UN857	Lateral occupancy between UN866 and UN857	Lateral occupancy between UN741 and UN866	Overall lateral occupancy
0.0	0.0000	0.1689	0.1892	0.3581
0.1	0.0514	0.1521	0.1892	0.3927
0.2	0.0952	0.1352	0.1892	0.4195
0.3	0.1313	0.1183	0.1892	0.4387
0.4	0.1597	0.1014	0.1892	0.4502
0.5	0.1804	0.0845	0.1892	0.4541
0.6	0.1935	0.0676	0.1892	0.4502
0.7	0.1989	0.0507	0.1892	0.4387
0.8	0.1966	0.0338	0.1892	0.4195
0.9	0.1866	0.0169	0.1892	0.3927
1.0	0.1689	0.0000	0.1892	0.3581

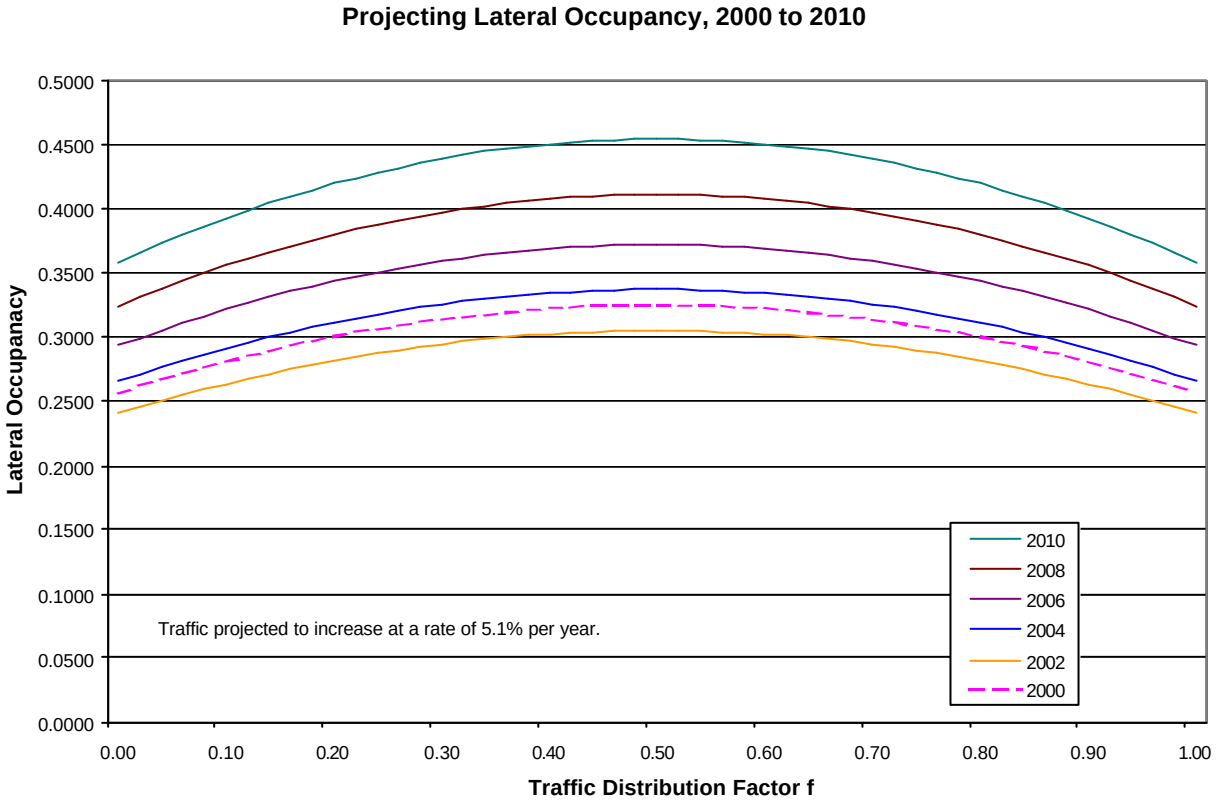

Figure 3-6a. Effect of the Traffic Distribution Factor (*f*) on Lateral Occupancy Over 10 Years at a Growth Rate of 5.1% per year.

The annual traffic growth rate of 5.1%, assumed above, is an ICAO global value. Adopting an annual traffic growth rate of 8%, proposed by IATA and adopted by the SAT/9, gives an overall traffic growth factor of 2.16. Including the assumed across-the-board 15% reduction in occupancy due to the introduction of RVSM in 2002 reduces this overall traffic growth factor to 1.84. Application of this factor to the estimates in Table 3.5 results in the numbers shown in Table 3.6b. The results given in Table 3.5 and Table 3.6b are summarized in Figure 3.6b.

The same direction lateral occupancy values shown in Table 3.5 are not extremely high. For example, for NAT MNPS airspace, the same direction lateral occupancy for the year 1999 was estimated as 0.671 (Ref. 19). The NOPAC system has a much lower value for same direction occupancy, e.g. 0.09/0.07 for 1995, but has a considerable opposite direction lateral occupancy (Refs. 9, 10). The future lateral occupancy values in ten years shown in Table 3.6b are projected to be 10-30% less than the current lateral occupancy in the North Atlantic.

Table 3-6b. Lateral Occupancy Estimates for Proposed Track System Based on Traffic Levels Projected Over a Ten Year Planning Horizon at 8% per year growth

Traffic distribution factor *f*	Lateral occupancy between UN866 and UN873 & UN873 and UN857	Lateral occupancy between UN866 and UN857	Lateral occupancy between UN741 and UN866	Overall lateral occupancy
0.0	0.0000	0.2218	0.2484	0.4702
0.1	0.0675	0.1996	0.2484	0.5155
0.2	0.1250	0.1774	0.2484	0.5508
0.3	0.1724	0.1553	0.2484	0.5760
0.4	0.2097	0.1331	0.2484	0.5911
0.5	0.2369	0.1109	0.2484	0.5961
0.6	0.2540	0.0887	0.2484	0.5911
0.7	0.2611	0.0665	0.2484	0.5760
0.8	0.2581	0.0444	0.2484	0.5508
0.9	0.2450	0.0222	0.2484	0.5155
1.0	0.2218	0.0000	0.2484	0.4702

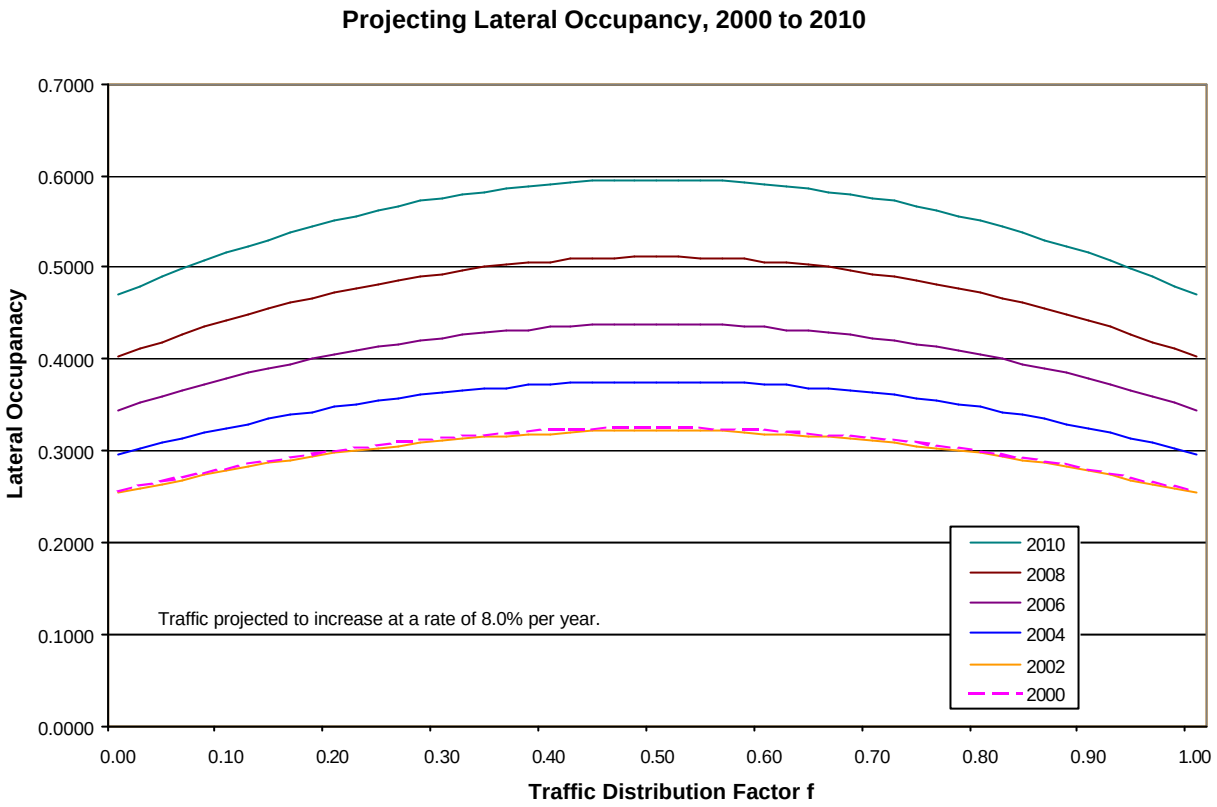

Figure 3.6b. Effect of the Traffic Distribution Factor (f) on Lateral Occupancy Over 10 Years at 8% per year.

3.5 The Probability of Vertical Overlap

The probability of vertical overlap of aircraft nominally flying at the same flight level of laterally adjacent flight paths is denoted by $P_z(0)$. It is defined by

$$P_z(0) = \int_{-l_z}^{l_z} f^{z_{12}}(z)dz \tag{3.19}$$

where $f^{z_{12}}(z)$ denotes the probability density of the vertical distance z_{12} between two aircraft with height deviations z_1 and z_2, nominally at the same flight level , i.e.

$$z_{12} = z_1 - z_2 \tag{3.20}$$

and

$$f^{z_{12}}(z) = \int_{-\infty}^{\infty} f^{TVE}(z_1) f^{TVE}(z_1 - z)dz_1 . \tag{3.21}$$

Note that equation (3.21) assumes that the deviations of the two aircraft are independent and have the same probability density, $f^{TVE}(z_1)$, say. As defined in Table 3.1, l_z denotes the average aircraft height. Substitution of equation (3.21) into equation (3.19) gives

$$P_z(0) = \int_{-l_z}^{l_z} \int_{-\infty}^{\infty} f^{TVE}(z_1) f^{TVE}(z_1 - z)dz_1 dz . \tag{3.22}$$

In practice, $P_z(0)$ is often approximated by

$$P_z(0) \approx 2\, l_z \int_{-\infty}^{\infty} f^{TVE}(z_1) f^{TVE}(z_1)dz_1 . \tag{3.23}$$

or

$$P_z(0) \approx 2\, l_z f^{z_{12}}(0) \tag{3.24}$$

Thus, the probability density $f^{TVE}(z_1)$ of the height-keeping deviations of aircraft is needed to calculate $P_z(0)$. The height-keeping performance of the aircraft population is dependent on whether, or not, the aircraft making up the population are MASPS approved. The better the height-keeping performance, the larger the value of $P_z(0)$. With a view to the planned implementation of RVSM on the 24th January 2002, it has been assumed for the RNAV RNP10 risk assessment, that the complete aircraft population has been MASPS approved. The MASPS puts constraints on the distributions of ASE and FTE/AAD, the two components of TVE. The probability density $f^{TVE}(z_1)$ can then be taken from Section 4.3 and $P_z(0)$ can be calculated by

means of equation (3.22) or equation (3.24). The resulting estimate, based on $l_z = 55.43$ (cf. Table 3.7), is

$$P_z(0) = 0.56565 \tag{3.25}$$

This may conservatively be rounded to $P_z(0) = 0.57$.

3.6 Aircraft Dimensions

Table 2.6 shows the dimensions of the various aircraft types in the SAT. The B741 – B747, A330 – A340, B772 and MD11 are the largest aircraft types common in the area. Average aircraft dimensions have been calculated using the proportions of flights by type shown in the 3rd column of Table 2.6 as weighting factors. Figure 2.7 shows the range of the aircraft dimensions. Because there are only few flights made by the smaller aircraft types, they contribute only marginally to the average aircraft dimensions.

The following averages have been computed:

- calculated weighted average length: 193.12 ft
- calculated weighted average width: 174.45 ft
- calculated weighted average height: 55.43 ft

The average aircraft dimensions are shown in Table 3.7, both in feet and Nautical Miles. By comparison, the corresponding values currently in use for the lateral collision risk model in the NAT are 185.93, 165.27 and 52.25 ft. In this context, it is remarked that the estimate of the collision risk is not very sensitive to the average aircraft dimensions.

Table 3-7. Average Aircraft Dimensions for the Lateral Collision Risk Model

aircraft dimension	parameter	value (ft)	value (NM)
length	l_x	193.12	0.03179
width	l_y	174.45	0.02871
height	l_z	55.43	0.009124

3.7 Relative Velocities

The lateral collision risk model equation (3.2) contains three relative speed parameters, namely $\overline{|\Delta V|}$, $\overline{|\dot{y}|}$ and $\overline{|\dot{z}|}$. Their estimation for the benefit of the RNAV RNP10 risk assessment is successively discussed below. Also, as it is a parameter of the vertical collision risk model to be discussed in Section 4, the average aircraft speed $\overline{|V|}$ has been included. The extent to which the relative speed components, particularly $\overline{|\dot{y}|}$ and $\overline{|\dot{z}|}$, are related to the magnitude of the lateral and vertical separation between a pair of aircraft are also addressed.

The best way to estimate the average aircraft speed parameter of the lateral collision risk model is on the basis of data on the cleared speeds of aircraft in the SAT. As stated in Section 2.2, the Mach Number Technique (MNT) is applied flight by flight to all flights operating in the SAT to maintain longitudinal separation. Data on the cleared speeds were not provided; so speeds and relative velocities were estimated by comparing waypoint report times for the 776 flights in the Recife data set to matching flights in the Canaries ACC primary data set. There are two assumptions that underlie this approach:

- Waypoint report times will always err to late rather than early.
- Errors in waypoint report times are small compared to the time difference between widely separated reports.

A total of 693 matching flights were identified, yielding the computed speed distributions shown in Figure 3.7. Average speeds by route and direction are listed in Table 3.8. The overall average speed computed in this manner is 474.4 knots.

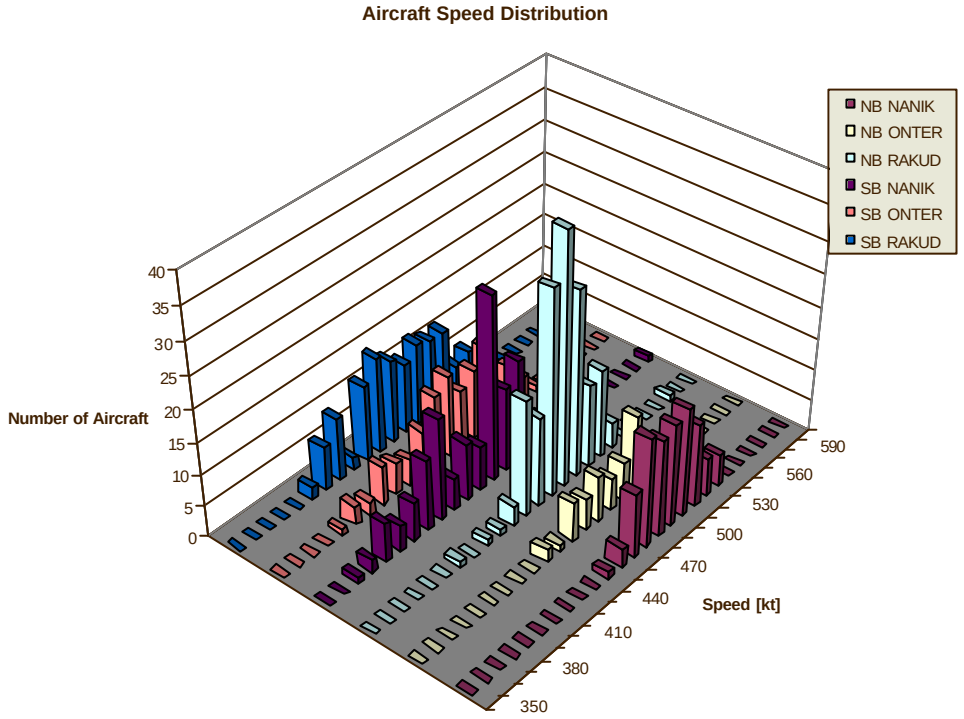

Figure 3-7. Distribution of computed aircraft speeds

Table 3-8. Average Aircraft Speeds, In Knots, for the Lateral Collision Risk Model

	NANIK	ONTER	RAKUD	Average
NB	494.0	489.5	483.5	489.0
SB	451.7	468.2	461.3	460.4
Average:	472.9	478.9	472.4	**474.7**

Table 2.6 includes typical cruising speeds of the different aircraft types operating in the SAT. Of the aircraft types for which the cruising speed was given as a range, the midpoint of their ranges has been noted. From this distribution, the average value for aircraft *cruising* speed was 538.3 knots. It was concluded that this value is out of line with values computed in Table 3.8, and therefore, was *not* used to compute collision risk, because the MN governs the aircraft speed in the Corridor. The following value for $\overline{|V|}$ to be used in the lateral (and vertical) collision risk model has been adopted:

$$\overline{|V|} = 475kt \tag{3.26}$$

This value is compared with that of 480 knots for both the NAT and the NOPAC (Refs. 19 and 9).

The average modulus of the relative along track speed, $\overline{|\Delta V|}$, can be derived from the distribution of the differences between computed speeds of pairs of aircraft. Strictly speaking, $\overline{|\Delta V|}$ applies to pairs of aircraft that have lost lateral separation. It is generally assumed, however, that the loss of lateral separation is not markedly related to the distribution of $|\Delta V|$ (it is related to $\overline{|\dot{y}|}$). Thus, Figure 3.8 shows the distribution of the modulus of the relative along track speeds for pairs of aircraft at the same flight level of adjacent tracks. Only proximate pairs of aircraft from the set of 793 flights for which speeds were computed above were used (cf. Section 3.4, lateral occupancy). The average value for this distribution is 17.0 kts (weighted average of 18.6 kts for Route 741/866 (49 events) and 15.4 kts for Route 857/866 (48 events)). A slightly conservative estimate of 20 kts was used to compute the lateral risk. The corresponding values for the NAT and the NOPAC are 13 and 29 kts, respectively.

Aside from $2\overline{|V|}$ for opposite direction traffic, $\overline{|\dot{y}|}$ is generally the most significant relative speed parameter of the lateral collision risk model. Values currently in use for the NAT and the NOPAC are 80 kts and 42.22 kts respectively (Refs. 14, 19 and 11). It is important to note that $\overline{|\dot{y}|}$ is the average value of the modulus of the relative cross track speed between a pair of aircraft that has lost lateral separation. Data on pairs of aircraft on adjacent routes that have actually lost lateral separation are scarce and the estimation of $\overline{|\dot{y}|}$ usually involves some extrapolation on the basis of data that are more readily available. In principle, the basic data source would be radar data on lateral deviations and speeds. From this, the relationship between $|\dot{y}|$ and $|y|$ could be examined and modeled. The model could then be used to extrapolate the data to obtain a

distribution of $|\dot{y}|$ at the lateral separation S_y, $|\dot{y}(S_y)|$, from which an average value could be calculated.

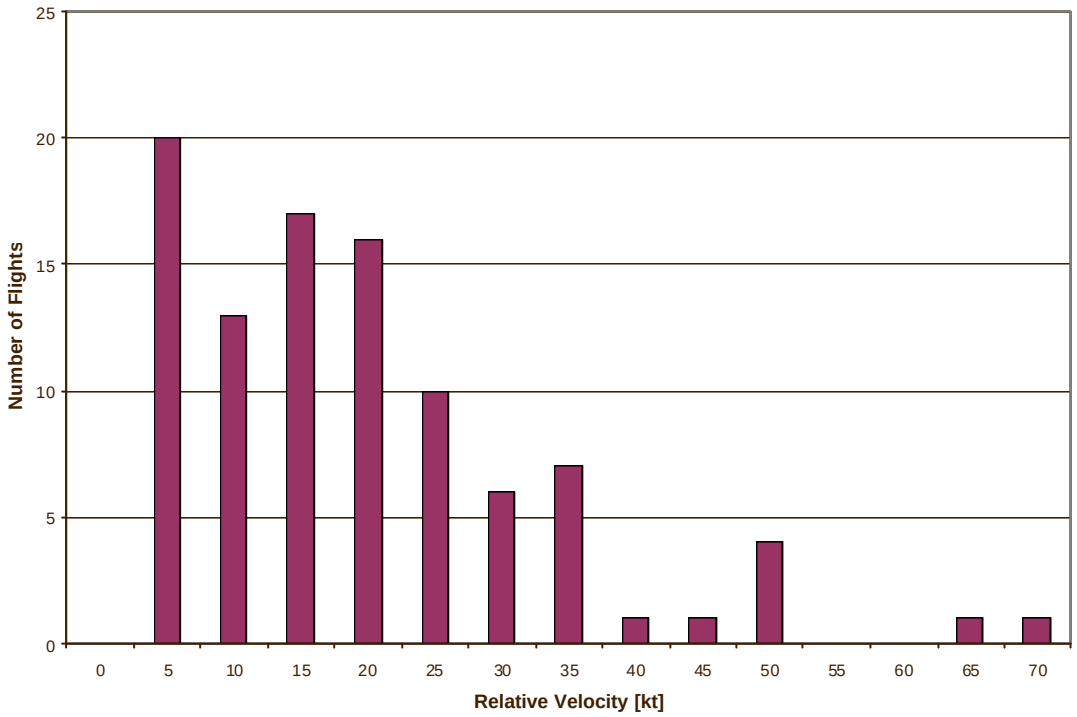

Figure 3-8. Distribution of Computed Relative Aircraft Speeds

Unfortunately, such radar data were not available for the current study. Empirical data from other studies such as References 11, 18 or 19 were not available either. In fact, the value of $\overline{|\dot{y}|} = 80kts$ used for the NAT is based on a model of a particular type of lateral error, i.e. a one-degree (60 NM) waypoint error, rather than empirical data (Ref.14). In general, the angle under which an aircraft starts deviating from its track, together with the aircraft's speed can be used to determine the time it takes to close a certain amount of lateral separation and hence the value of $|\dot{y}|$. When, as a rough approximation, the distance between successive waypoints on e.g. the UN866 is taken as 300 NM (cf. Table 2.2), a 50 NM waypoint error would define a deviation angle of approximately 9.5°. With an aircraft speed of 475 kts this would correspond with a lateral speed of approximately 80 kts. Thus, a value of $\overline{|\dot{y}|} = 80kts$ might also be taken for the lateral risk assessment of RNP10 airspace in the SAT. It should be noted, however, that, as argued in Reference 14, this value might be somewhat conservative for arbitrary random lateral deviations resulting in the complete loss of lateral separation. It must also be kept in mind that, currently, knowledge about the possible occurrence of waypoint and other types of operational errors in the SAT is limited. Current estimates from operators, ACCs and IATA representatives are that there are few if any waypoint type errors in the EUR/SAM Corridor due to the fixed track/waypoint nature of the airspace. In light of these arguments, the lateral risk is calculated on the basis of $\overline{|\dot{y}|} = 42kts$, which is consistent with the $\overline{|\dot{y}|} = 42.22kts$ value used in the NOPAC risk

assessment. Note that, at an aircraft speed of 475-480 kts, this value of the relative lateral speed relates to a deviation angle of approximately 5°. The sensitivity of the estimated risk to the value of this parameter is also examined.

Like $\overline{|\Delta V|}$ and $\overline{|\dot{y}|}$, $\overline{|\dot{z}|}$ denotes the average modulus of the relative vertical speed between a pair of aircraft on the same flight level of adjacent tracks that has lost lateral separation. As with the relative along track speed $|\Delta V|$, $|\dot{z}|$ is generally assumed to be independent of the size of the lateral separation between the aircraft. For aircraft in level flight, it may also be expected that there is virtually no dependence of $|\dot{z}|$ on the size of the vertical separation between the aircraft. Although data on $|\dot{z}|$ are relatively scarce, early data from the NAT showed that $\overline{|\dot{z}|}$ was of the order of 1kt for aircraft nominally in horizontal flight (Ref. 20). More recent data are available from the European studies of vertical separation above FL290 and showed an approximately constant relationship between $\overline{|\dot{z}|}$ and the vertical separation $|z|$ (Ref. 21, Part II, Annex A, Section 5.5.6). From that, a value of $\overline{|\dot{z}|} = 1.5$ kts may be taken. Based on this, and on the fact that the lateral models for the NAT as well as the NOPAC use a value of 1.5kts for $\overline{|\dot{z}|}$, $\overline{|\dot{z}|} = 1.5$ kts has also been taken for the lateral risk model for the SAT.

3.8 Summary and Comparison of Parameter Values

Table 3.9 summarizes the lateral collision risk model parameters for the SAT and shows a comparison with their counterparts used in the NAT and the NOPAC. The parameters of the lateral collision risk model for the Canaries routes between Spain and the Canaries Islands in RNP5 airspace have also been included (Ref. 17).

Table 3-9. Summary and Comparison of Lateral Collision Risk Model Parameters

	Airspace			
Parameter[1]	**SAT**	**NAT**	**NOPAC**	**Canaries**
RNP type	10	12.6	10	5
S_y	50	60	50	43
$P_y(S_y)$	7.858×10^{-8}			
$P_y(2S_y)$	2.101×10^{-8}			
$P_z(0)$	0.57	0.5	0.38	0.39/0.5[2]
l_x	193.12	185.93	232.11	139.76
l_y	174.45	165.27	213.27	121.52
l_z	55.43	52.25	63.80	42.53
$\tilde{S}_x$	80			
$E_y(same)$	Sect. 3.4			
$E_y(opp)$	0			
$\overline{\lvert V\rvert}$	475	480	480	450
$\overline{\lvert\Delta V\rvert}$	20	13	29	20
$\overline{\lvert\dot{y}\rvert}$	42	80	42.22	20
$\overline{\lvert\dot{z}\rvert}$	1.5	1.5	1.5	1.5

Notes: 1. Aircraft dimensions in feet, relative speeds in knots
2. Pre- and post-RVSM situation

3.9 Lateral Risk

The estimates of the different parameters of the collision risk model summarized in Table 3.9 can now be substituted into the model to estimate the lateral collision risk associated with a 50NM lateral separation minimum between three of the tracks in RNP10 airspace in the SAT. Two cases are considered namely current traffic levels and future traffic levels, projected forward over a 10 year planning horizon.

Recall from Section 3.2 that the collision risk model to be used is the following:

$$N_{ay} = \left\{P_y(S_y)E_y(same) + P_y(2S_y)E_y^{*}(same) + P_y(2S_y)E_y^{**}(same)\right\}\times P_z(0)\frac{l_x}{\tilde{S}_x}\left\{\frac{\overline{|\Delta V|}}{2l_x} + \frac{\overline{|\dot{y}|}}{2l_y} + \frac{\overline{|\dot{z}|}}{2l_z}\right\} \quad (3.27)$$

with $S_y = 50NM$. Use of the parameter values from the first column of Table 3.9 gives, for the latter part of the right-hand side of equation (3.27):

$$P_z(0)\frac{l_x}{\tilde{S}_x}\left\{\frac{\overline{|\Delta V|}}{2l_x}+\frac{\overline{|\dot{y}|}}{2l_y}+\frac{\overline{|\dot{z}|}}{2l_z}\right\}=0.57\times\frac{0.03179}{80}\times\left\{\frac{20}{2\times0.03179}+\frac{42}{2\times0.02871}+\frac{1.5}{2\times0.009124}\right\} \tag{3.28}$$

or

$$P_z(0)\frac{l_x}{\tilde{S}_x}\left\{\frac{\overline{|\Delta V|}}{2l_x}+\frac{\overline{|\dot{y}|}}{2l_y}+\frac{\overline{|\dot{z}|}}{2l_z}\right\}=0.57\times\frac{0.03179}{80}\times\{314.5643+731.4525+82.200789\} \tag{3.29}$$

$$=0.57\times3.9738\times10^{-4}\times1128.2176=0.2555$$

Thus, equation (3.27) becomes

$$N_{ay}=\left\{P_y(S_y)E_y(same)+P_y(2S_y)E_y^{*}(same)+P_y(2S_y)E_y^{**}(same)\right\}\times0.2555 \tag{3.30}$$

The next step is to substitute estimates of the occupancy parameters and the lateral overlap probabilities into equation (3.30). The lateral overlap probabilities have been given in Table 3.3, i.e. $P_y(S_y)=7.858\times10^{-8}$ and $P_y(2S_y)=2.101\times10^{-8}$, and the occupancies for current traffic levels in Table 3.5.

Table 3.10 shows the estimates of the lateral collision risk based on current traffic levels as a function of the traffic distribution factor f. It can be seen that the estimates are below the lateral TLS of 5×10^{-9} fatal accidents per flight hour for all values of f.

The sum of the occupancies $E_y^{*}(same)$ and $E_y^{**}(same)$ is seen to vary from 0.2562 to 0.1353 when the traffic distribution factor f varies between zero and one, whereas $E_y(same)$ varies from 0.0 to 0.1209 with a peak of 0.1423 at f = 0.7. As $P_y(2S_y)$ is not extremely small as compared to $P_y(S_y)$, a significant part of the calculated lateral risk is associated with the loss of lateral separation between aircraft that are nominally two separation standards apart. A better knowledge of the distribution of the lateral navigation deviations of the aircraft in the SAT might be able to show that the tails of the distribution are actually not as thick as was assumed in the current analysis due to lack of data on lateral deviations. This might make the effect of $P_y(2S_y)$ less significant as well as reduce the estimate of $P_y(S_y)$. Figure 3.9 illustrates the relative contribution of each track-to-track occupancy to the overall lateral collision risk.

Figure 3.9 illustrates the relative contribution of each track-to-track occupancy to the overall lateral collision risk. As traffic shifts from UN857 ($f=0$) to UN873 ($f=1$), the relative contribution from each route varies. Notice that, while the overall risk has a maximum around $f=0.7$, the contribution from the interaction between UN857 and UN873 has a maximum at

$f = 0.5$. The lateral risk is thus relatively sensitive to how the traffic is distributed over the available routes.

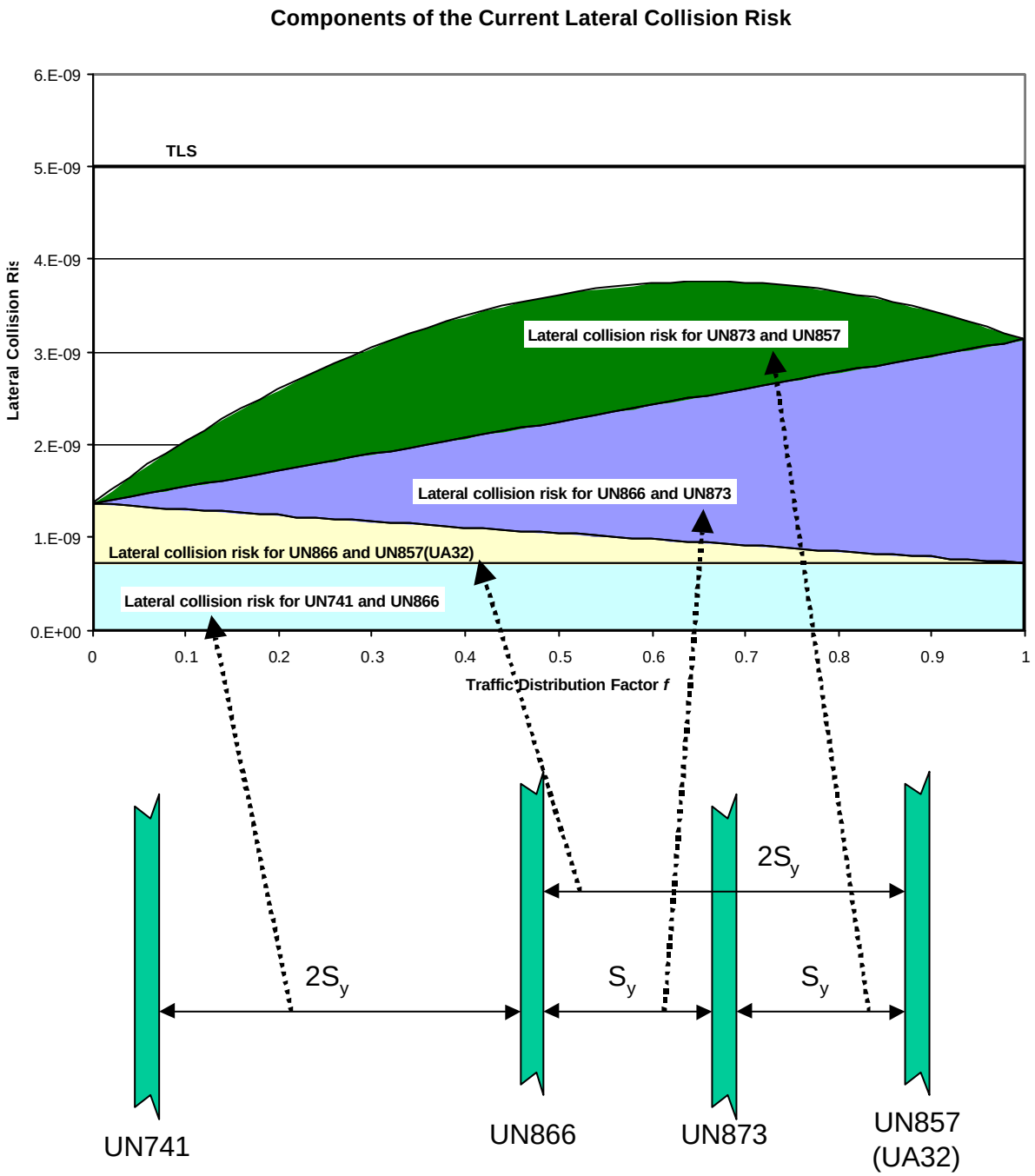

Figure 3-9. Sensitivity of Lateral Collision Risk to Relative Track Occupancy in 2000

Table 3-10. Lateral Collision Risk Estimates for Proposed Track System Based on Current Traffic Levels

Traffic distribution factor f	Lateral occupancy for UN866 and UN873 & UN873 and UN857 $E_y(same)$	Lateral occupancy for UN866 and UN857 $E_y^{**}(same)$	Lateral occupancy for UN741 and UN866 $E_y^{*}(same)$	Lateral collision risk N_{ay}
0	0.0000	0.1209	0.1353	1.365E-09
0.1	0.0368	0.1088	0.1353	2.034E-09
0.2	0.0681	0.0967	0.1353	2.593E-09
0.3	0.0939	0.0846	0.1353	3.043E-09
0.4	0.1143	0.0725	0.1353	3.384E-09
0.5	0.1291	0.0604	0.1353	3.615E-09
0.6	0.1384	0.0483	0.1353	3.737E-09
0.7	0.1423	0.0363	0.1353	3.749E-09
0.8	0.1406	0.0242	0.1353	3.652E-09
0.9	0.1335	0.0121	0.1353	3.445E-09
1	0.1209	0.0000	0.1353	3.129E-09

Table 3.11 shows the estimates of the lateral collision risk based on traffic levels projected forward over a ten-year planning horizon. The assumed traffic growth factor was 5.1% per annum, with an additional 15% drop due to the introduction of RVSM in 2002. As a result, the lateral risk estimates are a factor of 1.40 (overall growth factor) greater than their counterparts in Table 3.10 for current traffic levels. It can be seen that the risk estimate slightly exceeds the TLS of 5×10^{-9} for values of f between 0.5 and 0.8. The data in Table 3.10 and Table 3.11a are summarized in Figure 3.10a.

The effect of an 8% per annum growth rate is shown in Table 3.11b and Figure 3.10b. Note that, even with an 8% growth rate, all the estimates of the lateral risk are less than the *previous* lateral TLS of 2×10^{-8} accidents per flight hour.

Table 3-11a. Lateral Collision Risk Estimates for Proposed Track System Based on Traffic Levels Projected Over a Ten Year Planning Horizon with a 5.1% Growth Rate

Traffic distribution factor f	Lateral occupancy for UN866 and UN873 & UN873 and UN857 $E_y(same)$	Lateral occupancy for UN866 and UN857 $E_y^{**}(same)$	Lateral occupancy for UN741 and UN866 $E_y^{*}(same)$	Lateral collision risk N_{ay}
0	0.0000	0.1689	0.1892	1.908E-09
0.1	0.0514	0.1521	0.1892	2.843E-09
0.2	0.0952	0.1352	0.1892	3.625E-09
0.3	0.1313	0.1183	0.1892	4.254E-09
0.4	0.1597	0.1014	0.1892	4.730E-09
0.5	0.1804	0.0845	0.1892	5.053E-09
0.6	0.1935	0.0676	0.1892	5.223E-09
0.7	0.1989	0.0507	0.1892	5.240E-09
0.8	0.1966	0.0338	0.1892	5.104E-09
0.9	0.1866	0.0169	0.1892	4.816E-09
1	0.1689	0.0000	0.1892	4.374E-09

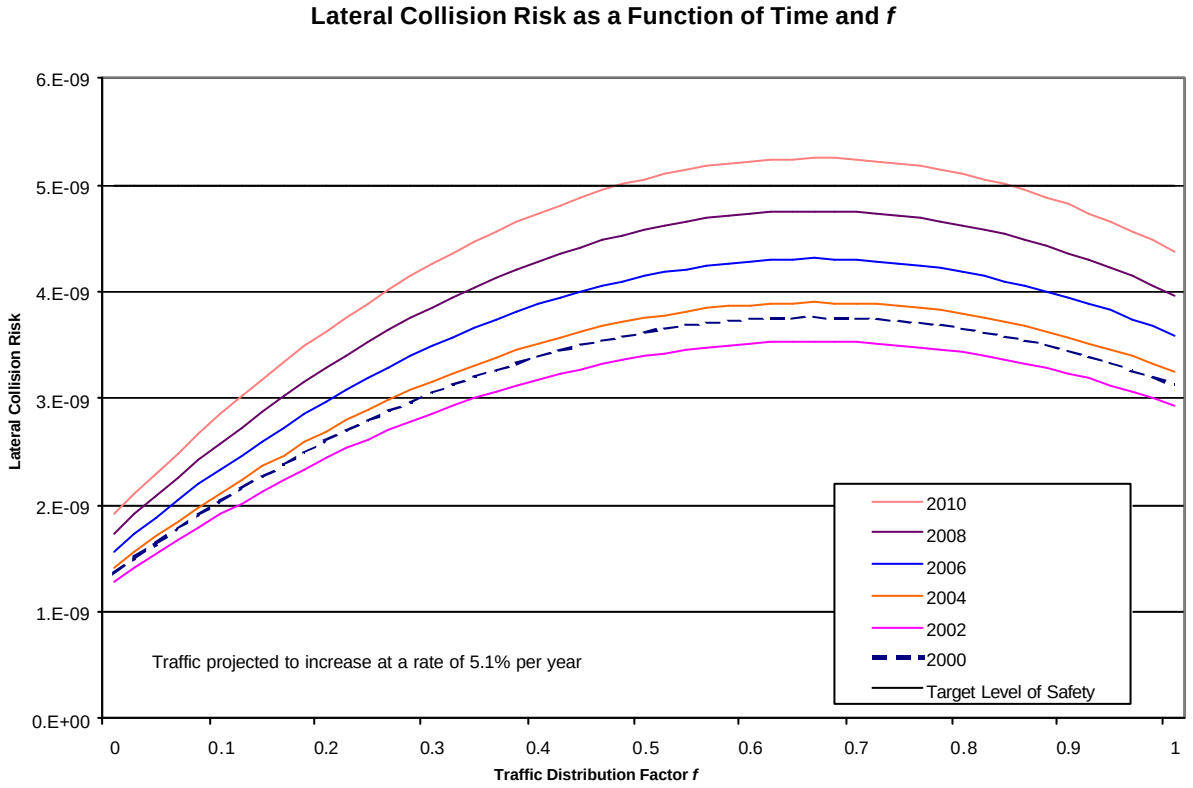

Figure 3-10a. Lateral Collision Risk as a Function Of Time and Traffic Distribution with a 5.1% Growth Rate

Table 3-11b. Lateral Collision Risk Estimates for Proposed Track System Based on Traffic Levels Projected Over a Ten Year Planning Horizon with an 8% Growth Rate

Traffic distribution factor f	Lateral occupancy for UN866 and UN873 & UN873 and UN857 $E_y(same)$	Lateral occupancy for UN866 and UN857 $E_y^{**}(same)$	Lateral occupancy for UN741 and UN866 $E_y^{*}(same)$	Lateral collision risk N_{ay}
0	0.0000	0.2218	0.2484	2.505E-09
0.1	0.0675	0.1996	0.2484	3.732E-09
0.2	0.1250	0.1774	0.2484	4.759E-09
0.3	0.1724	0.1553	0.2484	5.585E-09
0.4	0.2097	0.1331	0.2484	6.209E-09
0.5	0.2369	0.1109	0.2484	6.634E-09
0.6	0.2540	0.0887	0.2484	6.857E-09
0.7	0.2611	0.0665	0.2484	6.879E-09
0.8	0.2581	0.0444	0.2484	6.701E-09
0.9	0.2450	0.0222	0.2484	6.322E-09
1	0.2218	0.0000	0.2484	5.742E-09

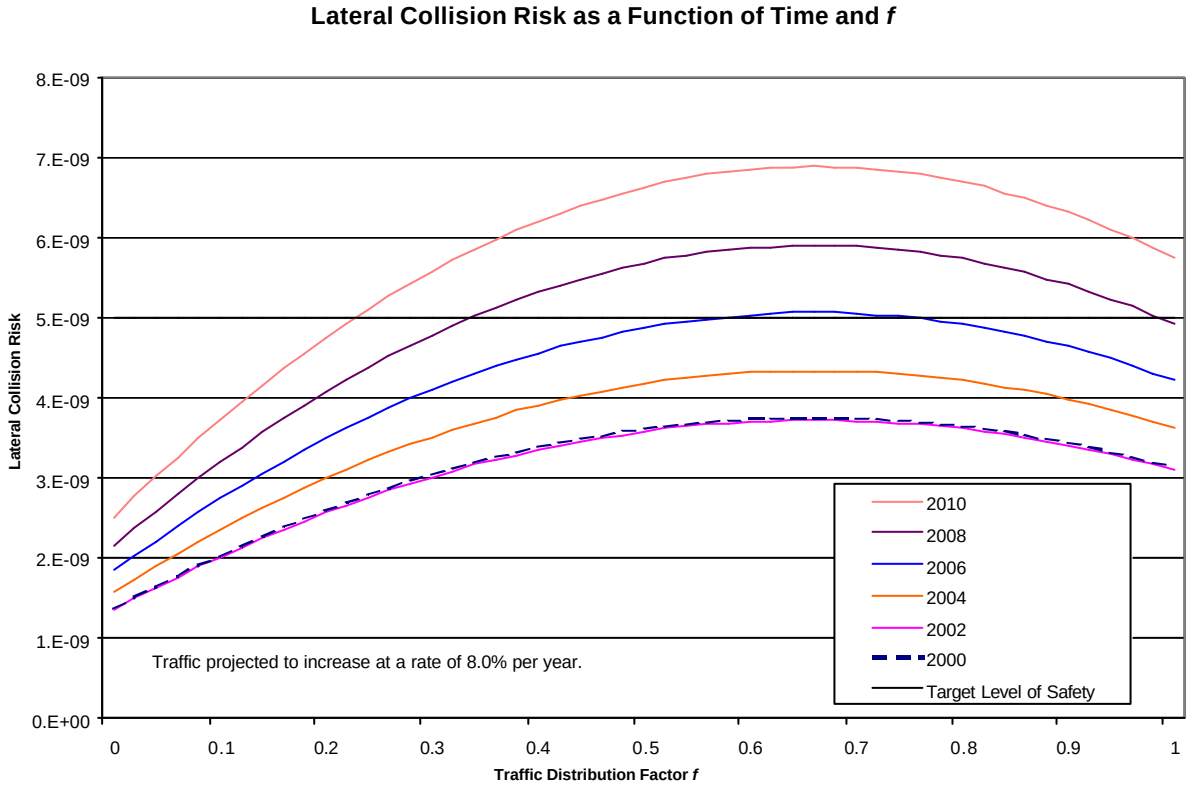

Figure 3-10b. Lateral Collision Risk as a Function of Time and Traffic Distribution with an 8% Growth Rate

In interpreting the above values, it should be kept in mind that several probably conservative assumptions have been made, e.g. concerning the proportion of flights/aircraft, a, having a lateral navigation deviation distribution with scale parameter a_2. The value of the scale parameter itself was shown to have little effect on the estimate of the probability of lateral overlap and hence on the collision risk in Section 3.3. Also, in the absence of data on individual types of large lateral deviations, it was necessary to base the overall distribution of the lateral deviations on the snap shot principle rather than on a weighted errors type of model. The former tends to be conservative as it assumes that each large error persists for the full duration of a flight. By comparison, a waypoint insertion error contributes to the risk only in a band of approximately 10 NM around the adjacent track.

Figures 3.11 and 3.12 show estimates of the lateral collision risk for the current and 2010 projected traffic levels for different values of the relative lateral speed $|\dot{y}|$, from 20 kts to 60 kts. These figures illustrate the sensitivity of the lateral risk to the value of this collision risk model parameter. Lateral speeds less than 60 kts have little impact on meeting the TLS at present (Figure 3.11); but the choice of lateral speed can determine whether or not the TLS will be exceeded in 2010.

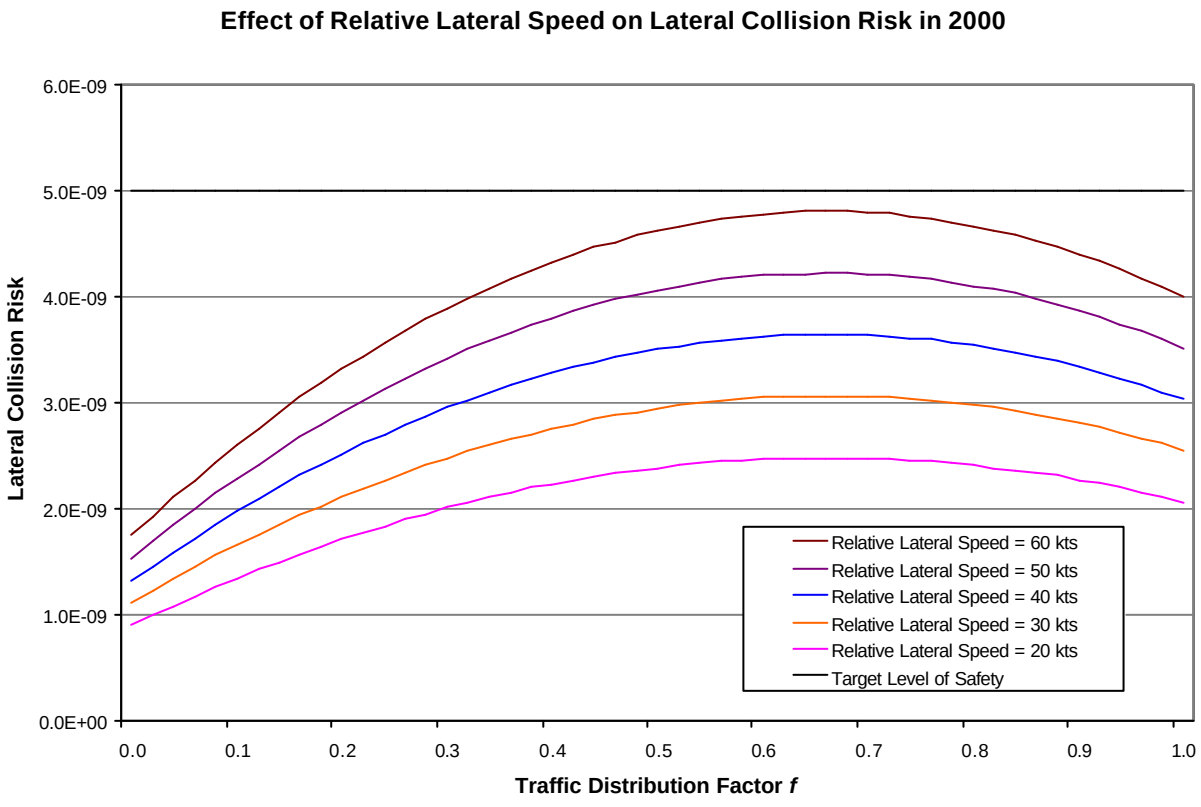

Figure 3-11. Sensitivity of lateral collision risk to relative lateral speed in 2000

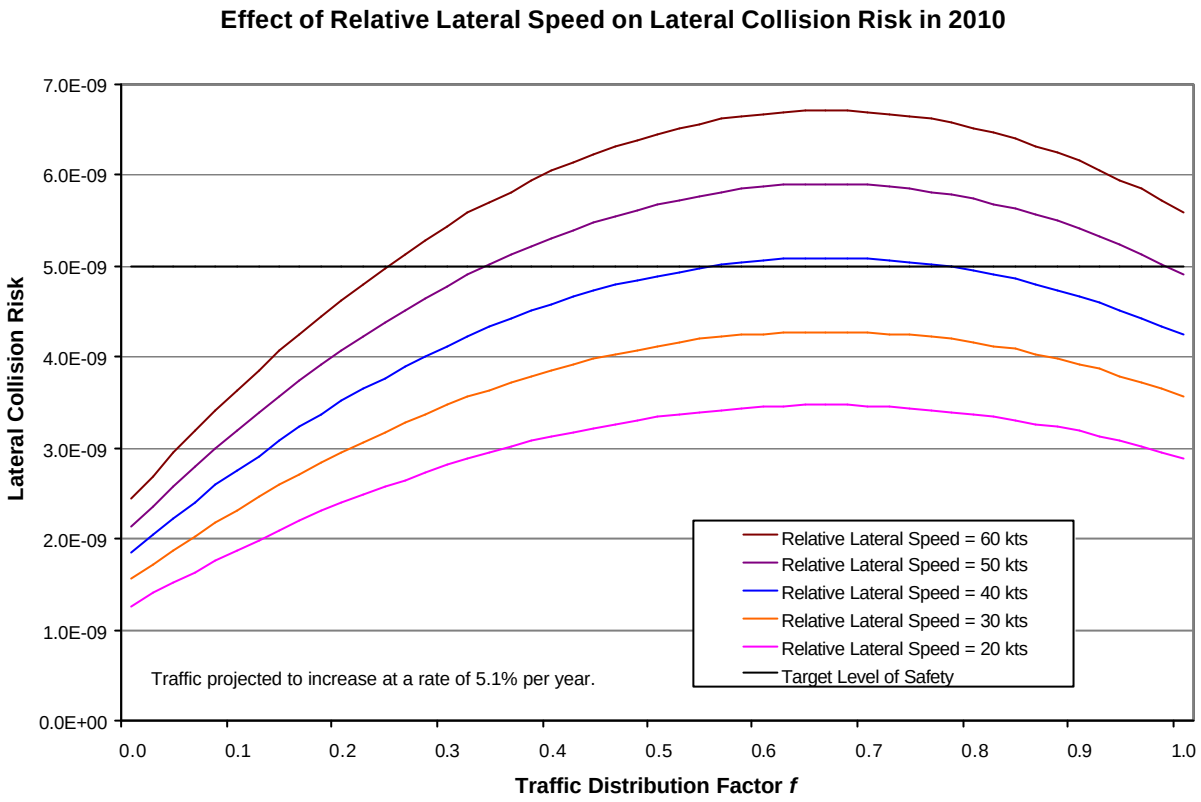

Figure 3-12. Sensitivity of Lateral Collision Risk to Relative Lateral Speed in 2010 Assuming a 5.1% Growth Rate

INCRUSTARINCRUSTARINCRUSTARINCRUSTAR**REFESTILOSECARÁBIGO**

4 Assessment of Technical Vertical Collision Risk

4.1 Introduction

The vertical collision risk assessment has to take into account two basic factors, namely different traffic components and different causes of height deviations. This section deals with the assessment of the technical vertical risk only. It takes into account the basic height-keeping performance of aircraft and the possible impact of meteorological conditions thereon and applies to aircraft in straight and level flight. The risk due to possible other causes such as ATC-loop errors or emergencies will be dealt with in Section 5 of this report.

Guidance material relating to vertical separation is contained in the *Manual on Implementation of a 300 m (1000 ft) Vertical Separation Minimum between FL 290 and FL 410 inclusive* (Ref. 22). In line with this guidance material and *ICAO Annex 11*, a safety assessment based on collision risk modeling is a part of the implementation process of RVSM in the SAT (Refs. 2, 7). Vertical collision risk, i.e. the risk due to the loss of vertical separation between aircraft on adjacent flight levels is generally made up of three traffic components, namely same direction traffic, opposite direction traffic and crossing traffic. As was mentioned in Section 2.1, there is some traffic crossing the EUR/SAM Corridor on the UR976/UA602 in the SAL UIR, some on routes to Johannesburg and to Cape Town in the Dakar UIR, , and some military crossing traffic in the Recife FIR. The total amount of crossing traffic is estimated at between 15% and 17% of the daily traffic, i.e., 9 to 10 crossing flights per day versus 60 flights in the Corridor. Crossing traffic is discussed further in this section and in Appendix C.

Vertical collision risk models for same and opposite direction traffic exist similar to those for lateral risk presented in Section 3.2. These models have also been extended to include crossing routes, see e.g. References 21 and 23. They apply to aircraft in straight and level flight. Recall from Section 2.1 that this condition can be assumed to be satisfied for the assessment of technical vertical risk. (As will be seen in Section 5, however, some operational causes of height deviations may lead to an aircraft climbing or descending through other flight levels, requiring a different type of modeling.) Section 4.2 presents the type of vertical collision risk model to be used for the technical safety assessment of RVSM in the SAT. Details of the estimation of the parameters of this model follow in Sections 4.3 to 4.7. Emphasis is on the estimation of the probability of vertical overlap and vertical occupancy. As expected, the values of some of the parameters of the vertical and lateral models are the same, such as the aircraft dimensions and the average aircraft speed. A summary of the different model parameter estimates is given in Section 4.8 and estimates of technical vertical collision risk under RVSM are presented in Section 4.9. Like the lateral risk estimates of Section 3.9, these will be based on current traffic levels and traffic levels projected forward to the year 2010.

4.2 Collision Risk Model for Technical Vertical Risk

Reference 21 gives the following model for the vertical collision risk between aircraft on adjacent flight levels of the same track, flying in either the same or the opposite direction:

$$N_{az} = P_z(S_z)P_y(0)\frac{l_x}{\tilde{S}_x}\left[E_z(same)\left\{\frac{\overline{|\Delta V|}}{2l_x}+\frac{\overline{|\dot{y}|}}{2l_y}+\frac{\overline{|\dot{z}|}}{2l_z}\right\}+E_z(opp)\left\{\frac{2\overline{|V|}}{2l_x}+\frac{\overline{|\dot{y}|}}{2l_y}+\frac{\overline{|\dot{z}|}}{2l_z}\right\}\right] \quad (4.1)$$

The various parameters are defined in Table 4.1. $E_z(same)$ and $E_z(opp)$ are referred to as same and opposite direction vertical occupancy. Again, one collision between two aircraft is counted as two aircraft accidents and the pertinent factor of two has been included in the occupancy parameters. The same type of model has been used for the technical vertical risk assessment in the NAT (Ref. 24, 25). It was also used for the same and opposite direction vertical risk components of the Australian RVSM safety assessment (Ref. 23).

Table 4-1. Definition of Parameters of the Vertical Collision Risk Model of Equation (4.1)

Parameter	Description
N_{az}	The expected number of accidents per flight hour due to the loss of vertical separation
S_z	The vertical separation minimum
$P_z(S_z)$	The probability of vertical overlap of aircraft nominally flying on adjacent flight levels of the same track
$P_y(0)$	The probability of lateral overlap of aircraft nominally flying at the same track
l_x	The average length of an aircraft
l_y	The average width of an aircraft
l_z	The average height of an aircraft
$\tilde{S}_x$	A parameter used in the calculation of E_z values
$E_z(same)$	The average number of same direction aircraft flying on adjacent flight levels of the same track within segments of length $2\tilde{S}_x$ centered on the typical aircraft
$E_z(opp)$	The average number of opposite direction aircraft flying on adjacent flight levels of the same track within segments of length $2\tilde{S}_x$ centered on the typical aircraft
$\overline{\lvert\Delta V\rvert}$	The average relative along-track speed of two aircraft flying at the same track in the same direction
$\overline{\lvert V\rvert}$	The average ground speed of an aircraft
$\overline{\lvert\dot{y}\rvert}$	The average relative cross-track speed of aircraft flying at the same track
$\overline{\lvert\dot{z}\rvert}$	The average relative vertical speed between aircraft which have lost S_z ft of separation

As can be seen from equation (4.1), the elements of the collision risk model for same and opposite direction traffic are the probabilities of overlap and the average duration of overlaps in the different co-ordinate directions. In the model for same and opposite direction traffic, overlap of two aircraft is defined as overlap of rectangular boxes enveloping the aircraft. It is also assumed that during a situation of overlap, the sides of the boxes remain parallel. This facilitates an easy computation of the average duration of an overlap in each dimension. Similar elements play a part in a model of vertical collision risk on crossing routes, but in a somewhat more complicated way. The geometry of a pair of crossing routes, intersecting at an arbitrary angle, has an effect on the computation of both the probability of overlap and the average duration of an overlap, i.e. the longitudinal and lateral dimensions get coupled into a horizontal dimension.

Firstly, due to the geometry of a crossing, the sides of the rectangular boxes enveloping the aircraft will not be parallel during a situation of horizontal overlap. As a result, the computation of the average duration of an overlap becomes rather complicated. This problem has been addressed by modeling the aircraft by (standing) cylinders and calculating the average duration of a horizontal overlap from the overlap of the circular cross sections of the cylinders, see Reference 21. The diameter of the cylinders is taken as the larger of the length and the width of the aircraft. The calculation uses the average relative speed between the aircraft on the crossing routes, which depends on the average aircraft speeds and the crossing angle.

To be consistent between the crossing and same/opposite direction cases, the aircraft should then also be represented by cylinders for the same and opposite direction cases. (Then the aircraft might also be represented by cylinders in the lateral collision risk model.)

Secondly, for a pair of crossing routes, the probability of horizontal overlap cannot be factored into the probabilities of overlap in the longitudinal and lateral directions. As the occurrence of an actual horizontal overlap between two aircraft on crossing routes is a very rare event this has an impact on the way this probability is to be estimated.

The vertical collision risk model for crossing routes developed by RGCSP on the basis of the cylindrical aircraft model can be expressed as (Ref. 21)

$$N_{az} = P_z(S_z)\frac{l_{xy}}{S_{xy}}E_z(q)\left\{\frac{V_{rel}(q)}{\frac{p}{2}\,l_{xy}} + \frac{|\dot{z}|}{2l_z}\right\} \tag{4.2}$$

where the relative velocity $V_{rel}(q)$ is given by

$$V_{rel}(q) = |V|\sqrt{2(1-\cos q)} \tag{4.3}$$

and Table 4.2 defines the new parameters. Note that the lateral overlap probability does not appear explicitly anymore, as it is incorporated into $E_z(q)$, the crossing track vertical occupancy (as a function of the crossing angle q). See Section 4.4 for more details of this parameter. The expression for the relative speed assumes the same average speed for both the aircraft. The

reciprocal of the first term inside the brackets of equation (4.2) is the average duration of a horizontal overlap of two circles with diameter l_{xy}.

Table 4-2. Definition of Additional Parameters of the Vertical Collision Risk Model of Equation (4.2) For Crossing Routes

Parameter	Description
q	The angle between two crossing routes, i.e. the angle between the aircraft headings
l_{xy}	The average diameter of a cylinder representing an aircraft
$\tilde{S}_{xy}$	A parameter used in the calculation of $E_z(q)$ values
$E_z(q)$	Twice the probability of horizontal overlap of circles representing horizontal cross sections of aircraft on crossing routes.
$V_{rel}(q)$	The average relative speed between aircraft flying on crossing routes

When there are several pairs of crossing routes with different crossing angles $q_i, i=1,...,n$, say, the model equation (4.2) can be applied to each pair of routes and combined subsequently to give

$$N_{az} = P_z(S_z)\frac{l_{xy}}{\tilde{S}_{xy}}\sum_{i=1}^{n} E_z(q_i)\left\{\frac{V_{rel}(q_i)}{\frac{p}{2} l_{xy}} + \frac{|\dot{z}|}{2 l_z}\right\} \qquad (4.4)$$

It is worth noting that a similar type of model is being used for the safety assessment of RVSM in European airspace (Ref. 26). Because of the large number of different crossing angles in the European route network and an increasing number of direct routings, radar data is being used to identify the geometry and relative velocity for all individual pairs of aircraft. This leads, in turn, to a model of the type of equation (4.4) with the summation extending over all the aircraft pairs.

When the number of crossing angles is relatively large, it may be desirable to approximate equation (4.4) by the model of equation (4.2) by taking conservative estimates of $E_z(q_i)$ and $V_{rel}(q_i)$, valid for each value of $i, i=1,...,n$. This approach was followed in Reference 23.

See also References 27 and 28 for additional details of modeling the vertical collision risk on intersecting oceanic routes.

The vertical collision risk model for crossing tracks equation (4.4) can be combined with the model equation (4.1) to give the complete technical vertical risk model for the RVSM safety assessment for the EUR/SAM Corridor in the SAT, i.e.,

$$N_{az} = P_z(S_z)P_y(0)\frac{l_x}{\tilde{S}_x}\left[E_z(same)\left\{\frac{\overline{|\Delta V|}}{2l_x}+\frac{\overline{|\dot{y}|}}{2l_y}+\frac{\overline{|\dot{z}|}}{2l_z}\right\}+E_z(opp)\left\{\frac{2\overline{|V|}}{2l_x}+\frac{\overline{|\dot{y}|}}{2l_y}+\frac{\overline{|\dot{z}|}}{2l_z}\right\}\right]+$$
$$P_z(S_z)\frac{l_{xy}}{\tilde{S}_{xy}}\sum_{i=1}^{n}E_z(q_i)\left\{\frac{V_{rel}(q_i)}{\frac{p}{2}l_{xy}}+\frac{\overline{|\dot{z}|}}{2l_z}\right\} \qquad (4.5)$$

Note that the original rectangular box dimensions l_x and l_y have been retained for the same and opposite direction components of the model of equation (4.5).

As mentioned in Sections 2.1 and 4.1, there are only four locations where aircraft are crossing the EUR/SAM traffic flow, namely on the route UR976/UA602 in the SAL UIR and on the routes to Johannesburg, Asuncion and Cape Town. Hence, $n = 4$ in equation (4.5) provided that all the tracks crossed at each individual location are taken into account in the estimation of the pertinent crossing track vertical occupancy.

Equation (4.5) may be simplified slightly as follows. The crossing angles for the different crossing routes are approximately 89°, 85°, 85°, and 77°, respectively. These angles may well be approximated by 90° angles, thereby reducing equation (4.5) to

$$N_{az} = P_z(S_z)P_y(0)\frac{l_x}{\tilde{S}_x}\left[E_z(same)\left\{\frac{\overline{|\Delta V|}}{2l_x}+\frac{\overline{|\dot{y}|}}{2l_y}+\frac{\overline{|\dot{z}|}}{2l_z}\right\}+E_z(opp)\left\{\frac{2\overline{|V|}}{2l_x}+\frac{\overline{|\dot{y}|}}{2l_y}+\frac{\overline{|\dot{z}|}}{2l_z}\right\}\right]+$$
$$P_z(S_z)\frac{l_{xy}}{\tilde{S}_{xy}}E_z(90)\times\left\{\frac{\overline{|V|}\sqrt{2}}{\frac{p}{2}l_{xy}}+\frac{\overline{|\dot{z}|}}{2l_z}\right\} \qquad (4.6)$$

where $E_z(90)$ is the crossing track vertical occupancy for a 90° crossing angle for **all** of the four locations where traffic crosses the main traffic flow. Details of the estimation of the different occupancy parameters are given in Section 4.4.

For a 90° crossing angle, it also makes sense again to represent the aircraft by rectangular boxes and to assume that the sides of the boxes remain parallel during a situation of horizontal overlap. The duration of an overlap in each of the two dimensions involved is given by

$$t_{90} = 2\times\frac{\frac{l_x}{2}+\frac{l_y}{2}}{\overline{|V|}} \qquad (4.7)$$

or

$$t_{90} = \frac{l_x + l_y}{\overline{|V|}} \tag{4.8}$$

Substitution of its reciprocal into a model for 90° crossing tracks based on rectangular boxes, similar to the models for same and opposite direction traffic gives

$$N_{az} = P_z(S_z)\frac{l_{xy}}{\tilde{S}_{xy}} E_z(90)_{rect}\left\{\frac{\overline{|V|}}{l_x + l_y} + \frac{\overline{|V|}}{l_x + l_y} + \frac{\overline{|\dot{z}|}}{2\,l_z}\right\} \tag{4.9}$$

where the symbol $E_z(90)_{rect}$ formally denotes 90° crossing track vertical occupancy based on rectangular boxes. Equation (4.9) can be combined with the model equation (4.1) for same and opposite direction vertical collision risk to the following complete model:

$$N_{az} = P_z(S_z)P_y(0)\frac{l_x}{\tilde{S}_x}\left[E_z(same)\left\{\frac{\overline{|\Delta V|}}{2\,l_x} + \frac{\overline{|\dot{y}|}}{2\,l_y} + \frac{\overline{|\dot{z}|}}{2\,l_z}\right\} + E_z(opp)\left\{\frac{2\overline{|V|}}{2\,l_x} + \frac{\overline{|\dot{y}|}}{2\,l_y} + \frac{\overline{|\dot{z}|}}{2\,l_z}\right\}\right] +$$
$$P_z(S_z)\frac{l_{xy}}{\tilde{S}_{xy}} E_z(90)_{rect}\left\{\frac{\overline{|V|}}{l_x + l_y} + \frac{\overline{|V|}}{l_x + l_y} + \frac{\overline{|\dot{z}|}}{2\,l_z}\right\} \tag{4.10}$$

When the aircraft dimensions from Table 3.7 are used, the coefficients of $\overline{|V|}$ in the crossing track components of the vertical collision risk models of equations (4.6) and (4.10) are found to be 28.325 and 32.96, respectively. This suggests that the rectangular box model might be slightly more conservative for a 90° crossing angle.

4.3 The Probability of Vertical Overlap

4.3.1 Approach

The probability of vertical overlap of a pair of aircraft nominally flying at adjacent flight levels separated by S_z is denoted by $P_z(S_z)$. It is defined by

$$P_z(S_z) = \int_{-l_z}^{l_z} f^{z_{12}}(z)dz \tag{4.11}$$

where $f^{z_{12}}(z)$ denotes the probability density of the vertical distance z_{12} between the two aircraft. This distance may be defined as

$$z_{12} = S_z + z_1 - z_2 \tag{4.12}$$

with z_1 and z_2 representing the height-keeping deviations of two aircraft. Height-keeping deviations of aircraft are usually defined in terms of Total Vertical Error (TVE) where

$$TVE = actual\ pressure altitude\ flown by\ an\ aircraft - assigned altitude \tag{4.13}$$

(measured in geometric feet). Notice that when vertical separation has been established correctly, i.e. assigned by ATC as S_z and adhered to by the aircraft, equation (4.12) gives the correct expression for the vertical distance in the sense that the nominal value of z_{12} will be S_z. When vertical separation has not been established correctly, the nominal value of z_{12} will normally not be equal to S_z (cf. Section 5.2).

Assuming that the height-keeping deviations of the two aircraft are independent and denoting their probability densities by $f_1^{TVE}(z_1)$ and $f_2^{TVE}(z_2)$, the probability density $f^{z_{12}}(z)$ and the probability of vertical overlap can be written as

$$f^{z_{12}}(z) = \int_{-\infty}^{\infty} f_1^{TVE}(z_1) f_2^{TVE}(S_z + z_1 - z)dz_1 . \tag{4.14}$$

and

$$P_z(S_z) = \int_{-l_z}^{lz} \int_{-\infty}^{\infty} f_1^{TVE}(z_1) f_2^{TVE}(S_z + z_1 - z)dz_1 dz . \tag{4.15}$$

In practice, $P_z(S_z)$ may be able to be approximated by

$$P_z(S_z) \approx 2 l_z \int_{-\infty}^{\infty} f_1^{TVE}(z_1) f_2^{TVE}(S_z + z_1) dz_1 \ . \tag{4.16}$$

or

$$P_z(S_z) \approx 2 l_z f^{z_{12}}(0) \tag{4.17}$$

Thus, to calculate the probability of vertical overlap, the probability density $f^{TVE}(z)$ of the aircraft height-keeping deviations is needed.

The probability distribution of the height-keeping deviations depends first of all on the height-keeping characteristics of the aircraft as specified by the MASPS. Data on the height-keeping performance of MASPS-approved aircraft can be obtained by means of aircraft height monitoring as set out in Reference 22. Currently, height monitoring data are not yet available from the South Atlantic Monitoring Agency (SATMA). However, as the majority of the aircraft types and operators in the EUR/SAM Corridor are also flying in the (planned) European (RVSM) airspace, monitoring data from the European RVSM height monitoring program was initially used. As there is a close co-ordination between the European Monitoring Agency (EMA) and the CMA for the NAT, height-monitoring data from the NAT was also incorporated where appropriate. In addition to the normal height deviations of MASPS approved aircraft, large height deviations may occasionally occur due to adverse meteorological conditions (Refs. 22, 24). Such conditions may cause turbulence and (relatively) large height oscillations of the aircraft. Following the approach used in the NAT (Ref. 24), the latter height deviations will be included in the distribution of technical height-keeping deviations although it might be argued that they should rather be included in the operational vertical risk due to all causes. (See Section 5 for possible other, non-technical, causes of large height deviations.)

The approach that has been followed in the NAT and in Europe is based on the available height monitoring data and consists of separately modeling the two components of TVE, Altimetry System error (ASE) and Flight Technical Error (FTE). The large height deviations due to turbulence are included in the distribution of FTE. The probability distribution or density $f^{TVE}(z)$ can then be obtained as follows. Let

$$TVE = ASE + FTE \tag{4.18}$$

where

$$ASE = actual\ pressure altitude\ flown by\ an\ aircraft - displayed altitude \tag{4.19}$$

$$FTE = displayed altitude - assigned altitude \tag{4.20}$$

and assume that the two components are statistically independent. The probability density of TVE follows from

$$f^{TVE}(z) = \int_{-\infty}^{\infty} f^{ASE}(a) f^{FTE}(z-a) da \tag{4.21}$$

In practice, FTE is difficult to determine and is approximated by Assigned Altitude Deviation (AAD),

$$AAD = transponded\ altitude - assigned altitude \tag{4.22}$$

and equation (4.21) is approximated by

$$f^{TVE}(z) = \int_{-\infty}^{\infty} f^{ASE}(a) f^{AAD}(z-a) da \tag{4.23}$$

The difference between FTE and AAD is referred to as correspondence error. Data on AAD can be obtained by evaluating archived mode C data.

The same approach was followed for the assessment of the technical vertical collision risk associated with RVSM in the SAT. The modeling of the two component densities is described below.

4.3.2 ASE Distribution Modeling

Analogous to the approaches followed in the NAT and in Europe, an overall distribution of ASE is formed as a mixture of ASE distributions by aircraft type, i.e.

$$f^{ASE}(a) = \sum_{i=1}^{n_{tg}} b_i f_i^{ASE}(a) \tag{4.24}$$

where n_{tg} denotes the number of different aircraft type groups, b_i is the proportion of flight time contributed by aircraft type group i and $f_i^{ASE}(a)$ is the probability density of the ASE of aircraft type group $i, i = 1,...,n_{tg}$ (Refs. 24, 26).

The probability densities $f_i^{ASE}(a)$, $i = 1,...,n_{tg}$, are to be determined on the basis of height monitoring data of MASPS approved aircraft. As was mentioned before, such monitoring data are not yet available from the SATMA. Table 4.3 gives preliminary results on the type of probability densities and associated parameter values for the aircraft types operating in the SAT and included in Table 2.6, based on data from the European and NAT height monitoring programs (Ref. 29). Note that there are three aircraft types that are not MASPS-approved, namely the B703, IL76 and LJ55. A service bulletin is under development for the Embraer 145 (E145). Therefore, and because of their very small contribution to the total flight time, these four

aircraft types have not been included in the evaluation of the ASE probability density of a MASPS approved aircraft fleet for the SAT by means of equation (4.24). (The proportions of flight time from the second column of Table 4.3 have been re-normalized to ensure that the weighting factors b_i add up to one.) At this stage, it has been assumed that the above aircraft population will be representative of the MASPS approved aircraft population wanting to be flying in RVSM airspace in the SAT. The remaining 55 aircraft types were not included in Table 2.6 (and Table 4.3) because of their rare occurrence. They comprise a mixture of aircraft types, for which service bulletins do and do not exist.

Figures 4.1 and 4.2 show the resulting overall ASE density $f^{ASE}(a)$ for the SAT plotted against a linear and logarithmic scale respectively. The latter diagram gives a better indication of the tail of the ASE distribution. It should be emphasized that this density is only valid for the aircraft population in the SAT on the assumption that all individual aircraft are MASPS approved.

Table 4-3. Proportion of Flight Time and Preliminary Characteristics of ASE per Aircraft Type Group Operating in the SAT

Aircraft type	Proportion of flight time	Source of height monitoring data	Type of probability density	Probability density parameters	
				Mean	Standard deviation
B763	0.1764	NAT	DE	-31.89	45.05
MD11	0.1751	NAT	G	1.05	37.4
A340	0.1619	NAT	DE	8.78	42.06
B744	0.1200	NAT	DE	-23.24	46.25
B742	0.0648	NAT	DE	-12.72	58.84
A310	0.0526	NAT	G	-16.01	45.52
B772	0.0501	NAT	DE	45.07	43.87
B762	0.0458	NAT	DE	-4.04	47.83
B752	0.0438	NAT	DE	4.18	40.79
A330	0.0227	NAT	G	41.88	36.34
B747	0.0194	NAT	DE	-12.72	58.84
DC10	0.0185	NAT	DE	14.32	66.55
A320	0.0088	NAT	G	52.92	47.91
B767	0.0061	NAT	DE	-4.04	47.83
F900	0.0038	NAT	G	28.81	53.89
E145*	0.0023				
CL60	0.0023	NAT	DE	4.14	47.23
B733	0.0017	NAT	DE	-9.49	41.75
B741	0.0016	NAT	DE	-12.72	58.84
GLF4	0.0015	NAT	DE	-17.64	49.08
B703**	0.0014	NAT	DE	47.66	71.58
IL76**	0.0014				
MD80	0.0014	NAT	G	29.14	41.55
A124	0.0013	NAT	G	107.5	81.67
FA50	0.0013	NAT	DE	32.54	59.18
L101	0.0013	NAT	DE	20.42	57.96
B743	0.0012	NAT	DE	-12.72	58.84
H25B	0.0012	NAT	G	-5.34	60.08
B777	0.0011	NAT	DE	45.07	43.87
LJ55**	0.0007	NAT	DE	43.98	91.61

* Service bulletin under development
** Non-MASPS approved aircraft type

The mean of the ASE density $f^{ASE}(a)$ is given by

$$m\{ASE\} = \sum_{i=1}^{n_{tg}} b_i m_i \tag{4.25}$$

where m_i denotes the ASE mean of the *i*-th aircraft type as shown in Table 4.3. The standard deviation of the aggregate ASE density $f^{ASE}(a)$ follows from

$$s^2\{ASE\} = \sum_{i=1}^{n_{tg}} b_i s_i^2 + \sum_{i=1}^{n_{tg}} b_i m_i^2 - \left(m\{ASE\}\right)^2 \tag{4.26}$$

where s_i denotes the ASE standard deviation of type *i* as shown in Table 4.3. Thus, the mean and standard deviation of the overall ASE density $f^{ASE}(a)$ are - 4.38 ft and 44.14 ft respectively.

It might be of interest to examine the probability of vertical overlap between a MASPS approved aircraft and a non-MASPS approved aircraft on the assumption that for some reason some non-approved aircraft would show up in the SAT RVSM airspace. In that case, an ASE density (and an AAD density) representing non-MASPS approved aircraft height-keeping performance is needed. As this situation can be considered an operational error it could be dealt with in future iterations of the vertical collision risk model.

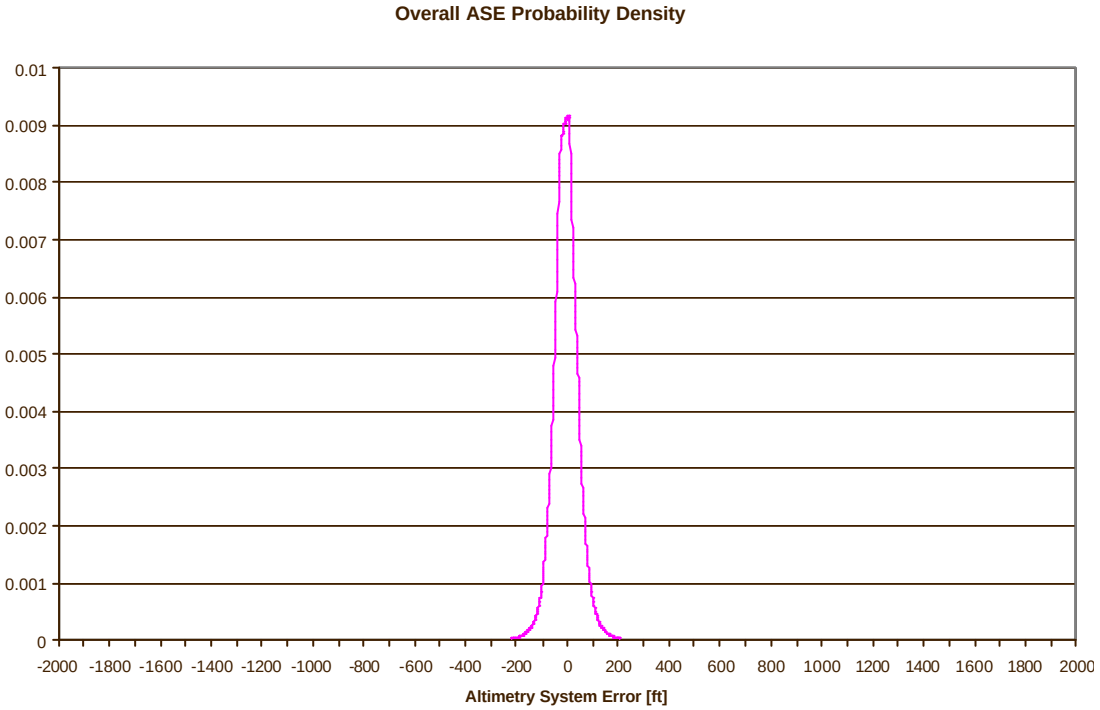

Figure 4-1. Overall ASE Density $f^{ASE}(a)$ for the MASPS Approved Aircraft Population in the SAT

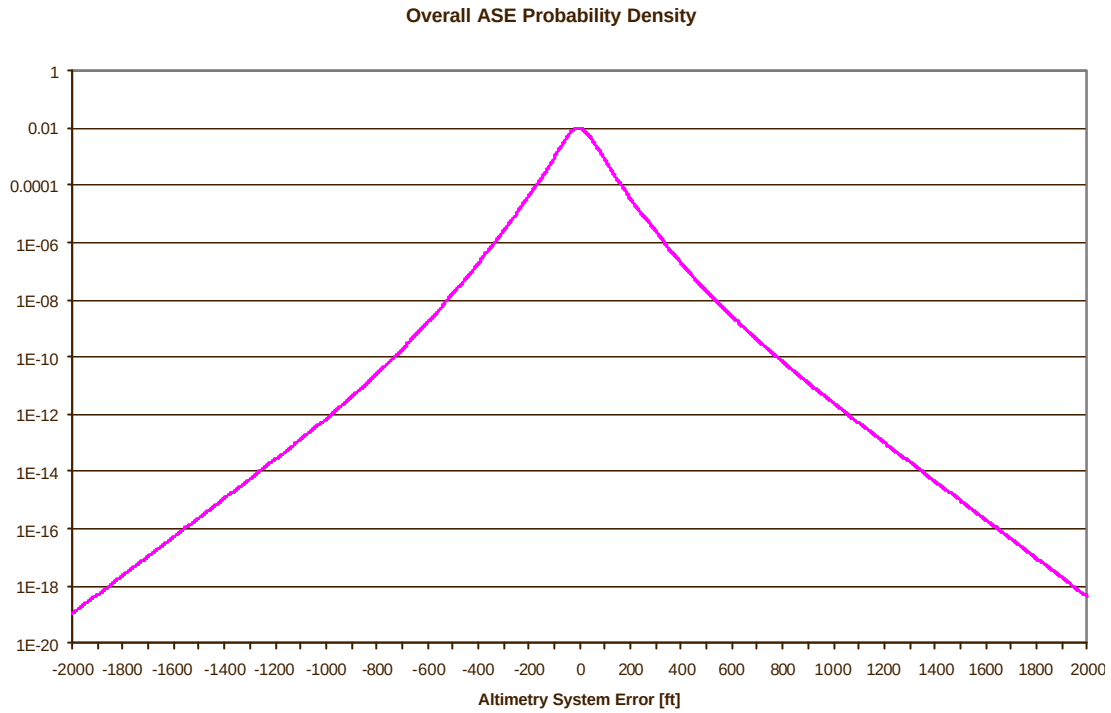

Figure 4-2. Overall ASE Density $f^{ASE}(a)$ for the MASPS Approved Aircraft Population in the SAT, Logarithmic Scale

4.3.3 AAD Distribution Modeling

AAD performance is subdivided into typical performance and atypical performance. For the assessment of technical vertical risk, atypical performance was used to model large AADs due to turbulence only. AAD data on typical performance should be obtained from the height monitoring process as a part of the RVSM implementation program. AAD data on atypical performance should also be obtained from incident reports collected by the SATMA. The data is to be used to estimate the parameters of a suitable analytical probability density of AAD. In line with the modeling of the AAD component distribution in the NAT and in Europe, and also in conformity with the modeling of the distribution of the lateral navigation deviations set out in Section 3.3, a composite model made up of two components is used (Refs. 24-26):

$$f^{AAD}(a) = (1-a) \times f_{typ}^{AAD}(a) + a \times f_{atyp}^{AAD}(a). \tag{4.27}$$

Both the component densities are taken as exponential densities and equation (4.27) becomes

$$f^{AAD}(a) = (1-a) \times \frac{1}{2a_1} \exp - \left| \frac{a}{a_1} \right| + a \times \frac{1}{2a_2} \exp - \left| \frac{a}{a_2} \right| \tag{4.28}$$

Unfortunately, no data on either typical or atypical AAD performance in the SAT are currently available. As a substitute, therefore, use was made of AAD data and models from the NAT. Reference 30 describes the modeling of a set of AAD data from the NAT. The data set consisted of about one million minutes worth of mode C data on typical AAD performance collected for aircraft in level flight above FL290 east of the coast of Canada and within coverage of their surveillance radars. These data were supplemented with data on large atypical assigned altitude deviations from the entire year of 1997 in NAT MNPS airspace. The latter data set included in particular a 1200-ft deviation due to turbulence, which had lasted for several minutes. A DDE model of the form of equation (4.28) was then obtained as the best model of the data. The parameter values of the model are shown in Table 4.4. Note that the data set was also modeled without the 1200ft deviation.

Table 4-4. Parameters of Double Double Exponential AAD Densities for the NAT

Data set	DDE model parameters	Statistics
Canadian mode C and large height deviations	$a_1 = 22.3$ $a_2 = 216.8$ $a = 3.8 \times 10^{-6}$	$s_1 = 31.5$ $s_2 = 306.6$
Canadian mode C and large height deviations after removing one 6-minute 1200ft deviation	$a_1 = 22.3$ $a_2 = 123.9$ $a = 1.1 \times 10^{-5}$	$s_1 = 31.5$ $s_2 = 175.2$

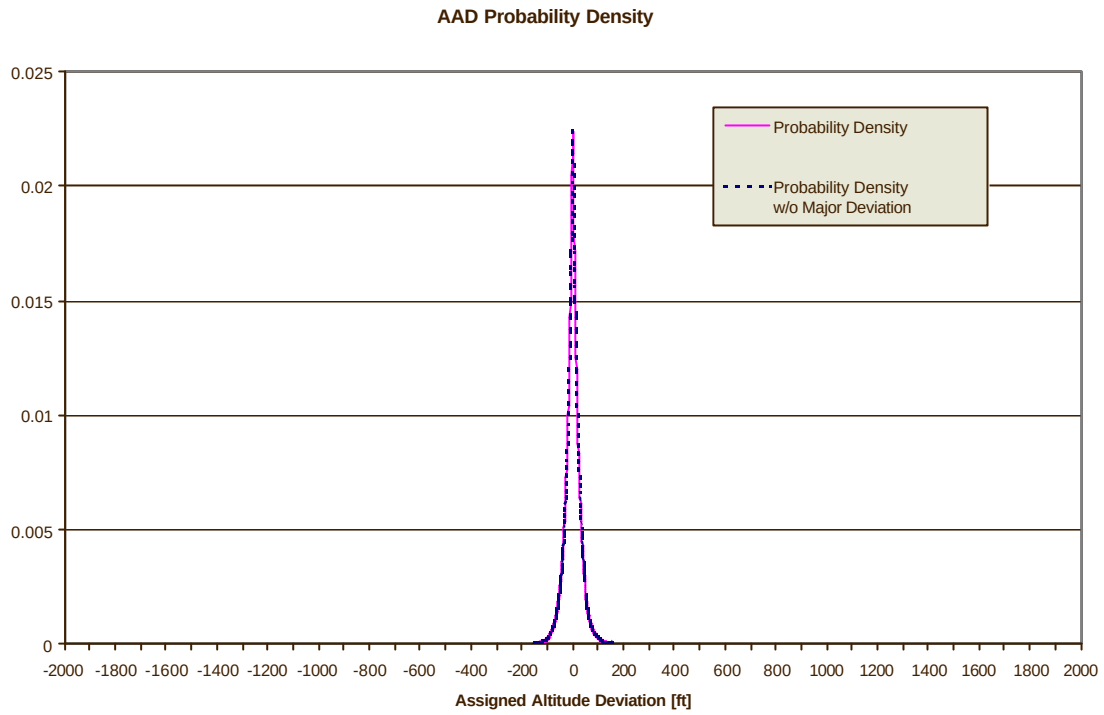

INCRUSTAR

Figure 4-3. Assumed AAD Density $f^{AAD}(a)$ for the Aircraft Population in the SAT

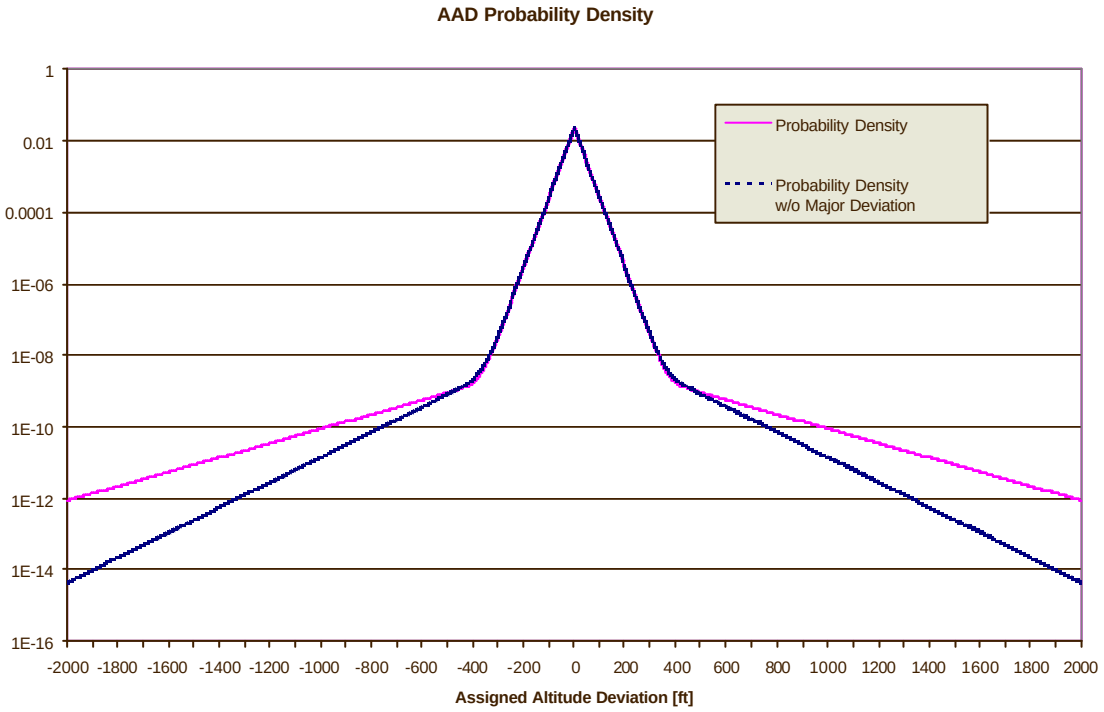

Figure 4-4. Assumed AAD Density $f^{AAD}(a)$ for the Aircraft Population in the SAT, Logarithmic Scale

On the assumption that there is some similarity between the oceanic environments in the NAT and the SAT, the AAD density models specified in Table 4.4 were used in this risk assessment for the SAT. It must be stressed that it is important to verify this assumption on a short-term basis, i.e. prior to the implementation of RVSM by establishing a monitoring program at Canaries and Recife ACCs to capture and document AAD deviations.

Figures 4.3 and 4.4 show the AAD mixture densities, $f^{AAD}(a)$, from Table 4.4 plotted against a linear and logarithmic scale respectively. Again, the latter emphasizes the tail of the AAD distribution. The effect on the tail of the mixture density of the single 6-minute large AAD deviation is clearly visible, approximately from a deviation size of 600 ft onwards.

4.3.4 Resulting TVE Distribution and Probability of Vertical Overlap

Substitution of the ASE and AAD densities of the foregoing two subsections into equation (4.23) yields the TVE density $f^{TVE}(z)$ for the SAT shown in the Figures 4.5 and 4.6. Like Figure 4.4, Figure 4.6 demonstrates the effect of the single 6-minute large AAD deviation on the tail of the TVE density. Due to the smoothing effect of the convolution of the AAD density with the ASE density (cf. equation (4.23)), the effect becomes visible at an altitude deviation size of about 700 ft. This will also be seen to have an impact on meeting the criteria of the global height-keeping performance specification. As argued in Section 4.3.3, it remains to be verified that the assumed AAD densities are representative of the RVSM airspace in the SAT.

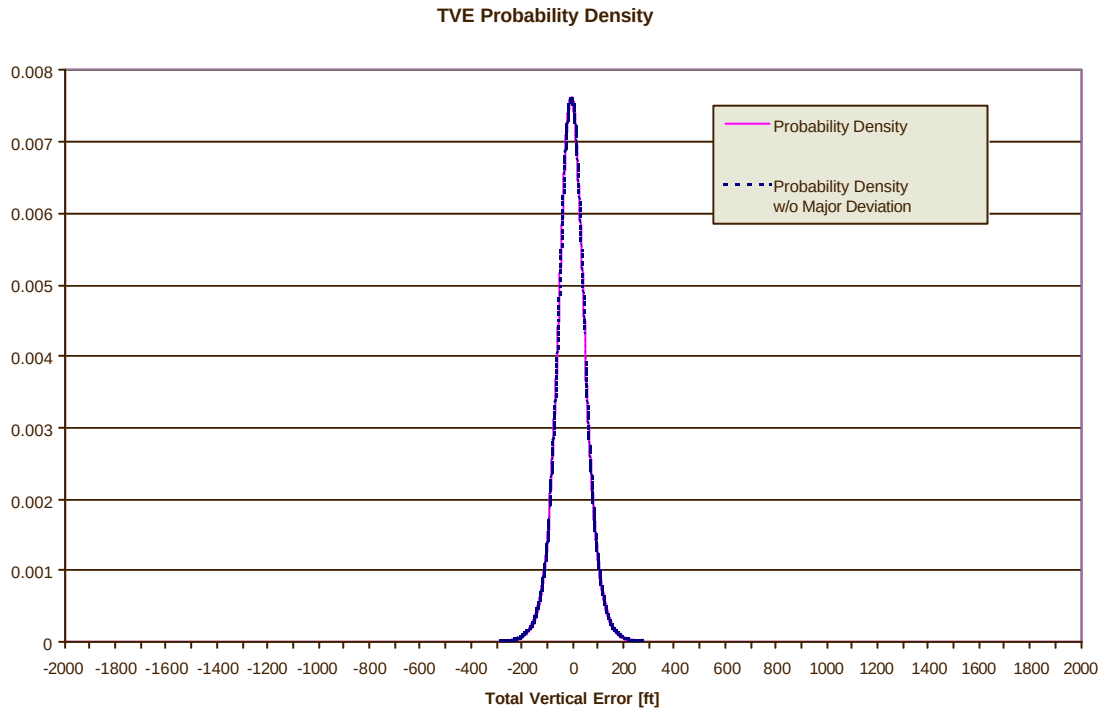

Figure 4-5. TVE Density $f^{TVE}(z)$ for the Aircraft Population in the SAT

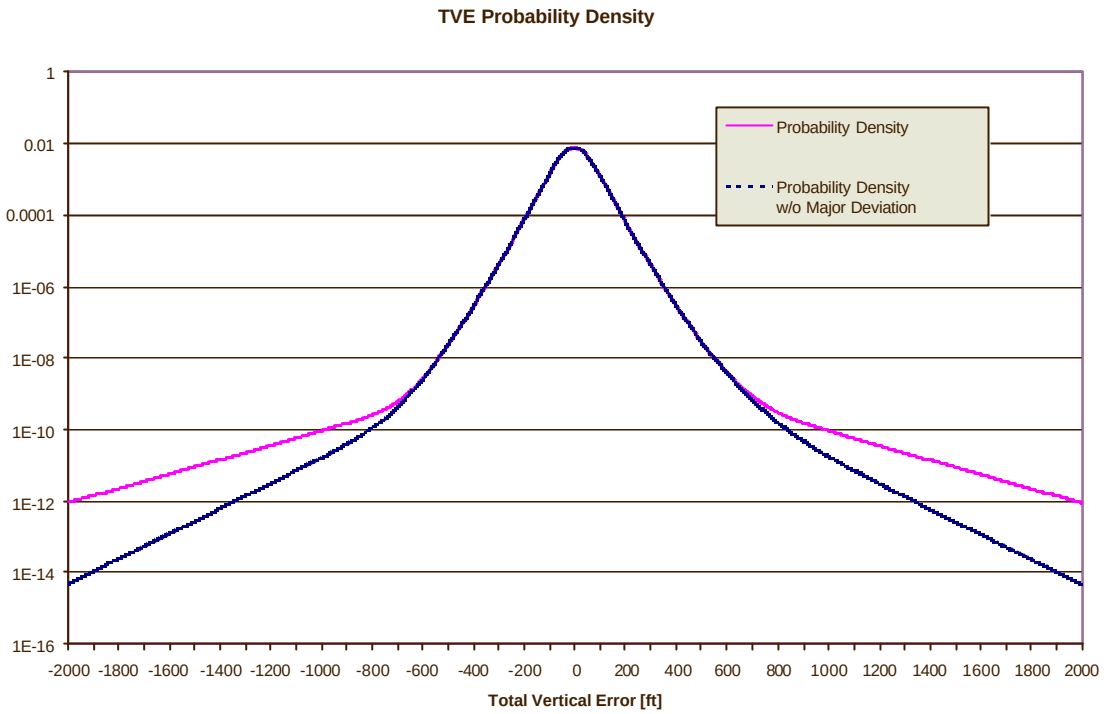

Figure 4-6. TVE Density $f^{TVE}(z)$ for the Aircraft Population in the SAT, Logarithmic Scale

The probability of vertical overlap was calculated by means of equations (4.14) and (4.17) for the two TVE densities of Figure 4.5. The nominal separation between adjacent flight levels, denoted by S_z, is taken as 1000 and 2000 feet. The resulting values are given in Table 4.5.

Table 4-5. Estimates of Probability of Vertical Overlap for the SAT

Data for TVE density model	Probability of vertical overlap $P_z(S_z = 1000\,ft)$	Probability of vertical overlap $P_z(S_z = 2000\,ft)$
ASE combined with Canadian mode C and large height deviations	2.1346E-08	1.6058E-10
ASE combined with Canadian mode C and large height deviations after removing one 6-minute 1200ft deviation	4.5263E-09	9.7130E-13

In addition to the TLS of 2.5×10^{-9} for the technical vertical risk, there are some constraints to be met by the TVE-performance of aircraft (Ref. 22). Firstly, the global system performance specification requires the probability of vertical overlap $P_z(S_z)$ not to exceed a value of 1.7×10^{-8}. Secondly, the global height-keeping performance specification specifies bounds for the proportions of height-keeping deviations larger in magnitude than 300 ft, 500 ft, 650 ft, and between 950 and 1050 ft as follows:

a) The proportion of height-keeping errors beyond 90 m (300 ft) in magnitude is less than 2.0×10^{-3};
b) The proportion of height-keeping errors beyond 150 m (500 ft) in magnitude is less than 3.5×10^{-6};
c) The proportion of height-keeping errors beyond 200 m (650 ft) in magnitude is less than 1.6×10^{-7};
d) The proportion of height-keeping errors between 290 m and 320 m (950 ft and 1050 ft) in magnitude is less than 1.7×10^{-8}.

Meeting the criteria of the global height-keeping performance specification provides additional confidence in the estimate of the probability of vertical overlap $P_z(S_z)$. The various quantities have been calculated for the probability density $f^{TVE}(z)$ of TVE above and are shown in Table 4.6. The difference between the two AAD densities and hence that between the two TVE densities is reflected in the estimates of the proportions of TVE values larger than 650 and between 950 and 1050 ft in magnitude. Without the major deviation, three out of the four criteria are well met, with the remaining one being slightly exceeded. By comparing Figures 4.2 and 4.4, it can be seen that the frequency of large AAD values, either with or not with the inclusion of the major deviation, is the driving force behind the tails of the TVE density. These values should be monitored periodically to ensure that the criteria of the global height-keeping performance specification are not exceeded.

Table 4-6. Estimates of Proportions of Height-Keeping Errors

Quantity	Estimate	Estimate w/o Major Deviation	Upper Bound
$Prob\{\|TVE\| \geq 300\}$	2.9880E-04	2.9888E-04	2.0×10^{-3}
$Prob\{\|TVE\| \geq 500\}$	2.6066E-06	2.4298E-06	3.5×10^{-6}
$Prob\{\|TVE\| \geq 650\}$	2.9313E-07	1.6203E-07	1.6×10^{-7}
$Prob\{950 \leq \|TVE\| \leq 1050\}$	1.86344E-08	3.54695E-09	1.7×10^{-8}

4.4 Vertical Occupancy

Vertical occupancy can be defined for same and opposite direction traffic in the same way as lateral occupancy. Thus, "same direction, single separation minimum vertical occupancy" is the average number of aircraft, which are, in relation to the typical aircraft:

a) flying in the same direction as it;
b) nominally on the same track as it;
c) nominally flying at flight levels one vertical separation minimum away from it; and
d) within a longitudinal segment centered on it.

A similar set of criteria can be used to define opposite direction vertical occupancy.

The vertical equivalent of equation (3.18) is

$$E_z = \frac{2T_z}{H} \tag{4.29}$$

where

T_z: The total same direction proximity time generated in the system, i.e. the total time spent by same direction aircraft pairs on the same flight paths at adjacent flight levels and within a longitudinal distance $\tilde{S}_x$ of each other; and

H: The total number of flying hours generated in the system during the period considered.

Vertical occupancy is used to estimate the probability of aircraft pairs being in longitudinal overlap in the system and converts numbers of collisions into numbers of accidents through the factor of 2 in the numerator of equation (4.29).

In principle, the same methods apply to the estimation of vertical occupancy as apply to the estimation of same and opposite direction lateral occupancy. In practice, the "*direct estimation from time at waypoint passing*" method is most useful. Its use is even slightly easier in the case of vertical occupancy as the condition that "The points utilized should be approximately on a plane at right angles to the track system" is automatically satisfied for aircraft on the same track. As this method was used for the estimation of lateral occupancy, it has also been used for the estimation of vertical occupancy.

Thus, for a given day in the traffic sample, the flight progress information for all flights is examined and the times reported at each required point in the system are grouped by track and vertical occupancy is estimated by

$$E_z = \frac{2n_z}{n} \tag{4.30}$$

where n_z is the total number of vertically proximate pairs of aircraft and n is the total number of aircraft. The adjective "total" here refers to all the pairs of adjacent flight levels on all the tracks. The determination of whether or not an aircraft pair is vertically proximate is carried out directly from the times at which waypoint position reports were given.

Crossing track occupancy $E_z(q)$ and $E_z(90)_{rect}$ were introduced in Section 4.2 for cylindrically shaped aircraft on routes intersecting at an angle q and for aircraft shaped like boxes on routes intersecting at 90°. Crossing track occupancy may, in principle, be defined in the same way as same and opposite direction vertical occupancy, e.g.

$$E_z(q) = \frac{2T_z(q)}{H} \tag{4.31}$$

where

$T_z(q)$: The total time spent by aircraft pairs on routes crossing at an angle q at adjacent flight levels within a distance $\tilde{S}_{xy}$ of each other.

Note that a symbol $\tilde{S}_{xy}$ rather than $\tilde{S}_x$ (for same and opposite direction traffic) has been used although the numerical values of both may be the same in practice.

Crossing track occupancy $E_z(q)$ may also be estimated by

$$E_z(q) = \frac{2n_z(q)}{n} \tag{4.32}$$

where $n_z(q)$ is the total number of vertically proximate pairs on the routes intersecting at an angle q and n is the total number of aircraft. An obvious way of determining whether or not an aircraft pair is vertically proximate would be on the basis of the times t_c, say, of passing the crossing point. If the crossing point is a reporting point for both the aircraft, then the reported times of passing the crossing can be used. If the crossing point is not a reporting point for both the aircraft, then interpolated values based on the surrounding reporting points have to be used. An analysis of various errors affecting an interpolated reporting time is given in Reference 28.

Equation (4.32) may also be used to estimate the crossing track occupancy $E_z(90)_{rect}$. This is multiplied by $l_{xy}/\tilde{S}_{xy}$ in the collision risk model equation (4.10) to obtain (twice) the probability of horizontal overlap between two aircraft. The scope of this relation, however, is not fully clear yet. Therefore, at this stage, it is preferred to approximate $E_z(90)_{rect}$ by $E_z(90)$ in the model equation (4.10).

Table 4.7 shows some results on same and opposite vertical occupancy for the existing track system. Note that same direction vertical occupancy is zero due to the flight level allocation scheme in use (cf. Figure 2.4). Opposite direction vertical occupancy is seen to be made up mainly by both the outer tracks which together have approximately 85% of the opposite direction vertical proximate events. It was verified that the relationship between $\tilde{S}_x$ and vertical occupancy was linear. Vertical collision risk, therefore, will be calculated on the basis of $\tilde{S}_x = 80NM$.

Table 4-7. Vertical Occupancy for Existing Track System and Some Associated Quantities Based on Traffic Flow Data for the Period of Time August 1999 to September 2000

Quantity	Estimate
same direction vertical occupancy $E_z(same)$ for existing track system with $\tilde{S}_x = 80NM$	0.0
opposite direction vertical occupancy $E_z(opp)$ for existing track system with $\tilde{S}_x = 80NM$	0.1440
number of flights on UN741	8526
number of flights on UN866	5167
number of flights on UA32	11740
number of flights on UN741, UN866 and UA32	25433
number of opposite direction vertical proximate events for UN741	629
number of opposite direction vertical proximate events for UN866	280
number of opposite direction vertical proximate events for UA32	922
number of opposite direction vertical proximate events for UN741, UN866 and UA32	1831

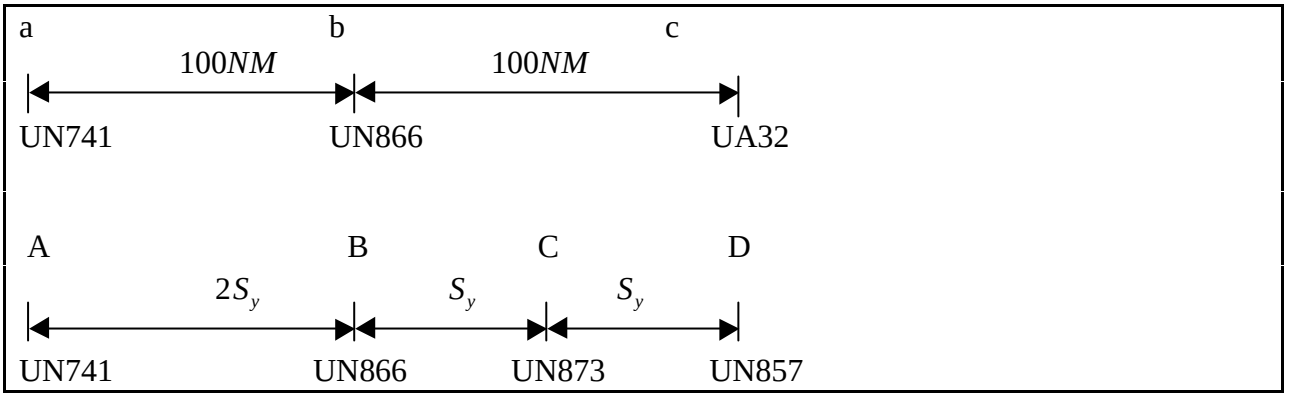

Figure 4-7. Existing and Proposed Track System

For the occupancies to be used in the risk assessment of RVSM, the effect of two changes to the existing track system have to be taken into account, namely the planned implementation of RNP10 in September 2001 and the implementation of RVSM itself. The implementation of RNP10 will be accompanied with the introduction of a new route in the east as shown in Figure 4.7. As described extensively in Section 3.4, this will lead to a redistribution of traffic on the two then eastern most routes UN873 and UN857. This redistribution affects the vertical occupancy with the current vertical separation minimum of 2000ft.

As for the lateral risk assessment, assume that the two new routes UN873 and UN857 will carry proportions f and $1-f$ of the current traffic on the existing route UA32. Assume also that the

distribution of the traffic over the flight levels of these two new routes will be the same as the distribution of the traffic over the flight levels of the existing route UA32. It is then possible to project opposite direction vertical occupancy for the proposed track system with the current vertical separation minimum in the manner of Appendix B. Using the notation of Appendix B, this results in

$$E_z^{ABCD}(opp;2S_z) = 2\times\frac{n_z^a + n_z^b + \left(f^2 + (1-f)^2\right)\times n_z^c}{n^a + n^b + n^c} \tag{4.33}$$

Because the factor in front of n_z^c is less than one for $0 < f < 1$, opposite direction vertical occupancy in the proposed four-track system would be projected to be smaller than in the current three-track system. In practice, due to the lower traffic load per route, the traffic distribution over the flight levels may shift somewhat to the economically preferred flight levels, which would tend to make the contribution of those routes to the vertical occupancy for the system somewhat bigger than projected by equation (4.33). To be cautious, one might ignore the reduction in vertical occupancy suggested by equation (4.33). However, the above describes only the effect of the first system change on vertical occupancy in an RVSM environment, the other being the introduction of RVSM itself. This approximately doubles the number of flight levels available and would theoretically, with the same traffic load on each flight level, half the vertical occupancy. In reality, not all the flight levels are equally loaded and there would be a strong tendency to use the economically best flight levels in an RVSM environment. This could limit the theoretical reduction of occupancy to the expected range of a 20 to 30 percent as seen in the NAT.

In the absence of precise information on the future use of the flight levels under RVSM in the SAT, it is assumed that the reduction in vertical occupancy due to the availability of additional flight levels will depend on the redistribution of traffic over the flight levels resulting from the implementation of both RNP10 and RVSM. There remains, however, the reduction in occupancy due to the redistribution of traffic over the new routes as given by equation (4.33) that also applies also when the vertical separation minimum is S_z rather than $2S_z$, i.e.

$$E_z^{ABCD}(opp) = 2\times\frac{n_z^a + n_z^b + \left(f^2 + (1-f)^2\right)\times n_z^c}{n^a + n^b + n^c} \tag{4.34}$$

Table 4.8 shows the projected occupancy as a function of the traffic distribution factor f based on current traffic levels. For the nominal situation of an equal split of the traffic on the existing UA32 between the new UN873 and UN857, the opposite direction vertical occupancy has decreased by approximately 25% from 0.1440 to 0.1077. Clearly, the effect on vertical occupancy of the additional route is smaller when the amount of traffic on either of the two new eastern most routes is more similar to that on the original route UA32.

Table 4-8. Vertical Occupancy in the Proposed Track System Under RVSM Based on Current Traffic Levels

Traffic distribution factor f	$f^2 + (1-f)^2$	Opposite direction Vertical Occupancy
0.0	1.00	0.1440
0.1	0.82	0.1309
0.2	0.68	0.1208
0.3	0.58	0.1135
0.4	0.52	0.1092
0.5	0.50	0.1077
0.6	0.52	0.1092
0.7	0.58	0.1135
0.8	0.68	0.1208
0.9	0.82	0.1309
1.0	1.00	0.1440

Table 4-9a. Vertical Occupancy in the Proposed Track System Under RVSM Based On Traffic Levels Projected Forward Over a Ten Year Planning Horizon With a 5.1% Annual Growth Rate

Traffic distribution factor f	$f^2 + (1-f)^2$	Opposite direction Vertical Occupancy
0.0	1.00	0.2368
0.1	0.82	0.2153
0.2	0.68	0.1986
0.3	0.58	0.1867
0.4	0.52	0.1796
0.5	0.50	0.1772
0.6	0.52	0.1796
0.7	0.58	0.1867
0.8	0.68	0.1986
0.9	0.82	0.2153
1.0	1.00	0.2368

Table 4-9b. Vertical Occupancy in the Proposed Track System Under RVSM Based on Traffic Levels Projected Forward Over a Ten Year Planning Horizon with an 8% Annual Growth Rate

Traffic distribution factor f	$f^2 + (1-f)^2$	Opposite direction Vertical Occupancy
0.0	1.00	0.3110
0.1	0.82	0.2827
0.2	0.68	0.2609
0.3	0.58	0.2452
0.4	0.52	0.2359
0.5	0.50	0.2326
0.6	0.52	0.2359
0.7	0.58	0.2452
0.8	0.68	0.2609
0.9	0.82	0.2827
1.0	1.00	0.3110

The effect of traffic growth on vertical occupancy is modelled in the same way as for lateral occupancy in Section 3.4. Assuming again a planning horizon of ten years and an annual traffic growth rate of 5.1%, an overall traffic growth factor of 1.64 is found. Application of this factor to the vertical occupancy numbers in Table 4.8 produces the values shown in Table 4.9a. When an annual traffic growth rate of 8% is assumed, an overall traffic growth factor of 2.16 is found, which produces the values shown in Table 4.9b.

In a similar way as for the projection of lateral occupancy in the proposed track system, a number of assumptions have again had to be made to project vertical occupancy under RVSM in the proposed track system. It is equally important that these assumptions be verified after each change to the structure of the system to confirm the validity of the projections.

Consider finally the crossing track occupancy $E_z(90)/E_z(90)_{rect}$. Data on traffic crossing the main EUR/SAM Corridor was obtained from Brazil (Recife FIR) for August and September 2000. The crossing routes indicated by this data are plotted in Figure 4.8. The data available was processed to obtain vertically proximate events between aircraft crossing at adjacent flight levels. Approximately 25 percent of the proximate events appeared from the data to be on the same flight level. In general, aircraft crossing the Corridor that identify themselves to the Recife ACC are separated vertically. There was insufficient data available to determine if there was communication and subsequent vertical separation between 10 of these proximate pairs that crossed within 80 NM of each other. It is recommended that further data be gathered and examined in these events. However, it was assumed that the required vertical separation was maintained and therefore that *all* of the vertically proximate events involved aircraft crossing at adjacent flight levels. The data from the crossing traffic and the resulting crossing track vertical occupancy are summarized in Table 4.10. A linear relationship was again established between $\tilde{S}_{xy}$ and crossing track vertical occupancy $E_z(90)$ and, consequently, technical vertical collision

risk will be calculated on the basis of $\tilde{S}_{xy} = 80NM$. Again, this means that any aircraft within 80 NM when another aircraft crosses its track is considered vertically proximate to the crossing aircraft. As described in Appendix C, the crossing track vertical occupancy computed in this manner is corrected by a factor of 0.15 to account for the non-uniform distribution of crossing events along the portion of the Corridor examined.

Figure 4-8. Crossing Routes Reported in the Recife FIR

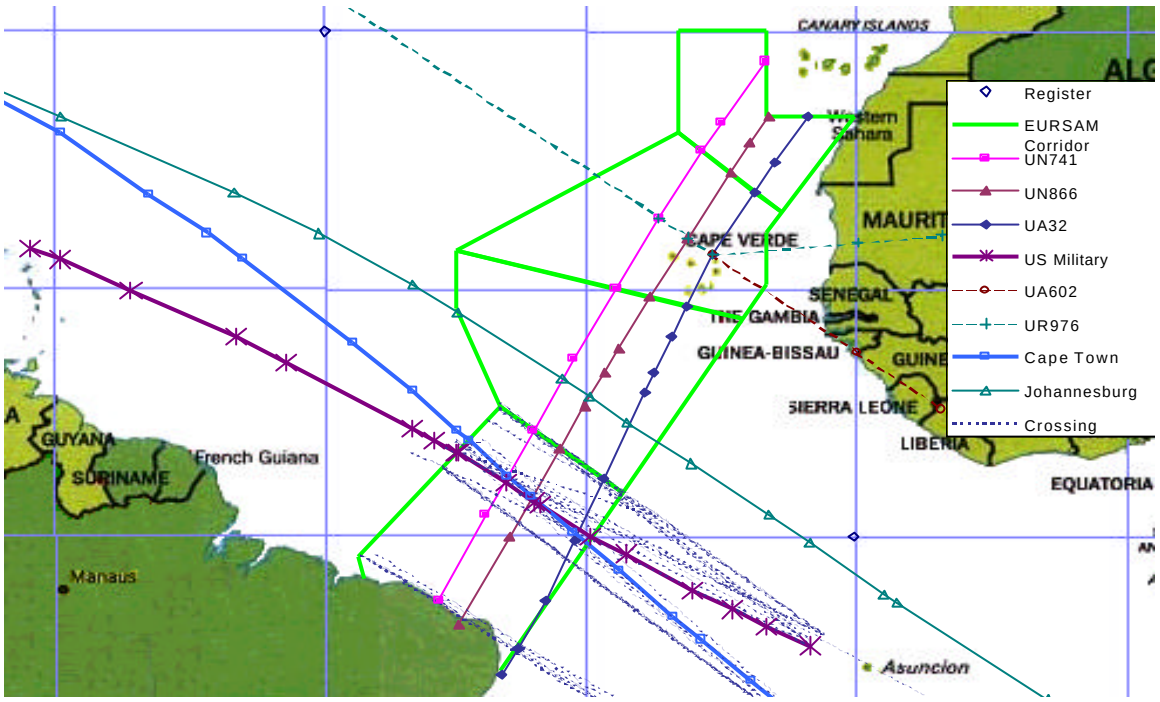

Table 4-10. Crossing Track Vertical Occupancy for Existing Track System and Some Associated Quantities Based On Traffic Flow Data From Recife FIR for the Period of Time August and September 2000

Quantity	Estimate
crossing track vertical occupancy $E_z(90)$ for existing track system with $\tilde{S}_{xy} = 80NM$ (corrected)	0.003471
number of flights on main route (UN741, UN866 and UA32)	3444
number of crossing flights	273
total number of flights	3717
number of crossing traffic vertical proximate events	43

Crossing track vertical occupancy is needed for the proposed rather than the existing track system. As the total *amount* of traffic on the main routes remains the same (for current traffic levels), it is assumed that the change to the new track system does not affect crossing track occupancy for current traffic levels. Hence, $E_z(90) = 0.003471$ will be used for the proposed track system at current traffic levels. In addition, crossing traffic vertical occupancy for future traffic levels projected forward over a ten year planning horizon are needed. If both the traffic flow in the EUR/SAM Corridor and the crossing traffic flow would be growing with the overall traffic growth factor of 1.64, then crossing traffic vertical occupancy would be projected to grow by this factor, i.e. $E_z(90)^{future} = 0.005707$. This value has been used for the estimation of vertical collision risk for future traffic levels. If both the traffic flow in the EUR/SAM Corridor and the crossing traffic flow are assumed to increase with the overall traffic growth factor of 2.16, then crossing traffic vertical occupancy would be projected to grow by this factor, i.e. $E_z(90)^{future} = 0.007497$.

No data on crossing traffic was available from SAL UIR for the UR976/UA602 or from Dakar Oceanic UIR for the Atlanta-Johannesburg route. Hence, the vertical collision risk component due to crossing traffic is underestimated to this extent. One possibility would be to assume that the total traffic on these two routes is approximately equal to the traffic on the two routes identified through the Recife FIR, implying that the crossing traffic vertical occupancy numbers should be doubled. This is accounted for in the correction factor defined in Appendix C.

The crossing traffic flow data from Recife FIR indicate that 10 of the 43 crossing traffic proximity events involved aircraft at the same flight level within ten minutes of each other. Four possible explanations for this apparent violation of the required separation come to mind:
A tactical flight level change to separate crossing traffic was not included in the data provided;

1) The air traffic controller did not register a flight level change on the strip (Recife's system is manual);
2) The aircraft made contact too late to allow an action by the air traffic controller; or
3) There was an operational error that was not registered by the air traffic controller and/or by the aircraft.

For this analysis, a request was made to the Recife ATC to investigate these proximity events, and to date the Recife ATC has indicated that three of the events involved aircraft that were cleared to a different altitude. The records do not readily allow further clarification of the other seven events. For the purpose of accounting for these events in the collision risk model, the "same flight level" crossing proximity events were counted as "adjacent flight level" crossing proximity events. If it could be shown that these events were in fact violations of the vertical separation standard by a whole vertical separation standard (2,000 ft), then these events would be treated as large height keeping deviations and be accounted for in the vertical collision risk due to all causes model. Reporting, collection and evaluation of these events are critical to further assessment of the collision risk.

4.5 The Probability of Lateral Overlap

The probability of lateral overlap for aircraft nominally flying at adjacent flight levels of the same flight path is denoted by $P_y(0)$. It is defined by

$$P_y(0) = \int_{-l_y}^{l_y} f^{y_{12}}(y)dy \tag{4.35}$$

where $f^{y_{12}}(y)$ denotes the probability density of the lateral distance y_{12} between two aircraft with lateral deviations y_1 and y_2, nominally at the same track, i.e.

$$y_{12} = y_1 - y_2 \tag{4.36}$$

and

$$f^{y_{12}}(y) = \int_{-\infty}^{\infty} f^Y(y_1) f^Y(y_1 - y)dy_1 . \tag{4.37}$$

Note that equation (4.37) assumes that the deviations of the two aircraft are independent and have the same probability density, $f^Y(y_1)$, say. As defined in Table 4.1, l_y denotes the average aircraft width. Substitution of equation (4.37) into equation (4.35) gives

$$P_y(0) = \int_{-l_y}^{l_y} \int_{-\infty}^{\infty} f^Y(y_1) f^Y(y_1 - y)dy_1 dy \tag{4.38}$$

which, in practice, is often approximated by

$$P_y(0) \approx 2l_y \int_{-\infty}^{\infty} f^Y(y_1) f^Y(y_1)dy_1 \tag{4.39}$$

or

$$P_y(0) \approx 2l_y f^{y_{12}}(0) \tag{4.40}$$

Thus, the probability density $f^Y(y_1)$ of the lateral navigation deviations of aircraft is needed to calculate $P_y(0)$. This density was extensively described in Section 3.3. Essentially the core part of $f^Y(y_1)$ is needed for the estimation of $P_y(0)$. Using equation (3.16) with $a = 0.0$ and $a_1 = 3.338$, the resulting estimate based on $l_y = 174.45$ ft (cf. Table 4.11) is $P_y(0) = 0.0043$. Some care, however, is required with regard to this value. As can be seen from equation (4.10),

the vertical collision risk for same and opposite direction traffic is directly proportional to the probability of lateral overlap $P_y(0)$. This means that any underestimation of this parameter leads almost directly to an underestimation of the vertical risk. As the risk estimate is to cover a planning horizon up to the year 2010, expected improvements in actual navigation performance over this period need to be taken into account. Satellite navigation in particular will lead to a track keeping accuracy which will be well within the RNP value and will thus lead to a value of the probability of lateral overlap $P_y(0)$ which is considerably larger than calculated above. As a tentatively conservative approach, therefore, the value of $P_y(0)$ from the Global System Performance Specification underlying the use of RVSM and the MASPS will be used, i.e. $P_y(0) = 0.058$. This value is based on a standard deviation of lateral navigation deviations of 0.3 NM. It will, again, be important to monitor this parameter after the implementation of RVSM to ensure that the actual vertical collision risk is not being underestimated.

4.6 Aircraft Dimensions

Table 3.7 showed the average aircraft dimensions for the lateral collision risk model. Clearly, the same dimensions apply to the vertical model. In addition, the vertical model for crossing traffic needs the average diameter of a cylinder enveloping the aircraft. Table 4.11 shows the pertinent average aircraft dimensions.

Table 4-11. Average Aircraft Dimensions for the Vertical Collision Risk Model

aircraft dimension	parameter	value (ft)	value (NM)
length	l_x	193.12	0.03179
width	l_y	174.45	0.02871
height	l_z	55.43	0.009124
diameter	l_{xy}	193.12	0.03179

4.7 Relative Velocities

The vertical collision risk model equation (4.10) contains four relative speed parameters, $2\overline{|V|}$, $\overline{|\Delta V|}$, $\overline{|\dot{y}|}$ and $\overline{|\dot{z}|}$. Note that the relative speed components between aircraft crossing at an angle of (approximately) 90° have been taken as $\overline{|V|}$. (See the derivation of equation 4.7 for why this value is not $\sqrt{2}\overline{|V|}$.) The average relative along track speeds $\overline{|V|}$ and $\overline{|\Delta V|}$ are taken the same as for the lateral collision risk model.

An issue is again the extent to which the relative speed components, $\overline{|\dot{y}|}$ and $\overline{|\dot{z}|}$, are related to the magnitude of the lateral and vertical separation between a pair of aircraft (cf. Section 3.7). For the vertical collision risk model, $\overline{|\dot{y}|}$ is the mean of the (modulus of the) relative cross-track speed between aircraft on the same track. Consequently, there is no operational reason why this relative

velocity should have a particularly large value. The vertical risk assessments for the NAT and the Australian FIRs assumed values of 20 and 4 kts respectively (Refs. 31 and 23). The more conservative value of 20 kts will be used here. (It may be somewhat outdated, however, see Reference 24.) The mean (modulus of the) relative vertical speed $\overline{|\dot{z}|}$ of the vertical collision risk model applies to aircraft that have lost their assigned vertical separation minimum of S_z. The relationship between the relative vertical speed and the vertical separation between two aircraft was discussed in Section 3.7. An approximately constant relationship was quoted from Annex A of Part II of Reference 21 at a value of 1.5 kts. Thus, $\overline{|\dot{z}|}=1.5$ kts will be taken here. The same value has been used for the NAT. The vertical collision risk assessment for the Australian FIRs used a value of 10 kts as in the development of the global system performance specification, but the accuracy of this value has been questioned in Annex A of Part II of Reference 21.

4.8 Summary and Comparison of Parameter Values

Table 4.12 summarizes the vertical collision risk model parameters other than occupancy and the probability of vertical overlap and shows a comparison with their counterparts used in the NAT and the Australian FIRs (Refs. 31 and 23).

Table 4-12. Summary and Comparison of Vertical Collision Risk Model Parameters

Parameter[1]	Airspace		
	SAT	**NAT**	**Australian FIRs**
$P_y(0)$	0.058	0.0263	0.058 (?)
l_x	193.12	185.93	221.17
l_y	174.45	165.27	195.04
l_z	55.43	52.25	61.37
l_{xy}	193.12	-	221.17
$\overline{\|V\|}$	475	480	470
$\overline{\|\Delta V\|}$	20	13	20
$\overline{\|\dot{y}\|}$	20	20	4
$\overline{\|\dot{z}\|}$	1.5	1.5	10

Note[1]: Aircraft dimensions in feet, speeds in knots

4.9 Technical Vertical Risk

The estimates of the different parameters of the vertical collision risk summarized in Table 4.12 can now be substituted into the model of equation (4.10), to estimate the technical vertical collision risk associated with RVSM in the proposed track system. Two cases are again examined; namely current traffic levels and future traffic levels projected forward over a ten-year planning horizon.

It follows that

$$N_{az} = P_z(S_z)E_z(opp)\times 0.058\times\frac{0.03179}{80}\times\left\{\frac{2\times 475}{2\times 0.03179}+\frac{20}{2\times 0.02871}+\frac{1.5}{2\times 0.009124}\right\}+$$
$$P_z(S_z)E_z(90)_{rect}\times\frac{0.03179}{80}\times\left\{\frac{475}{0.03179+0.02871}+\frac{475}{0.03179+0.02871}+\frac{1.5}{2\times 0.009124}\right\} \quad (4.41)$$

or

$$N_{az} = P_z(S_z)E_z(opp)\times 0.058\times 3.973\times 10^{-4}\times\{14944.9+348.301+82.2134\}+$$
$$P_z(S_z)E_z(90)_{rect}\times 3.973\times 10^{-4}\times\{7851.99+7851.99+82.2134\}= \quad (4.42)$$
$$= P_z(S_z)E_z(opp)\times 0.058\times 3.973\times 10^{-4}\times 15375.4+$$
$$P_z(S_z)E_z(90)_{rect}\times 3.973\times 10^{-4}\times 15786.2$$

i.e.

$$N_{az} = P_z(S_z)E_z(opp)\times 0.3543+P_z(S_z)E_z(90)_{rect}\times 6.2717 \quad (4.43)$$

The next step is to substitute the estimates of the probability of vertical overlap and vertical occupancy into equation (4.43). The vertical overlap probability has been given in Table 4.5, i.e. $P_z(1000)=2.1346\times 10^{-8}$ and $P_z(1000)=4.5263\times 10^{-9}$, and the occupancies for current traffic levels in Tables 4.8 and 4.10.

Table 4.13 shows the estimates of the technical vertical collision risk based on current traffic levels as a function of the traffic distribution factor f. It can be seen that for both the values of $P_z(1000)$ the estimates of the technical vertical collision risk are well below the TLS of 2.5×10^{-9}. Taking into account the opposite direction vertical occupancy values from Table 4.8 and the crossing traffic vertical occupancy from Table 4.10, equation (4.43) and Figure 4.9 show that the opposite direction traffic is in fact the main contributor to the technical vertical risk. Its contribution is between two and three times larger than that of the crossing traffic, depending on the value of the traffic distribution factor f. The technical vertical collision risk due to just the crossing traffic component is still significant. These results indicate that before RVSM is implemented, it may be necessary to reduce the uncertainty about the proper value of the probability of vertical overlap $P_z(1000)$ and about the crossing traffic in the Sal and Dakar

Oceanic UIRs. As explained in Section 4.3.4, the former uncertainty is mainly due to uncertainty about the distribution of FTE/AAD.

Table 4-13. Technical Vertical Risk Estimates in the Proposed Track System Under RVSM Based On Current Traffic Levels

Traffic distribution factor f	Technical vertical collision risk	
	$P_z(1000) = 2.1346 \times 10^{-8}$	$P_z(1000) = 4.5263 \times 10^{-9}$
0.0	1.554E-09	3.294E-10
0.1	1.455E-09	3.085E-10
0.2	1.378E-09	2.922E-10
0.3	1.323E-09	2.806E-10
0.4	1.290E-09	2.736E-10
0.5	1.279E-09	2.713E-10
0.6	1.290E-09	2.736E-10
0.7	1.323E-09	2.806E-10
0.8	1.378E-09	2.922E-10
0.9	1.455E-09	3.085E-10
1.0	1.554E-09	3.294E-10

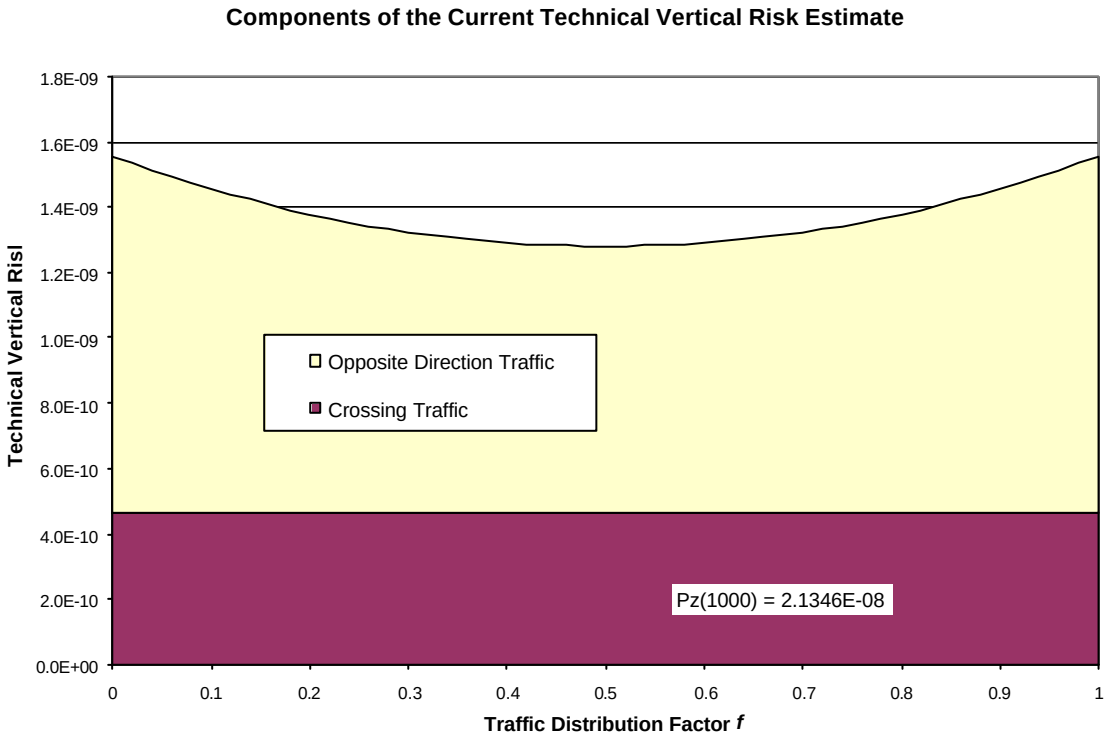

Figure 4-9. The Technical Vertical Risk is Dominated by the "Opposite" Traffic

Table 4.14a shows the estimates of the technical vertical collision risk based on traffic levels projected forward over a ten-year planning horizon. The assumed traffic growth factor was 5.1% per annum. As for current traffic levels, the estimates of the technical vertical collision risk are less than the technical TLS for the smaller value of $P_z(1000)$. As the vertical occupancies for future traffic levels are larger by a factor of 1.64, the technical vertical TLS is now barely exceeded in the year 2010 for the larger value of $P_z(1000)$ for the "end" values of the traffic distribution factor f. The data in Tables 4.13 and 4.14a are summarized in Figure 4.10a.

Table 4-14a. Technical Vertical Risk Estimates in the Proposed Track System Under RVSM Based On Traffic Levels Projected Forward Over a Ten-Year Planning Horizon With 5.1% Annual Growth

Traffic distribution factor f	**Technical vertical collision risk**	
	$P_z(1000) = 2.1346 \times 10^{-8}$	$P_z(1000) = 4.5263 \times 10^{-9}$
0.0	2.555E-09	5.417E-10
0.1	2.392E-09	5.073E-10
0.2	2.266E-09	4.805E-10
0.3	2.176E-09	4.614E-10
0.4	2.122E-09	4.500E-10
0.5	2.104E-09	4.461E-10
0.6	2.122E-09	4.500E-10
0.7	2.176E-09	4.614E-10
0.8	2.266E-09	4.805E-10
0.9	2.392E-09	5.073E-10
1.0	2.555E-09	5.417E-10

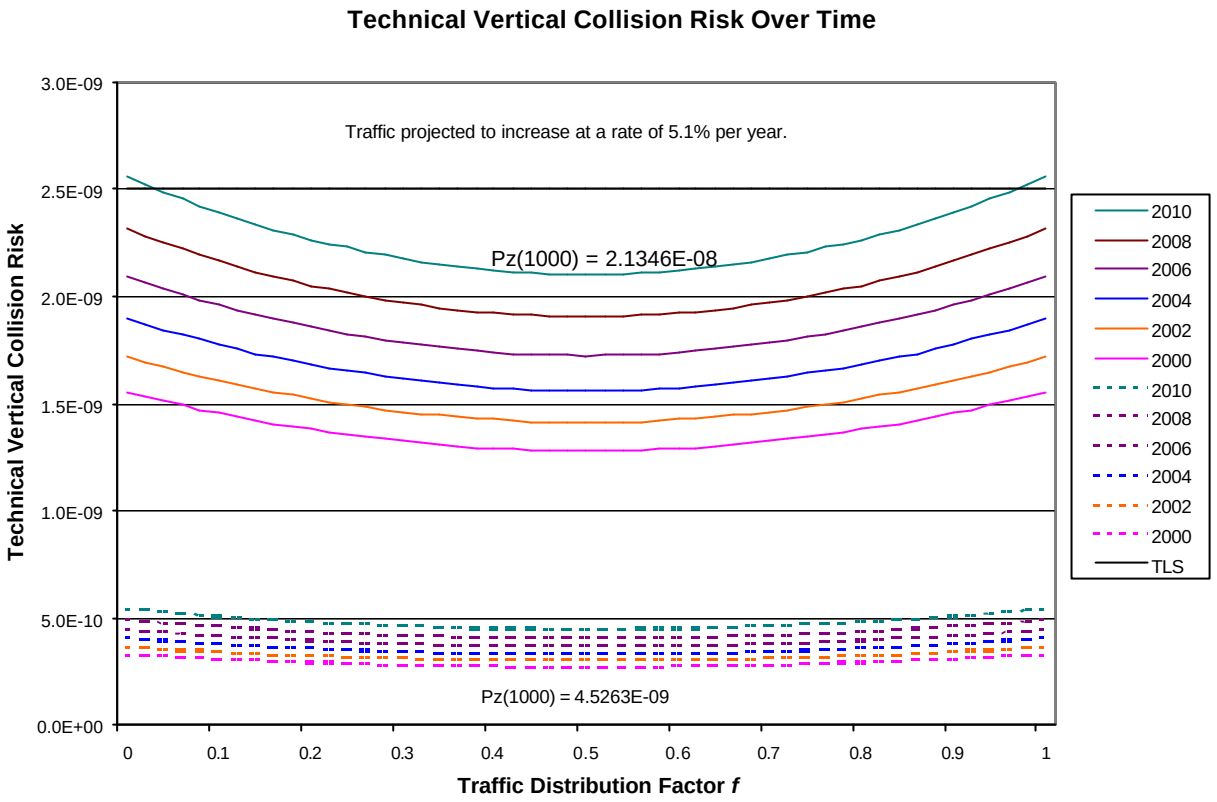

Figure 4-10a. Technical Vertical Collision Risk Increases as the Traffic Increases With Time With 5.1% Annual Growth

Table 4.14b shows the estimates of the technical vertical collision risk based on traffic levels projected forward over a ten-year planning horizon. The assumed traffic growth factor was 8% per annum. Again, the estimates of the technical vertical collision risk are less than the technical TLS for the smaller value of $P_z(1000)$. As the vertical occupancies for future traffic levels are larger by a factor of 2.16, the technical vertical TLS is now exceeded in the year 2010 for the larger value of $P_z(1000)$ for all values of the traffic distribution factor f. The data in Tables 4.13 and 4.14b are summarized in Figure 4.10b.

Table 4-14b. Technical Vertical Risk Estimates in the Proposed Track System Under RVSM Based On Traffic Levels Projected Forward Over a Ten-Year Planning Horizon With 8% Annual Growth

Traffic distribution factor f	Technical vertical collision risk	
	$P_z(1000) = 2.1346 \times 10^{-8}$	$P_z(1000) = 4.5263 \times 10^{-9}$
0.0	3.354E-09	7.112E-10
0.1	3.141E-09	6.660E-10
0.2	2.975E-09	6.309E-10
0.3	2.857E-09	6.058E-10
0.4	2.786E-09	5.907E-10
0.5	2.762E-09	5.857E-10
0.6	2.786E-09	5.907E-10
0.7	2.857E-09	6.058E-10
0.8	2.975E-09	6.309E-10
0.9	3.141E-09	6.660E-10
1.0	3.354E-09	7.112E-10

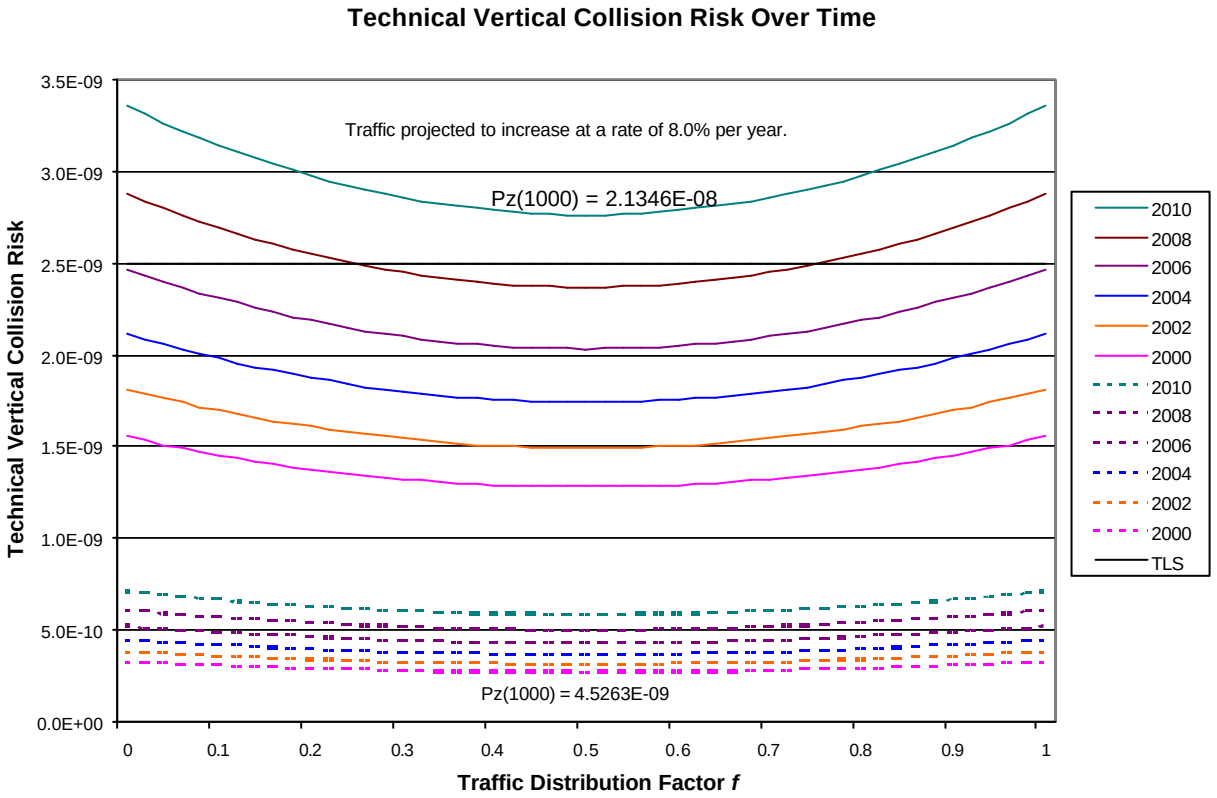

Figure 4-10b. Technical Vertical Collision Risk Increases as the Traffic Increases With Time With 8% Annual Growth

5 Assessment of Vertical Collision Risk Due to all Causes

5.1 Introduction

Section 4 discussed the assessment of the technical vertical collision risk associated with the implementation of RVSM in the SAT. However, there may be other causes of the loss of vertical separation between aircraft at adjacent flight levels and the combined effect of all those causes is to be assessed against a TLS of 5×10^{-9} aircraft accidents per flight hour. This section presents models for some non-technical causes with which the associated vertical risks can be estimated and added up to examine whether the TLS of 5×10^{-9} is being met.

Currently, there are insufficient data to estimate all the parameters of the different sub-models. Therefore, rather than actually estimating the risk and comparing it with the TLS of 5×10^{-9}, the TLS and the overall model will be used to derive upper bounds for the error rates which should not be exceeded.

From an operational point of view, experience in the NAT suggests that the following general types of causes be considered (Ref. 24):

- ATC-pilot loop errors and incorrect clearances;
- Aircraft contingency events; and
- Height deviations due to ACAS (TCAS).

These causes have been further subdivided as shown in Table 5.1 (Ref. 24). Error classes A-C belong to the second general type of cause and error classes D-G to the first. Error class I refers to a cause that was classified as technical in Section 4, viz. large height deviations due to meteorological effects (cf. Section 4.3.1).

Table 5-1. Classification of Large Height Deviations

Error class	Deviation type
A	Contingency action due to engine fault
B	Contingency action due to pressurization failure
C	Contingency action due to other cause
D	Failure to climb/descent as cleared
E	Climb/descent without ATC clearance
F	Entry to RVSM airspace at an incorrect level
G	ATC FL re-clearance resulting in loss of lateral or longitudinal separation
H	Deviation due to ACAS (TCAS)
I	Aircraft unable to maintain level
O	Other

The first two general types of causes may involve an aircraft leveling off at a wrong flight level and/or climbing or descending through one or more flight levels without clearance. Consequently, they have been called large height deviations involving whole numbers of flight

levels. It should be noted that for most of the contingency situations procedures are in place to effectively control the risk associated with the contingency event. Occasionally, it may not be possible to fully comply with the procedures, resulting in the type of effect mentioned. Height deviations due to ACAS (TCAS) do not usually involve whole numbers of flight levels, but may be much larger than the normal height deviations of MASPS approved aircraft.

Appropriate vertical collision risk models needed for each of the above cases are described in Section 5.2. These models differ from the technical vertical collision risk model with respect to the computation of the probability of vertical overlap and the relative vertical speed. As the first two general types of causes each may involve two types of risk initiating events, collision risk models are presented first for aircraft leveling off at a wrong level, and climbing/descending through a flight level. These two models have in common that they work on a 'per event basis." They are then used as building blocks for models of the collision risk associated with ATC-pilot loop errors/incorrect clearances and aircraft contingency events. Vertical risk estimates are examined in Section 5.3.

5.2 Collision Risk Models

5.2.1 Aircraft Leveling Off at a Wrong Level

An aircraft leveling off at a wrong flight level is still in level flight. Therefore, the same type of collision risk model is applicable as for aircraft at adjacent flight levels but with a modified calculation of the probability of vertical overlap.

Consider a pair of aircraft, one of which has leveled off at a wrong level. For such a pair, their vertical distance z_{12} reduces to (cf. equation (4.12))

$$z_{12} = z_1 - z_2 \tag{5.1}$$

and the probability of vertical overlap given the event becomes

$$P_z(S_z;0) = \int_{-l_z}^{lz} \int_{-\infty}^{\infty} f_1^{TVE}(z_1)\, f_2^{TVE}(z_1 - z)\, dz_1 dz \tag{5.2}$$

Note that P_z has two arguments: the latter indicates that the actual nominal vertical separation between the two aircraft is zero and the former indicates that the intended nominal vertical separation is S_z. Numerically, its value is equal to that of $P_z(0)$ given by equation (3.22), i.e.

$$P_z(S_z;0) = P_z(0)\,. \tag{5.3}$$

When the number of aircraft leveling off at a wrong level during a given period of calendar time is n^{wl}, the average time spent at a wrong level is $\bar{t}^{wl}$ and the amount of flying time is T, it follows that the probability of vertical overlap associated with this type of event is

$$P_z(S_z) = \frac{P_z(S_z;0) \times n^{wl} \times \bar{t}^{wl}}{T} \tag{5.4}$$

or, using equation (5.3),

$$P_z(S_z) = \frac{P_z(0) \times n^{wl} \times \bar{t}^{wl}}{T}\,. \tag{5.4}$$

The average sojourn time of an aircraft at a wrong level after having leveled off there may be estimated by

$$\bar{t}^{wl} = \frac{1}{n^{wl}} \sum_{i=1}^{n^{wl}} t_i^{wl} \tag{5.5}$$

where t_i^{wl}, $i = 1,\ldots,n^{wl}$, denotes the time spent by an aircraft at a wrong level during the i-th event.

Equation (5.4) can be substituted for $P_z(S_z)$ into the collision risk model of equation (4.10) to obtain the vertical risk due to aircraft leveling off at a wrong level, i.e.

$$\begin{aligned} N_{az}^{wl} = \frac{P_z(0) \times n^{wl} \times \bar{t}^{wl}}{T} P_y(0) \frac{l_x}{\tilde{S}_x} \Bigg[& E_z(same) \left\{ \frac{\overline{|\Delta V|}}{2\,l_x} + \frac{\overline{|\dot{y}|}}{2\,l_y} + \frac{\overline{|\dot{z}|}}{2\,l_z} \right\} + \\ & E_z(opp) \left\{ \frac{2\overline{|V|}}{2\,l_x} + \frac{\overline{|\dot{y}|}}{2\,l_y} + \frac{\overline{|\dot{z}|}}{2\,l_z} \right\} \Bigg] + \\ \frac{P_z(0) \times n^{wl} \times \bar{t}^{wl}}{T} & \frac{l_{xy}}{\tilde{S}_{xy}} E_z(90)_{rect} \left\{ \frac{\overline{|V|}}{l_x + l_y} + \frac{\overline{|V|}}{l_x + l_y} + \frac{\overline{|\dot{z}|}}{2\,l_z} \right\} \end{aligned} \tag{5.6}$$

Except for the parameters making up $P_z(S_z)$, the values of the parameters of the model of equation (5.6) are the same as those summarized in Table 4.12 for the technical vertical collision risk model.

5.2.2 Aircraft Climbing or Descending Through a Flight Level

In a similar way as for aircraft on crossing routes (cf. Section 4.2), the two main elements of a collision risk model for aircraft climbing or descending through a flight level without clearance depend on the probability of two aircraft being in joint longitudinal and vertical overlap and on the average duration of a joint overlap in the vertical plane. Clearly, the relative vertical speed plays a part. This depends on the rate of climb/descent during the event and determines the angle at which the flight level is crossed. A model is described below that is applicable for relatively small level crossing angles determined by climb/descent speeds up to approximately 40kts. See Reference 24 for a model that might be used in case of higher climb/descent speeds.

Starting point for the model is the assumption that the probability of joint longitudinal and vertical overlap can still be factored into the product of the overlap probabilities in the individual dimensions. It is also assumed that during the event the sides of the boxes representing the aircraft remain parallel. The differences then concern the calculation of the probability of vertical overlap and the value of the relative vertical speed. As one of the aircraft is climbing/descending and the other is in level flight, the relative vertical speed can be taken as the climb/descent rate of the former aircraft.

Per event, i.e. an aircraft crossing through a flight level, the aircraft are in vertical overlap, on average, for t_z flight hours, where

$$t_z = \frac{2 l_z}{\overline{|\dot{z}_c|}} \tag{5.7}$$

and $\overline{|\dot{z}_c|}$ denotes the average climb/descent rate.

As, on average again, an aircraft is in longitudinal overlap with other aircraft for P_x flight hour per flight hour, the time they are in both longitudinal and vertical overlap <u>per event</u> is taken as the product of the two quantities, i.e.

$$t_{xz} = \frac{2 l_z}{\overline{|\dot{z}_c|}} P_x \tag{5.8}$$

Given the assumptions underlying this approach, the time in joint longitudinal and vertical overlap per event may be converted into number of collisions per event by means of the factors within accolades in equation (4.10) and into number of accidents by multiplying by a factor of 2. Taking also into account the relation between probability of longitudinal overlap and occupancy, the expected number of accidents <u>per event</u> due to the loss of vertical separation caused by an aircraft crossing a flight level without clearance can be written as

$$N_{az/event}^{lc} = \frac{2 l_z}{\overline{|\dot{z}_c|}} P_y(0) \frac{l_x}{\tilde{S}_x} \left[E_z(same) \left\{ \frac{\overline{|\Delta V|}}{2 l_x} + \frac{\overline{|\dot{y}|}}{2 l_y} + \frac{\overline{|\dot{z}_c|}}{2 l_z} \right\} + E_z(opp) \left\{ \frac{2\overline{|V|}}{2 l_x} + \frac{\overline{|\dot{y}|}}{2 l_y} + \frac{\overline{|\dot{z}_c|}}{2 l_z} \right\} \right] +$$
$$\frac{2 l_z}{\overline{|\dot{z}_c|}} \frac{l_{xy}}{\tilde{S}_{xy}} E_z(90)_{rect} \left\{ \frac{\overline{|V|}}{l_x + l_y} + \frac{\overline{|V|}}{l_x + l_y} + \frac{\overline{|\dot{z}_c|}}{2 l_z} \right\} \tag{5.9}$$

The same and opposite direction parts of this model correspond with a model for a quantity C_t, given by equation (31) of paragraph 5.5.28 of Reference 24.

When the number of flight levels crossed during a given period of calendar time is n^{lc} and the amount of flying time is T, it follows that the expected number of accidents per flight hour due

to the loss of vertical separation caused by an aircraft crossing a flight level without clearance is given by

$$N_{az}^{lc} = \frac{n^{lc}}{T} N_{az/event}^{lc} \tag{5.10}$$

or,

$$N_{az}^{lc} = \left(\frac{n^{lc}}{T} \frac{2 l_z}{\overline{|\dot{z}_c|}} \right) P_y(0) \frac{l_x}{\tilde{S}_x} \left[E_z(same) \left\{ \frac{\overline{|\Delta V|}}{2 l_x} + \frac{\overline{|\dot{y}|}}{2 l_y} + \frac{\overline{|\dot{z}_c|}}{2 l_z} \right\} + E_z(opp) \left\{ \frac{2\overline{|V|}}{2 l_x} + \frac{\overline{|\dot{y}|}}{2 l_y} + \frac{\overline{|\dot{z}_c|}}{2 l_z} \right\} \right] +$$
$$\left(\frac{n^{lc}}{T} \frac{2 l_z}{\overline{|\dot{z}_c|}} \right) \frac{l_{xy}}{\tilde{S}_{xy}} E_z(90)_{rect} \left\{ \frac{\overline{|V|}}{l_x + l_y} + \frac{\overline{|V|}}{l_x + l_y} + \frac{\overline{|\dot{z}_c|}}{2 l_z} \right\} \tag{5.11}$$

It follows from equation (5.11) that the probability of vertical overlap associated with aircraft crossing flight levels without clearance may be interpreted as

$$P_z(S_z)^{lc} = \frac{n^{lc} \frac{2 l_z}{\overline{|\dot{z}_c|}}}{T} \tag{5.12}$$

which is precisely the proportion of flying time spent in longitudinal overlap due to this particular cause.

5.2.3 Aircraft Deviating in Response to ACAS (TCAS)

Large height deviations due to ACAS (TCAS) do not usually involve whole numbers of flight levels and have been termed as such in the NAT. From a modeling point of view, they may be considered as realizations of zero mean random processes and their modeling is not different from that of large height deviations due to turbulence described in Section 4.3.3. Thus, an AAD distribution made up of typical performance and atypical performance due to ACAS induced large height deviations not involving whole numbers of flight levels is to be built. The model could again be of the form of a double double exponential density, i.e.

$$f_{ACAS}^{AAD}(a) = (1-a) \times \frac{1}{2a_1} \exp - \left| \frac{a}{a_1} \right| + a \frac{1}{2a_2} \exp - \left| \frac{a}{a_2} \right|. \tag{5.13}$$

The three parameters a, a_1 and a_2 could be estimated using the same data on typical performance as mentioned in Section 4.3.3, supplemented with data on the occurrence of ACAS related incident events from the SATMA. Unfortunately, no data on the latter type of events are currently available. Therefore, the somewhat arbitrary assumption could be made that the AAD density associated with ACAS-related large height deviations has the same parameter values as

the AAD density associated with turbulence induced large height deviations. The parameter values of the latter density are given in Table 4.4. By comparison, three TCAS related risk bearing height deviation incidents (not involving whole numbers of flight levels) between FL290 and FL410 in NAT MNPS airspace during the year 1999 are reported in Appendix A to Reference 31. (The number of flights for the NAT MNPS in 1999 was estimated at 324,295.)

The AAD density $f_{ACAS}^{AAD}(a)$ can be convoluted with the ASE density $f^{ASE}(a)$ defined by equation (4.24) to give a TVE density $f_{ACAS}^{TVE}(z)$. This density can be used in equations (4.14) and (4.17) to produce an estimate $P_z(S_z)_{ACAS}$, say, of the probability of vertical overlap due to ACAS induced large height deviations not involving whole numbers of flight levels. The resulting vertical risk then follows from the model equation (4.10) with $P_z(S_z) = P_z(S_z)_{ACAS}$.

5.3 Vertical Risk Due to all Causes

Let N_{az} denote the vertical collision risk due to all causes. With the modeling discussed above and in Section 4, it follows that

$$N_{az} = N_{az}^{wl} + N_{az}^{lc} + N_{az}^{ACAS} + N_{az}^{tech} \tag{5.14}$$

where

- N_{az}^{wl} is the vertical risk due to aircraft leveling off at a wrong level (equation (5.6));
- N_{az}^{lc} is the vertical risk due to aircraft crossing a flight level without a clearance (equation (5.11));
- N_{az}^{ACAS} is the vertical risk due to ACAS related incidents (equation 4.10 and $P_z(S_z)_{ACAS}$); and
- N_{az}^{tech} is the technical vertical risk (equation (4.10)).

(The direct addition of N_{az}^{ACAS} and N_{az}^{tech} would be expected to be somewhat conservative as the density of typical AAD performance is counted almost twice, i.e. it is used in combination with the densities of atypical AAD due to both non-technical and technical causes. On the other hand, typical AAD does not contribute much to the vertical risk.)

The collision risk models equations (5.6) and (5.11) still have four unknown parameters, namely:

$$a^{wl} = \frac{n^{wl}}{T} \tag{5.15}$$

$$\bar{t}^{wl} \tag{5.16}$$

$$a^{lc} = \frac{n^{lc}}{T} \tag{5.17}$$

$$\overline{|\dot{z}_c|} \tag{5.18}$$

Aena's incident reporting system was queried for large height deviations due to non-technical causes. Only a single vertical incident was found for the years 1999 and 2000. It might be inferred from the description of the incident that it involved an aircraft crossing through two flight levels without a clearance. The description also suggests that it might have concerned a normal climb rate of 20 kts, say. It is not unlikely that there is an issue of underreporting of this kind of large height deviation. Therefore, rather than trying to estimate the risk at the likely cost of it being seriously underestimated, upper bounds for the error rates a^{wl} and a^{lc} based on equating N_{az} to the TLS of 5×10^{-9} were derived. These upper bounds should provide some insight into the level of operational system performance necessary to meet the TLS. It is expected that with additional emphasis on the importance of reporting of large height deviations, some data will become available to confirm that the actual error rates are less than the upper bounds derived from the TLS.

Despite the absence of sufficient data on the four parameters defined by equations (5.15) to (5.18), it is possible to examine the risk as a function of the four parameters over suitable ranges. Reference 24 presents assumed climb/descent rates for different types of incidents as follows:

Table 5-2. Assumed Climb/Descent Rates for Some Height Deviation Incidents (Ref.24)

Event	Assumed climb/descent rate (kts)
Engine failure (aircraft with 3 or more engines)	2
Engine failure (twin engine aircraft)	5
Normal climb/descent	20
Turbulence or TCAS incident	20
Pressurization failure	50

Equation (5.14) has been used to evaluate the vertical risk N_{az} as a function of combinations of a^{wl} and a^{lc} and parameterized by $\bar{t}^{wl}$ and $\overline{|\dot{z}_c|}$. Using the parameter values from Table 4.12, N_{az} can be expressed as

$$\begin{aligned} N_{az} = {} & a^{wl}\times\bar{t}^{wl}\times\left[\left\{E_z(opp)\times0.3543+E_z(90)_{rect}\times6.2717\right\}\times P_z(0)\right]+ \\ & a^{lc}\times\frac{1}{\overline{|\dot{z}_c|}}\times\left[4.2043\times10^{-7}\times\left\{E_z(opp)\times\left(14944.9+348.301+54.8089\times\overline{|\dot{z}_c|}\right)\right\}+\right. \\ & \left.4.2043\times10^{-7}\times\left\{E_z(90)_{rect}\times\left(7851.99+7851.99+54.8089\times\overline{|\dot{z}_c|}\right)\right\}\right]+ \\ & P_z(S_z)_{ACAS}\times\left[E_z(opp)\times0.3543+E_z(90)_{rect}\times6.2717\right]+ \\ & P_z(S_z)\times\left[E_z(opp)\times0.3543+E_z(90)_{rect}\times6.2717\right] \end{aligned} \tag{5.19}$$

or

$$N_{az} = a^{wl} \times \bar{t}^{wl} \times \left[\{E_z(opp) \times 0.3543 + E_z(90)_{rect} \times 6.2717\} \times P_z(0)\right] +$$

$$a^{lc} \times \frac{1}{\overline{|\dot{z}_c|}} \times \left[E_z(opp) \times \left(6.4296 \times 10^{-3} + 2.3043 \times 10^{-5} \times \overline{|\dot{z}_c|}\right) + E_z(90)_{rect} \times \left(6.6023 \times 10^{-3} + 2.3043 \times 10^{-5} \times \overline{|\dot{z}_c|}\right)\right] +$$

$$\left(P_z(S_z)_{ACAS} + P_z(S_z)\right) \times \left[E_z(opp) \times 0.3543 + E_z(90)_{rect} \times 6.2717\right] \tag{5.20}$$

Substitution of $P_z(0) = 0.57$, $P_z(S_z)_{ACAS} = 1.7 \times 10^{-8}$ and $P_z(S_z) = 1.7 \times 10^{-8}$ gives

$$N_{az} = a^{wl} \times \bar{t}^{wl} \times \left[E_z(opp) \times 0.2019 + E_z(90)_{rect} \times 3.5748\right] +$$

$$a^{lc} \times \frac{1}{\overline{|\dot{z}_c|}} \times \left[E_z(opp) \times \left(6.4296 \times 10^{-3} + 2.3043 \times 10^{-5} \times \overline{|\dot{z}_c|}\right) + E_z(90)_{rect} \times \left(6.6023 \times 10^{-3} + 2.3043 \times 10^{-5} \times \overline{|\dot{z}_c|}\right)\right] +$$

$$\left[E_z(opp) \times 1.2046 \times 10^{-8} + E_z(90)_{rect} \times 2.1324 \times 10^{-7}\right] \tag{5.21}$$

Vertical occupancies can be taken from Tables 4.8, 4.9, and 4.10 for current and projected future traffic levels. For current traffic levels and the nominal traffic distribution factor $f = 0.5$, the value for $E_z(opp)$ is 0.1077; and the value for $E_z(90)_{rect}$ is 0.003471. Substitution of these values into equation (5.21) gives

$$N_{az} = a^{wl} \times \bar{t}^{wl} \times 0.034156 + a^{lc} \times \frac{1}{\overline{|\dot{z}_c|}} \times \left[6.9495 \times 10^{-4} + 2.5617 \times 10^{-6} \times \overline{|\dot{z}_c|}\right] + 2.0374 \times 10^{-9} \tag{5.22}$$

Equation (5.22) clearly shows that the vertical risk increases with the error rates a^{wl} and a^{lc} and with the average time $\bar{t}^{wl}$ an aircraft spends at a wrong level after leveling off. It also shows that the risk decreases when the speed $\overline{|\dot{z}_c|}$ with which a flight level is traversed increases.

Figures 5.1A to 5.1C show the vertical risk due to all causes as a function of the error rates a^{wl} and a^{lc} for three different values of the sojourn time $\bar{t}^{wl}$ and a rate of climb/descent of $\overline{|\dot{z}_c|} = 2$ kts. Figures 5.2A to 5.2C and Figures 5.3A to 5.3C show similar dependencies, but for climb rates of 5 and 20kts.

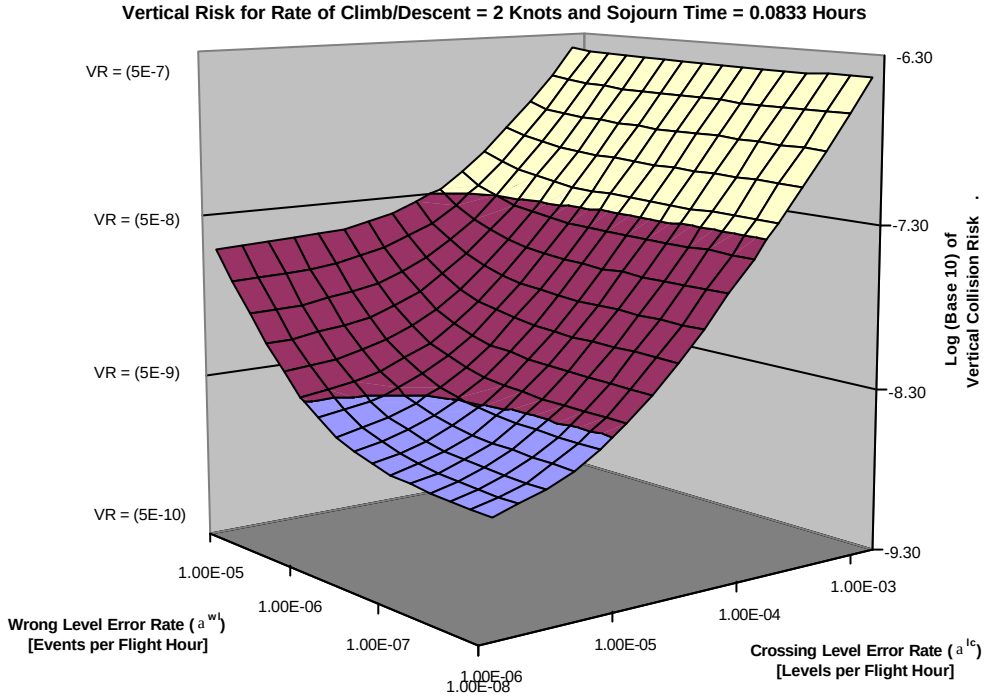

Figure 5-1a. The Vertical Risk Due to All Causes as a Function of the Error Rates a^{wl} and a^{lc}, with $\bar{t}^{wl} = 0.0833$ Flight Hour and $\overline{|\dot{z}_c|} = 2$ kts

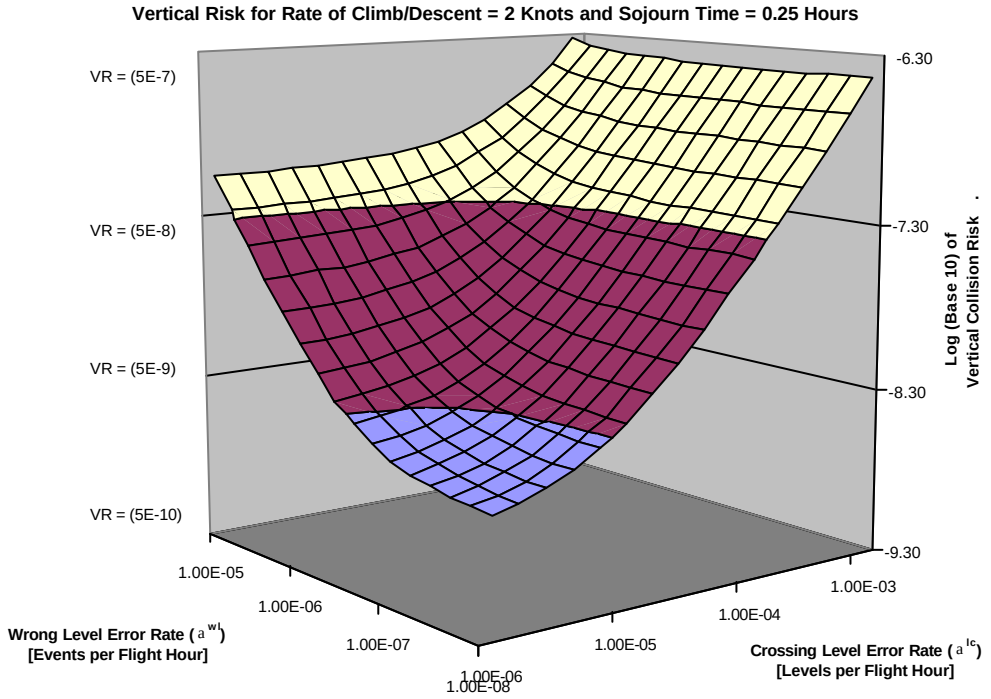

Figure 5-1b. The Vertical Risk Due To All Causes as a Function of the Error Rates a^{wl} and a^{lc}, With $\bar{t}^{wl} = 0.25$ Flight Hour and $\overline{|\dot{z}_c|} = 2$ Kts

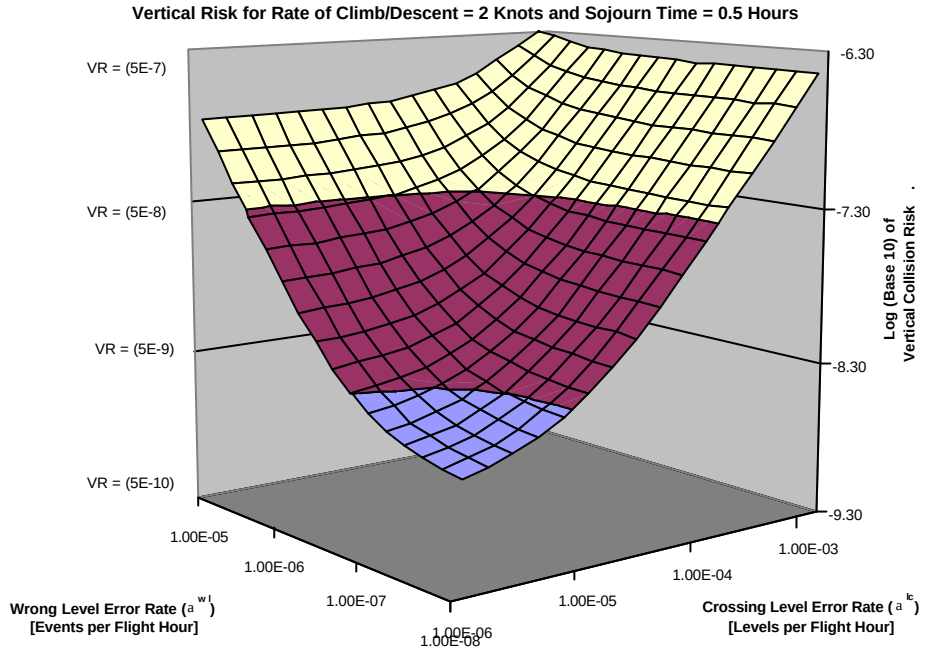

Figure 5-1c. The Vertical Risk Due To All Causes as a Function of the Error Rates a^{wl} and a^{lc}, With $\bar{t}^{wl} = 0.5$ Flight Hour and $\overline{|\dot{z}_c|} = 2$ Kts

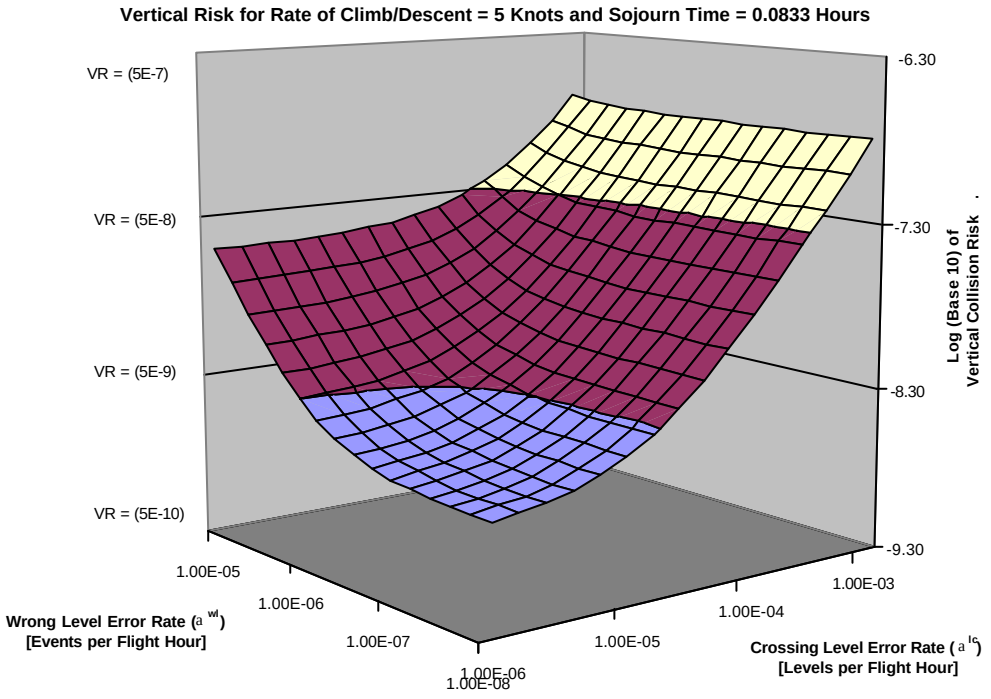

Figure 5-2a. The Vertical Risk Due to All Causes as a Function of the Error Rates a^{wl} and a^{lc}, With $\bar{t}^{wl} = 0.0833$ Flight Hour and $\overline{|\dot{z}_c|} = 5$ Kts

INCRUSTARINCRUSTARINCRUSTARINCRUSTAR

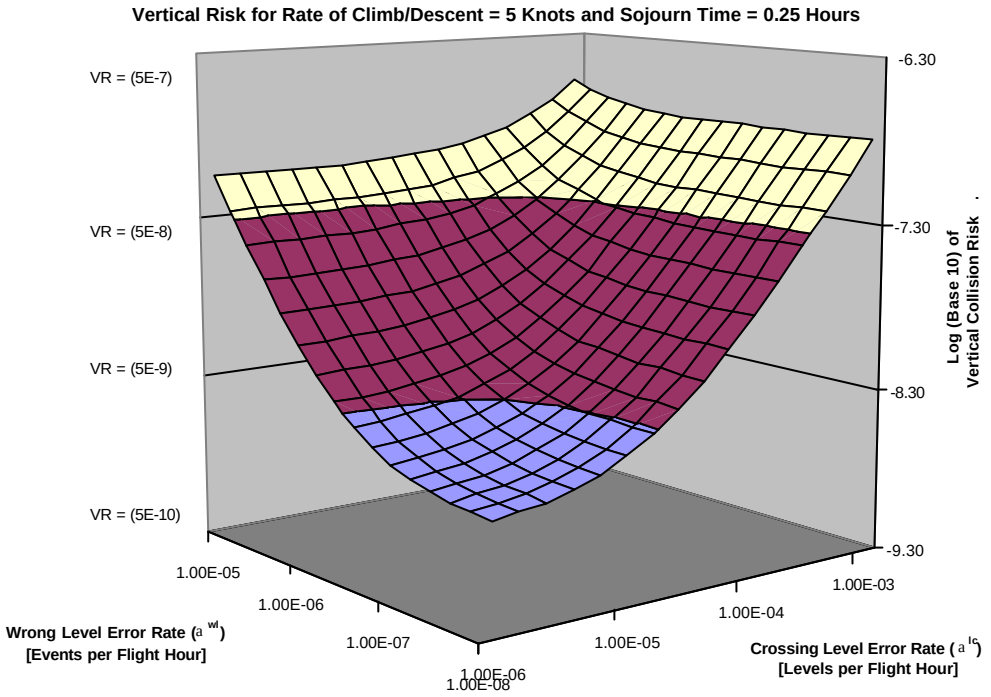

Figure 5-2b. The Vertical Risk Due to all Causes as a Function of the Error Rates a^{wl} and a^{lc}, With $\bar{t}^{wl} = 0.25$ Flight Hour and $\overline{|\dot{z}_c|} = 5$ Kts

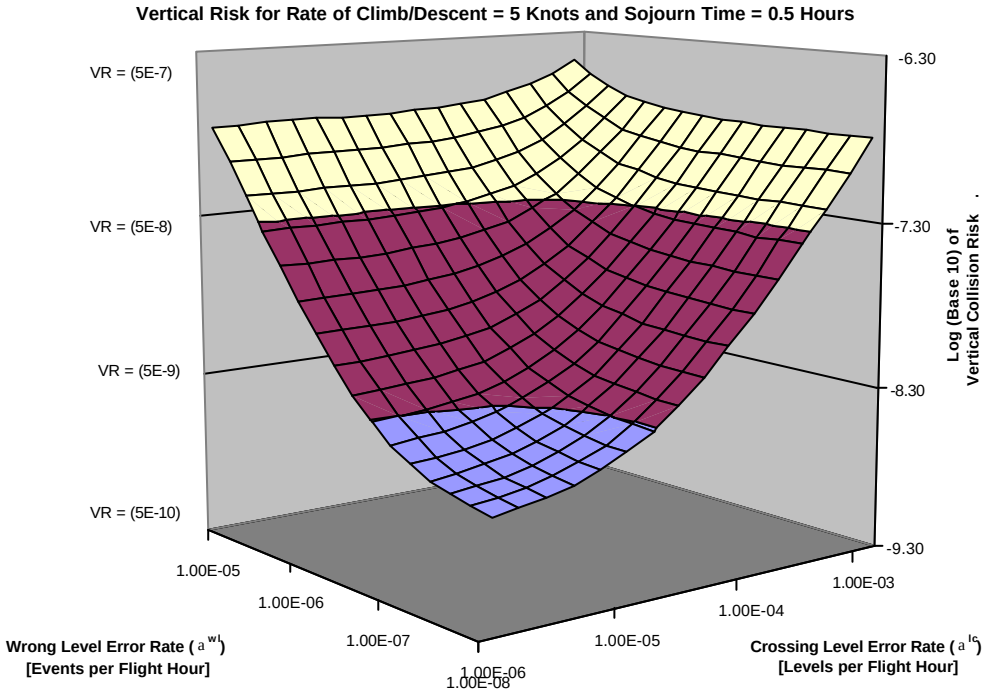

Figure 5-2c. The Vertical Risk Due to all Causes as a Function of the Error Rates a^{wl} and a^{lc}, With $\bar{t}^{wl} = 0.5$ Flight Hour and $\overline{|\dot{z}_c|} = 5$ Kts

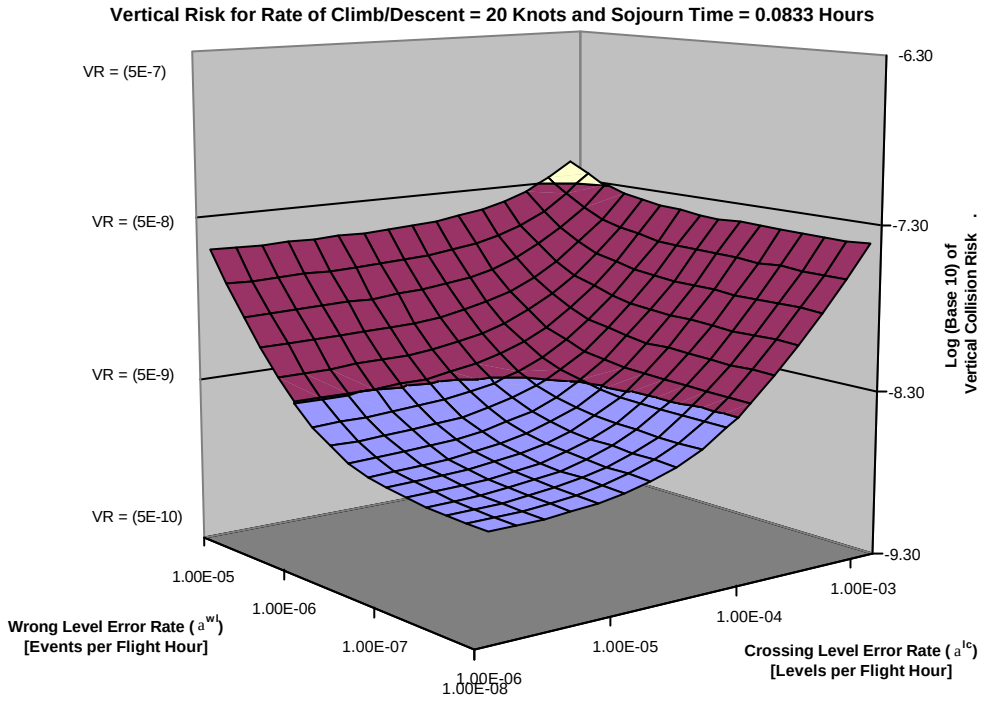

Figure 5-3a. The Vertical Risk Due to all Causes as a Function of the Error Rates a^{wl} and a^{lc}, With $\bar{t}^{wl} = 0.0833$ Flight Hour and $\overline{|\dot{z}_c|} = 20$ Kts

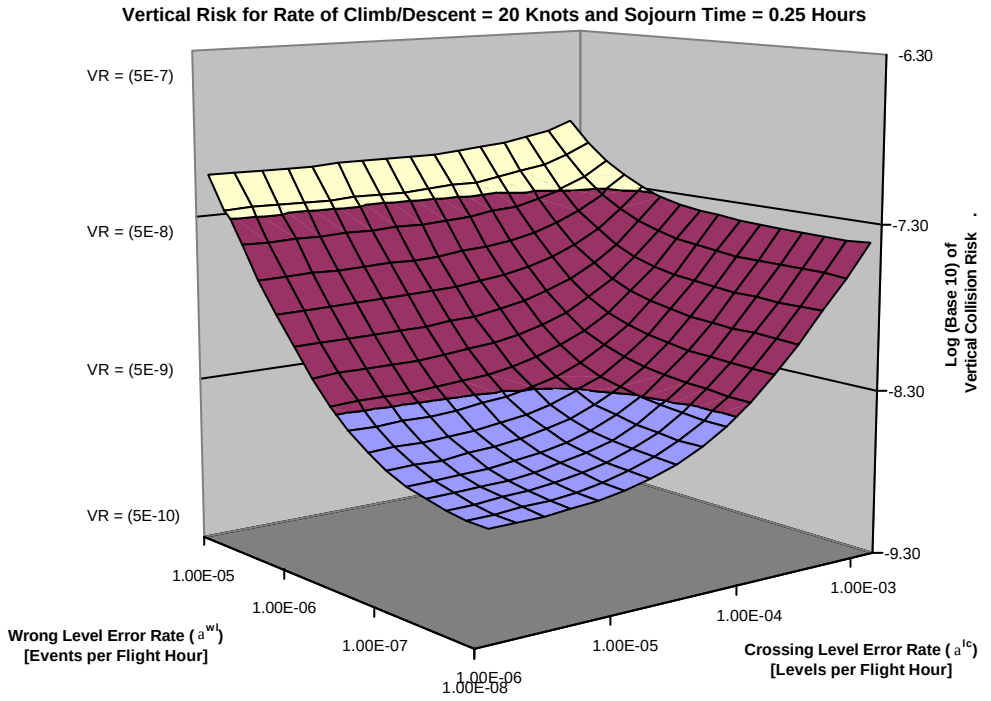

Figure 5-3b. The Vertical Risk Due to all Causes as a Function of the Error Rates a^{wl} and a^{lc}, With $\bar{t}^{wl} = 0.25$ Flight Hour and $\overline{|\dot{z}_c|} = 20$ Kts

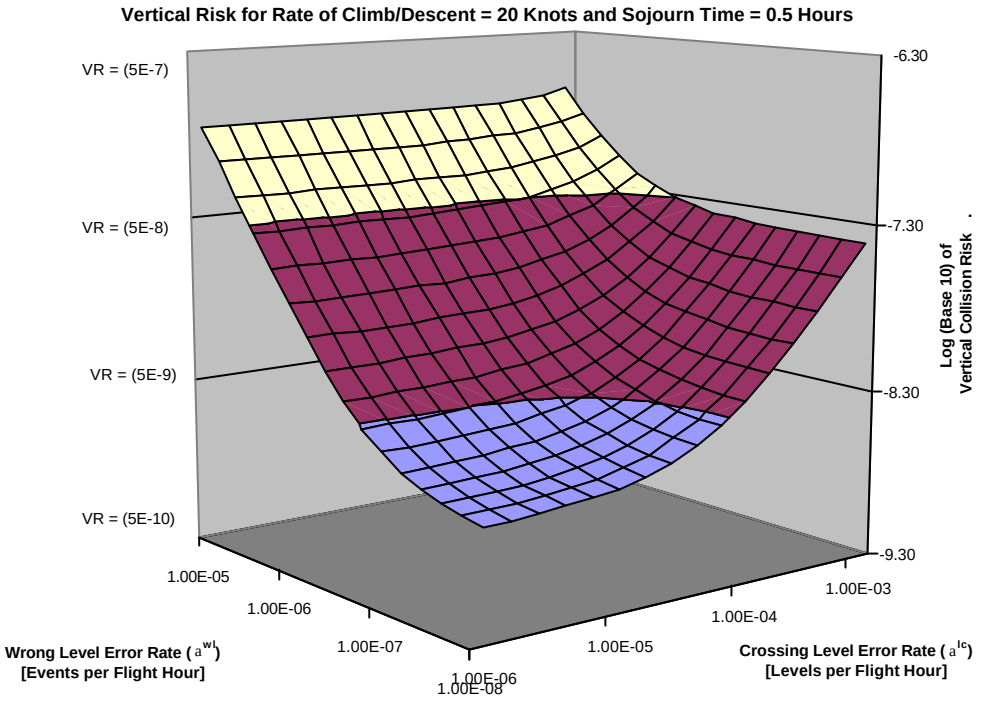

Figure 5-3c. The Vertical Risk Due to all Causes as a Function of the Error Rates a^{wl} and a^{lc}, With $\bar{t}^{wl} = 0.5$ Flight Hour and $\overline{|\dot{z}_c|} = 20$ Kts

As N_{az} represents the vertical risk due to all causes, it needs to be compared with a TLS of 5×10^{-9} accidents per flight hour. The diagrams above have been constructed such that the 5×10^{-9} level coincides with the boundary between the blue and purple parts of the risk surfaces. Thus, the acceptable combinations of the error rates a^{wl} and a^{lc}, acceptable in the sense of making the risk no greater than the TLS, are defined by the lowest, blue-colored, region of the risk surfaces.

The precise boundaries are shown in the Figures 5.4 to 5.6, which are two-dimensional views *down* through the plane defined by the TLS at surfaces for *all three* of the sojourn times. Keep in mind that both axes on these plots are logarithmic. Figure 5.6 shows that if indeed only two flight levels would have been crossed without a clearance during the years 1999 and 2000, and if there would have been no leveling-off at the wrong flight level, then this number of errors would have been acceptable, i.e. the TLS of 5×10^{-9} would not have been exceeded. This is based on an error rate a^{lc} of approximately 2.6×10^{-5}, i.e. $2/(60\times365\times3.5)$. The same diagram shows that this error rate in combination with wrong level errors would not lead to breaching the TLS provided the rate of the latter error is not greater than about 6×10^{-8}.

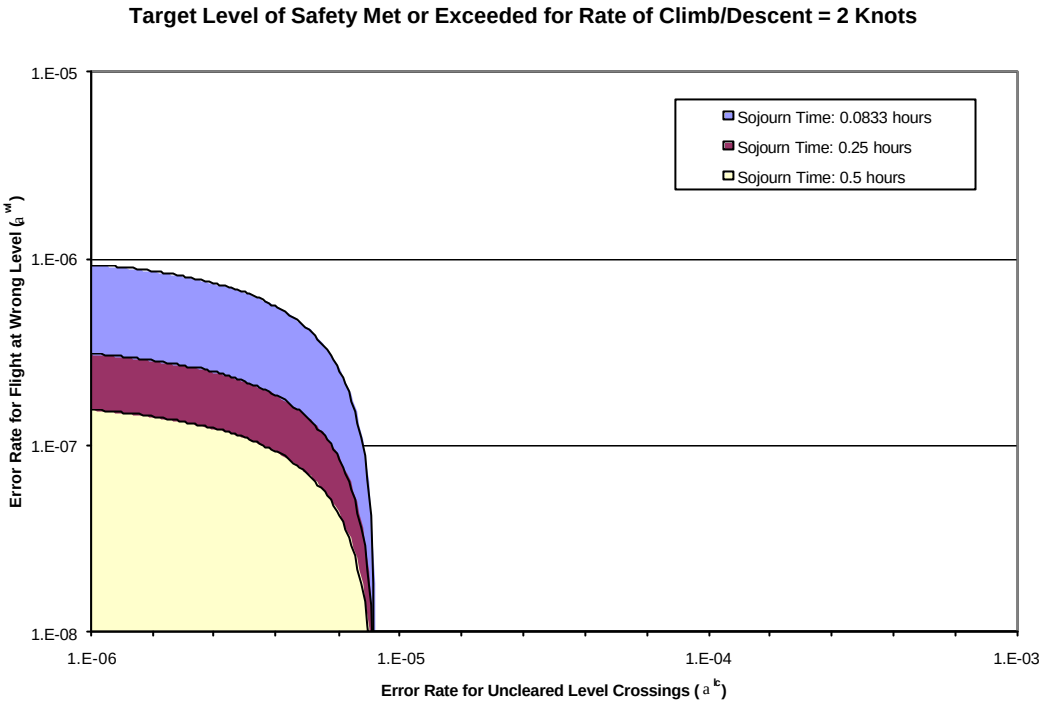

Figure 5-4. Acceptable Combinations of the Error Rates a^{wl} and a^{lc} for Three Different Values of $\bar{t}^{wl}$ and $\overline{|\dot{z}_c|} = 2$ kts

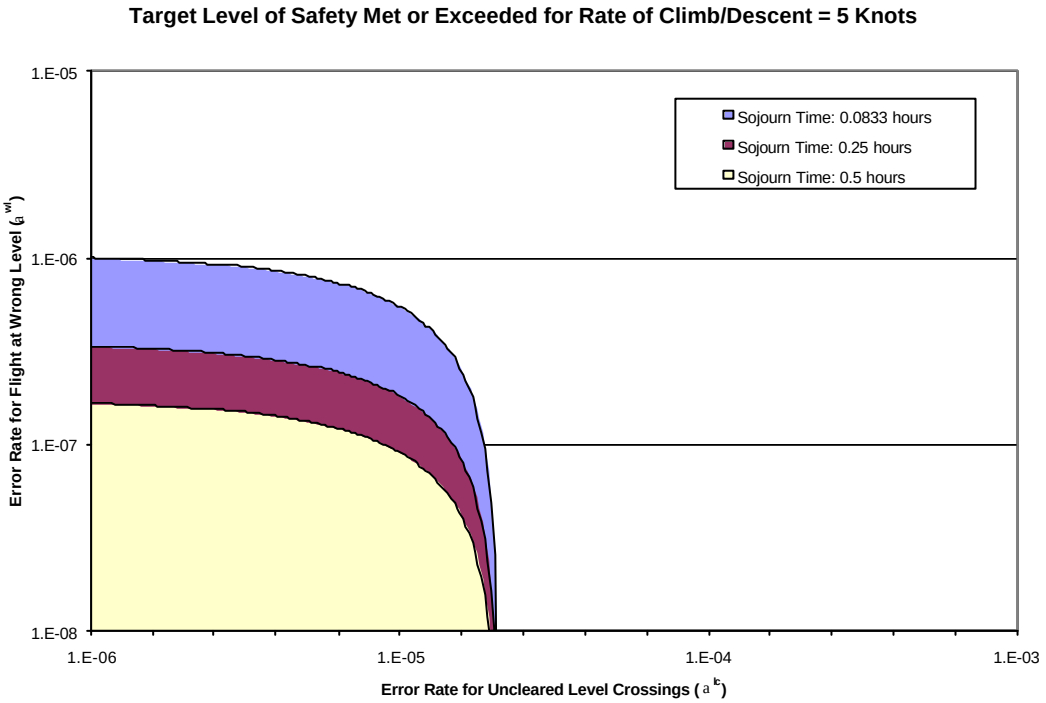

Figure 5-5. Acceptable Combinations of the Error Rates a^{wl} and a^{lc} for Three Different Values of $\bar{t}^{wl}$ and $\overline{|\dot{z}_c|} = 5$ kts

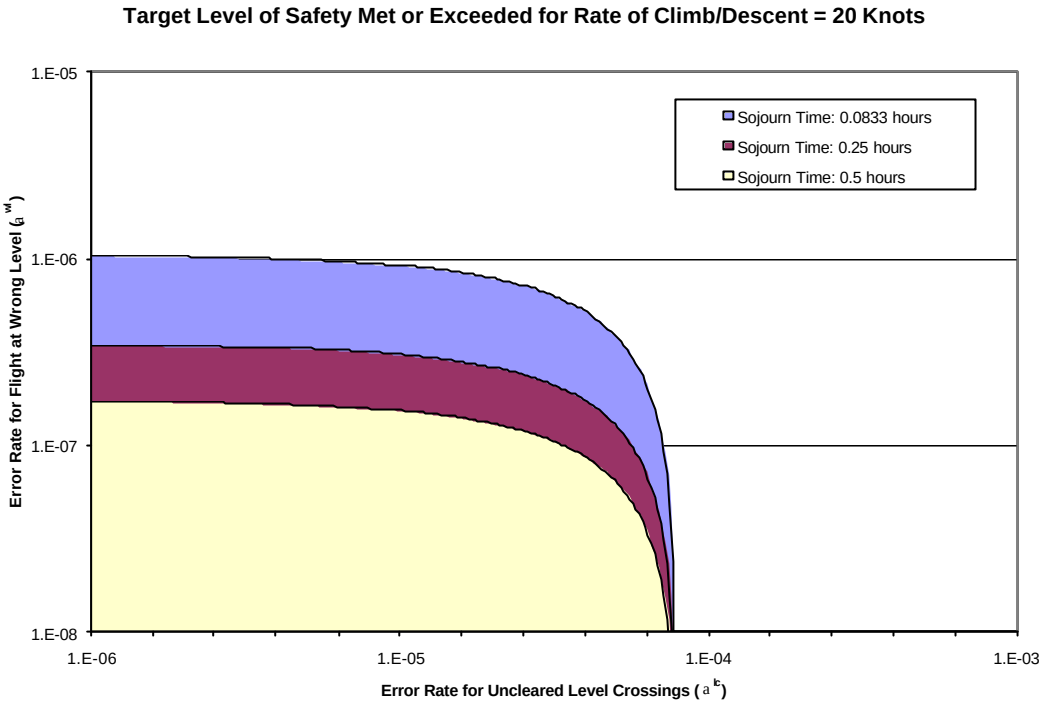

INCRUSTARINCRUSTARINCRUSTARINCRUSTAR

Figure 5-6. Acceptable Combinations of the Error Rates a^{wl} and a^{lc} for Three Different Values of $\bar{t}^{wl}$ and $\overline{|\dot{z}_c|} = 20$ kts

There are two simple cases that can easily be investigated. If no aircraft would be crossing any flight levels without a clearance, i.e. $a^{lc} = 0$, then equation (5.22) can be used to calculate the value of a^{wl} which would make the estimate of the risk just equal to the TLS of 5×10^{-9}. Table 5.3 shows this value as a function of the average sojourn time $\bar{t}^{wl}$.

Table 5-3. Maximum Value of Error Rate a^{wl} for Aircraft Leveling Off at a Wrong Level

Average sojourn time $\bar{t}^{wl}$ for an aircraft leveling off at a wrong level (flight hour)	Maximum value of error rate a^{wl} for aircraft leveling off at a wrong level (events per flight hour)
0.0833	8.464E-06
0.25	2.093E-05
0.50	7.941E-05

INCRUSTAR

Similarly, when no aircraft would be leveling off at a wrong level, i.e. $a^{wl} = 0$, then equation (5.22) can be used to calculate the value of a^{lc} which would make the estimate of the risk just equal to the TLS of 5×10^{-9}. Table 5.4 shows this value as a function of the rate of climb/descent $\overline{|\dot{z}_c|}$.

Table 5-4. Maximum Value of Error Rate a^{lc} for Aircraft Crossing a Flight Level Without Clearance

Rate of climb/descent (kts)	Maximum value of error rate a^{lc} for aircraft crossing a flight level without clearance (number of levels crossed per flight hour)
2	7.997E-06
5	1.829E-05
20	5.131E-05

INCRUSTAR

To tie these somewhat abstract numbers back to the EUR/SAM Corridor, assume that there are 60 flights a day, with an average flight time of 3.5 hours. This corresponds to 76,650 flight hours per year. Thus, at the current traffic levels, the EUR/SAM Corridor can tolerate about 34 seconds *per year* (corresponding to an error rate of a^{wl} = 1.25E-07) of aircraft leveling off at a wrong level, or about 4 flight levels crossed at 20 kts without clearance *per year*, without exceeding the TLS.

An issue that might need to be addressed at some stage is the possible risk due to non-MASPS approved aircraft entering the RVSM airspace in the SAT. This situation might occasionally occur during the early implementation of RVSM but should disappear quickly.

6 Conclusions

6.1 General

Two quantitative risk assessments based on suitable versions of the Reich collision risk model have been carried out for the EUR/SAM Corridor in the South Atlantic. The first assessment concerned the safety of 50 NM lateral separation between (some of) the tracks of a proposed new track structure based on the airspace becoming RNP10. The second concerned the safety of the implementation of the Reduced Vertical Separation Minimum (RVSM) between FL290 and FL410 inclusive.

In addition to the specific conclusions resulting from the quantitative safety assessments, it is important that the accomplishment of operational measures and procedures by the operators and state authorities as described in the pertinent ICAO regulations and guidance material for the implementation of RNP10/50 NM lateral separation minimum and RVSM be ensured by the SATMA. This concerns, for example, ensuring the approval status of the aircraft population.

6.2 Data Availability

The main parameters of the lateral and vertical collision risk models are the probabilities of lateral and vertical overlap, respectively. Data needed for the computation of lateral and vertical overlap probabilities are the distributions of the lateral and vertical deviations of aircraft from their assigned flight paths. The risk assessments in this report were hindered considerably by a lack of data on these deviations, particularly on the larger and more infrequent deviations. As a result, assumptions were made for certain parts of these distributions. Such assumptions, in the context of safety assessments, have to be conservative by definition. In order to confirm the validity of the assumptions made or to reduce the resulting, possibly too conservative, risk estimates, it is recommended that additional data collections be mounted and/or appropriate monitoring procedures be developed in all of the affected EUR/SAM Corridor FIR/UIRs on implementation of the proposed separation minima.

The next important parameters of the two collision risk models are the lateral and vertical occupancies. These are measures of the exposure to the loss of lateral and vertical separation in relation to the amount of traffic in the airspace. In general, a good amount of data was available for the estimation of occupancy. However, three issues relevant to the assessment of lateral and vertical separation maintenance need to be mentioned.

First, some inconsistencies in the data were anticipated as a result of a preliminary assessment of the current methodology of operation of the airspace. Such inconsistencies were found to be present indeed and an attempt to account for such inconsistencies has been made in the analysis. Second, data have not been equally available from the different FIR/UIRs that make up the airspace of the EUR/SAM Corridor. Additional data would improve the representation and precision of the occupancy estimates. Third, relatively little data were available on traffic crossing the main Corridor although there is ample evidence that such crossings are regularly occurring. Again, data from all ACCs would improve the quality of the estimates of crossing

track vertical occupancy. The establishment of crossing routes as "officially sanctioned" Trans-Atlantic air routes would also facilitate traffic data reporting for the crossing routes.

Although the amount of data on traffic crossing the main Corridor was limited, the available data did include a number of situations where aircraft at the same flight level seemed to be crossing one another's path with less than 10 minutes separation. Such situations would not be acceptable from a safety point of view and procedures should be developed to prevent their occurrence in future. There are some indications that these aircraft may have been vertically separated by ATC at the time of crossing, however, the data is incomplete and requires further investigation.

6.3 EUR/SAM Corridor Traffic Growth

Traffic growth affects lateral and vertical occupancies. Based on an annual traffic growth rate of 5.1%, occupancies have been projected forward over a ten-year planning horizon, resulting in an overall growth factor of 1.64. Comparison figures were also developed and presented for a projected growth rate of 8% per year resulting in an overall growth factor of 2.16. In the year 2002 with the implementation of RVSM, it is projected that the lateral occupancy will be reduced at least 15% due to the distribution of traffic over the new flight levels. The reduced occupancy will also reduce the projected 10-year growth factor from 1.64 to 1.40 for a growth rate of 5.1% per year and from 2.16 to 1.84 for the growth rate of 8% per year.

6.4 Lateral Collision Risk Assessment

A lateral collision risk assessment for 50 NM lateral spacing in the NOPAC RNP10 airspace as referred to in Attachment B to ICAO Annex 11 was taken as a basis for assessing the EUR/SAM Corridor lateral collision risk. It is important to recognize, however, that the NOPAC analysis was based on a Target Level of Safety of 2×10^{-8} accidents per flight hour whereas the current assessment, concerning an implementation after the year 2000, is based on the more stringent TLS of 5×10^{-9} accidents per flight hour. This puts, in particular, more stringent limits on the frequency of large lateral deviations that may be tolerated in EUR/SAM Corridor airspace.

Estimates of lateral collision risk in the proposed track system based on current and projected traffic levels have been calculated, taking into account the loss of lateral separation between aircraft on adjacent tracks with 50 NM spacing, S_y, as well as on non-adjacent tracks separated by twice S_y (*i.e.*, 100NM).

For current traffic levels, the estimated lateral collision risk was in the range of 1.365×10^{-9} to 3.749×10^{-9} accidents per flight hour, depending on the traffic distribution factor. The lower value corresponds with all the traffic being assigned to the new eastern-most route UN857 and is equivalent to the current track structure; the upper value corresponds with 70% of the traffic being assigned to the added route UN873. For an equal split of the traffic between the two new eastern-most routes, the estimate of the lateral collision risk is INCRUSTAR 3.615×10^{-9}. INCRUSTARThis shows that the TLS can be met with the implementation of RNP10 on the new proposed route structure for current traffic levels.

Given the assumptions made in the projection of occupancies over a ten year planning horizon, estimated lateral collision risk for future traffic levels were obtained by multiplying the estimates for current traffic levels by the overall growth factor of 1.40 and 1.84 corresponding to traffic growth rates of 5.1% and 8% per year respectively. Thus, the estimated lateral risk for future traffic levels using a growth factor of 1.40 was in the range of 1.908×10^{-9} to 5.240×10^{-9} depending on the traffic distribution factor. The lower value corresponds again with all the traffic on the existing route UA32 being assigned to the new eastern-most route UN857. Using the projected growth rate of 5.1% per year, the TLS of 5×10^{-9} accidents per flight hour is only exceeded in year 2010 when the traffic distribution factor is between $f = 0.5$ to 0.8, but the risk is below the TLS for the lower and higher distribution values.INCRUSTARINCRUSTAR

When the existing occupancy is projected over a ten year period using the 8% per year growth rate, the estimated lateral risk was in the range of 2.505×10^{-9} to 6.879×10^{-9} where the larger value occurred when the distribution of traffic was 70% on route UN873 or 30% on route UN857. At this level of growth, all lateral risk projections for the year 2010 were over the TLS when the distribution of traffic was more than 30% to UN873. For the nominal traffic distribution where $f = 0.5$, using an 8% growth rate the TLS begins to be exceeded in year 2006 and beyond.

Different causes of large lateral deviations result in different lateral risks. In the Reich-type collision risk model used for the analysis, this is reflected in the probability distribution of the lateral deviations associated with the anomaly and the average lateral speed between aircraft that have lost lateral separation. A query of the database of the Incident Reporting System maintained by AENA showed that data on individual causes of lateral deviations required to facilitate a such-like type of modeling were not available. A more global type of modeling, therefore, has had to be used. Of necessity, as this was to cover different types of causes, the analysis tends to be on the conservative side.

In fact, the query for data on individual causes of lateral deviation resulted in no data being available on lateral separation related incidents. Although it may be concluded that such incidents did not therefore occur in the EUR/SAM Corridor, there are two reasons for not drawing that conclusion. First, it is likely that not every occurrence of such incidents is being reported, because the incident may not have been perceived as a (major) safety related issue. Second, experiential information from other airspace analyses suggests that lateral separation related anomalies do occur in practice and are probably present in the EUR/SAM Corridor.

Within the global type of modeling, the probability distribution of the lateral deviations from flight path has been modeled as a "double double exponential probability distribution." This type of distribution has been used in various other lateral separation studies. The parameter related to the core part of the distribution used for the analysis was derived from the RNP type, i.e. RNP10. Given the lack of actual data from the FIR/UIRs for the EUR/SAM Corridor, the parameters of the tail part of the distribution have been determined in a conservative manner. The sensitivity of the probability of lateral overlap to the parameters of the distribution of the lateral deviations was examined within the analysis.

Based on the core part of the lateral deviation distribution alone, the probability of lateral overlap was equal to 2.1466×10^{-8}. Based on the full model of the lateral deviation distribution, the probability of lateral overlap $P_y(S_y)$ with $S_y = 50NM$ was found to be 7.858×10^{-8}, i.e. approximately four times larger. The probability of lateral overlap between aircraft on tracks separated by twice the lateral separation standard was also calculated and found to be $P_y(2S_y) = 2.101\times10^{-8}$, approximately the same value as the probability of lateral overlap between aircraft separated by the separation minimum of 50 NM due to RNP performance alone. In considering the values of $P_y(S_y)$ and $P_y(2S_y)$, it has been necessary to include in the collision risk model both the risks associated with the loss of S_y NM of lateral separation and that due to the loss of $2S_y$ NM of lateral separation.

Through use of global type of modeling of the lateral deviation distribution, a smaller value of the probability of lateral overlap can be obtained in two ways. The most important one is to show that the actual tail part of the distribution of the lateral deviations is smaller than that assumed in the current conservative analysis. Second, requiring a more stringent RNP type (such as RNP-8 or RNP-6) has a positive effect on the value of the probability of lateral overlap. In the latter context, actual data on the core part of the lateral deviation distribution might be used to demonstrate that the contribution of the core deviations to the probability of lateral overlap is less than that shown in the analysis due to the manner in which the RNP value contributes to the analysis results. In addition, when sufficient data is made available that will allow more accurate modeling of the probability distributions of large lateral deviations due to individual causes, a smaller value of the probability of lateral overlap is likely to result, based upon previous analytical projects of this type. At the same time, this should allow a more precise modeling of the relative lateral speed between two aircraft that have lost lateral separation due to a particular cause. This is important because the lateral risk is sensitive to the value of this parameter.

The estimation of occupancy for the proposed track system required the analysis team to make detailed assumptions of the distribution and flight level loading on the traffic flows in the proposed system. It is important to verify that the real traffic flows in the proposed system after implementation do not result in occupancy values that are larger than the current estimates in order to meet the TLS rate. The TLS begins to be exceeded in year 2006 and beyond.

Using the growth rate of 5.1%, the estimates of the lateral collision risk indicate that implementation of 50 NM lateral spacing between UN866 and the new routes UN873 and UN857 of the proposed track system in the EUR/SAM Corridor is currently fully supported by the analysis results. This conclusion is reached despite the conservative approach used in the assessment. More information on the types and number of lateral deviations in the region would allow less conservative modeling of the probability distribution of lateral deviations, which could lead to lower risk predictions in the future.
INCRUSTARINCRUSTARINCRUSTARINCRUSTARINCRUSTARINCRUSTARINCRUSTARINCRUST
ARINCRUSTARINCRUSTARINCRUSTARINCRUSTARINCRUSTARINCRUSTARINCRUSTARINCRU
STARINCRUSTAR
As a means of verifying the assumptions used in the assessment of lateral collision risk, it is recommended that accurate flight progress data for two (2) days a month, e.g. the 4th and the 15th

days be collected and made available from all the FIR/UIRs to facilitate estimation of same direction lateral occupancy after implementation of RNP10/50 NM lateral separation in the EUR/SAM Corridor. Continuous data, 24 hours per day for periods ranging from several months to a year would also facilitate computing speeds, identifying crossing traffic occupancies, and correcting erroneous manual data entries.

6.5 Vertical Collision Risk Assessment

The vertical collision risk assessment was split into two parts. The first part considered the vertical collision risk due to technical causes. The estimated risk was compared with a Target Level of Safety (TLS) of 2.5×10^{-9} accidents per flight hour. The second part examined the vertical collision risk due to all causes and compared this with an overall vertical TLS of 5×10^{-9} accidents per flight hour. The main difference between the collision risk models for vertical risk due to technical causes or to all causes concerns the modeling and estimation of the probability of vertical overlap.

Estimates of technical vertical collision risk in the proposed track system with RVSM based on current and projected traffic levels were calculated, taking into account both opposite direction and crossing traffic and two different models of the probability distribution of the aircraft height-keeping deviations. One model was based on the height keeping performance of similar aircraft in the NAT and did not contain deviations resulting from weather turbulence. This value was smaller than the result of the second model that did include deviation information from weather turbulence.

For current traffic levels, the estimated vertical collision risk based on the smaller value of the probability of vertical overlap ($P_z(1000) = 4.5263\times10^{-9}$) was in the range of 2.713 x 10^{-10} to 3.294 x 10^{-10} accidents per flight hour, depending on the traffic distribution factor. The lower value corresponds to an equal split of the traffic on the original route UA32 between the two new eastern-most routes UN873 and UN857. The technical vertical risk is symmetrical about an equal traffic split. Thus, the upper value corresponds with either no or all the traffic being assigned to the new eastern-most route UN857. The above range is well below the TLS of 2.5×10^{-9} for the technical vertical risk.

The estimated technical vertical collision risk for current traffic levels based on the larger value of the probability of vertical overlap ($P_z(1000) = 2.1346\times10^{-8}$) was in the range of 1.279 x 10^{-9} to 1.554 x 10^{-9} accidents per flight hour and also meets the TLS requirement of 2.5×10^{-9} for the technical vertical risk.

On the basis of the vertical occupancies projected forward over a ten year planning horizon, the estimated technical vertical collision risk for future traffic levels was obtained by multiplying the estimates for current traffic levels by the overall growth factors of 1.64 and 2.16 corresponding to traffic growth rates of 5.1% and 8% per year respectively. Thus, for the growth factor of 1.64, the estimated technical vertical risk for future traffic levels was in the range of 4.461 x 10^{-10} to 5.417 x 10^{-10} for the smaller value of the probability of vertical overlap and in the range of 2.104 x 10^{-9} to 2.555 x 10^{-9} for the larger value of the vertical overlap probability. The range of values

depends on the distribution of traffic over the two new routes UN857 and UN873. The former range is well below the TLS for technical vertical risk, but the latter range exceeds the TLS at the extreme limits of the traffic distributions in 2010. The estimated technical vertical risk for future traffic levels based on a growth factor 2.16 was in the range of 5.875×10^{-10} to 7.112×10^{-10} for the smaller value of the probability of vertical overlap and in the range of 2.762×10^{-9} to 3.354×10^{-9} for the larger value of the vertical overlap probability. The former range is also well below the TLS for technical vertical risk, but the latter range exceeds the TLS for all values of the traffic distributions in the year 2010.

Given the values of opposite direction and crossing track vertical occupancy, the above estimates of vertical collision risk are in fact dominated by the opposite direction traffic component. The other important factor is the probability of vertical overlap.

The estimation of the probability of vertical overlap due to technical causes was based on the probability distribution of Total Vertical Error (TVE). This was obtained by convoluting probability distributions of Altimetry System error (ASE) and Flight Technical Error (FTE). In the absence of any direct height monitoring data from the EUR/SAM Corridor, it was necessary to use height-keeping data and models from the North Atlantic (NAT) height-monitoring program for estimating these parameters. In order to approximate the characteristics of the aircraft population in the EUR/SAM Corridor, the proportions of flights by aircraft type were used to construct a representative ASE probability distribution as a weighted mixture of ASE probability distributions by aircraft type. Double double exponential probability distribution models of AAD obtained from the NAT approximated the probability distribution of FTE. Two different AAD models have been used, the models differing with regard to the amount of data on large deviations due to turbulence being included. Consequently, two different TVE distributions were obtained.

The probability of vertical overlap $P_z(S_z)$ with $S_z = 1000\,\text{ft}$ was found to be 4.53×10^{-9} or 2.13×10^{-8} depending on which TVE/AAD model was used. This range reflects the influence of the tail of the AAD distribution and hence the importance of verifying the representation of the AAD models for the South Atlantic.

INCRUSTARINCRUSTARINCRUSTARINCRUSTARINCRUSTARINCRUSTARA couple of routes cross the main traffic flow in the EUR/SAM Corridor under angles of approximately 90º. Based on flight progress data from some of the crossing routes for August and September 2000, a vertical crossing track occupancy estimate of 0.003471 was obtained for the proposed track system and current traffic levels. INCRUSTARThis value is about 30% of opposite direction vertical occupancy. Note that this estimate of the crossing traffic occupancy does not include any crossing traffic in the Sal or Dakar Oceanic UIRs, for which no data was made available.

The analysis of the data set on crossing traffic showed a number of anomalies involving aircraft crossing at the same flight level. Further examination of these anomalies is recommended to determine if it is necessary to develop suitable procedures for preventing their re-occurrence in the future.

In the same way as for the lateral risk assessment, the estimation of vertical occupancy for the proposed track system with RVSM required making a number of assumptions on the distribution of traffic over the available flight paths. Therefore, it is again important to verify these assumptions prior to RVSM implementation in the EUR/SAM Corridor. An appropriate correction factor should be defined when sufficient data becomes available.

Accurate flight progress data for two days a month, e.g. the 4^{th} and the 15^{th} days of the month, should be made available from all the FIR/UIRs to facilitate estimation of vertical occupancy after implementation of RVSM in the EUR/SAM Corridor. This should cover the main traffic flow as well as the crossing routes. Again, continuous data collection covering extended periods of time supports even more accurate evaluation of vertical occupancy.

The probability of lateral overlap for aircraft on the same track has considerable impact on the vertical collision risk. It is quite clear from the analysis that as lateral navigation performance becomes more accurate, the probability of lateral overlap increases and hence also the vertical collision risk. Formally, the lateral navigation performance for this probability may be estimated from the RNP value for the airspace. However, with a view to future improved lateral navigation performance due primarily to the use of GPS, the (larger) value of the probability of lateral overlap from the global system performance specification for aircraft on the same track has been used.

To predict the vertical collision risk due to all causes, several models have been developed for the identification of vertical collision risk due to non-technical deviations caused by ATC-pilot loop errors and incorrect clearances, aircraft contingency events, and deviations due to ACAS (TCAS). A distinction was made between large height deviations involving whole numbers of flight levels and large height deviations not involving whole numbers of flight levels. The latter category generally covers height deviations due to an ACAS (TCAS) alert. The former category covers ATC-pilot loop errors and incorrect clearances. For such errors it was assumed that they would result in an aircraft leveling off at a wrong flight level and/or climbing or descending through one or more flight levels without a clearance.

In order to effectively exercise these models it is necessary to analyze large height keeping deviations and model the distributions. Aena's incident reporting system database was queried for data on large height keeping deviations due to non-technical causes. It was concluded that there were insufficient data on these deviations to quantify the remaining collision risk model parameters. Therefore, rather than actually estimating the vertical risk due to all causes, upper bounds on the frequencies of aircraft leveling off at a wrong level or passing through other flight levels were derived using the difference between the technical vertical risk and the TLS of 5×10^{-9} accidents per flight hour to calculate the allowable deviations due to these causes.

In order to relate the resulting error rates back to the EUR/SAM Corridor, it was assumed that there are 60 flights a day, with an average flight time of 3.5 hours. This corresponds to 76,650 flight hours per year. Thus, at the current traffic levels, the EUR/SAM Corridor can tolerate about 34 seconds *per year* of aircraft leveling off at a wrong level, or about 4 flight levels crossed at 20 kts without clearance *per year*, without exceeding the TLS.

7 References

1. Manual on Airspace Planning Methodology for the determination of separation minima, Doc 9689-AN/953, ICAO, Montreal, First edition – 1998.
2. International Standards and Recommended practices AIR TRAFFIC SERVICES Air Traffic Control Service Flight Information Service Alerting Service, Annex 11 to the Convention on International Civil Aviation, ICAO, Montreal, Twelfth edition – July 1998.
3. P.G. Reich, Analysis of long-range air traffic systems: separation standards, Part I, Journal of Navigation (UK), Vol. 19, No. 115, pp. 88 – 98.
4. P.G. Reich, Analysis of long-range air traffic systems: separation standards, Part II, Journal of Navigation (UK), Vol. 19, No. 116, pp. 169 – 193.
5. P.G. Reich, Analysis of long-range air traffic systems: separation standards, Part III, Journal of Navigation (UK), Vol. 19, No. 117, pp. 331 – 347.
6. AIC for the implementation of RNP10 in the Corridor between Europe and South America (EUR/SAM Corridor), Spain, …..2000.
7. AIC for the implementation of RVSM in the Corridor between Europe and South America (EUR/SAM Corridor), Spain, …..2000.
8. Regional Supplementary Procedures, ICAO, Montreal, Doc 7030/4, Fourth edition – 1987.
9. Documenting the rationale supporting 50NM route spacing in North Pacific airspace, RGCSP/10-WP/22, ICAO, Montreal, May 2000.
10. Capabilities of FANS-1/A aircraft which can lead to separation standards reductions, RGCSP-WG/A-IP/17, Shizuoka, Japan, September 1994.
11. Analysis of 50NM lateral separation, Appendix to the PAC SUPP Amendment proposal in 1998, APAC-S 95/13, ICAO Bangkok Office, 1998.
12. Air Traffic Services Planning Manual, first edition – 1984, ICAO Montreal, Appendices A – C to Part II, Section 2, Chapter 4, ICAO, Montreal, Doc 9426-AN/924.
13. P. Brooker and F.A. White, Minimum Navigation Performance Specifications and other separation variables in the North Atlantic area, Journal of Navigation (UK), Vol. 32, No. 3, pp. 357 – 374.
14. L. Davies and A. Sharpe, Review of the North Atlantic lateral collision risk model, Air Traffic Control Quarterly. Vol. 1 No.3, pp. 225 –254, 1993.
15. Methodology for the derivation of separation minima applied to the spacing between parallel tracks in ATS route structures, ICAO, Montreal, Circular 120-AN/89/2, second edition, 1976.
16. L.Burt, Assessment of the safe separation between parallel tracks for aircraft with varying RNAV capabilities, RGCSP-WG/A-WP/12, Seattle, September 1993.
17. R. Rawlings, M.B. Perry and L. Burt, Operation on the BRNAV routes from the Iberian Peninsula to the Canaries, EURONTROL, NSSG, September 1997.
18. P. Olarte, Safety Analysis of GPS operations in the routes from the Iberian Peninsula to the Canaries, EUROCONTROL MDG/15-DP/03, December 1999.
19. K. Slater, 1999 Lateral collision risk estimate for NAT MNPS airspace, NAT SPG/36 MWG WP/6 (Revised), ICAO, Paris, May 2000.
20. A. Pool and J.J. Renes, Preliminary assessment of the safe separation between the centre lines of parallel routes with opposite-direction traffic using model studies, National

Aerospace Laboratory NLR, Amsterdam, The Netherlands, NLR TR 73091U, February 1974.
21. Review of the General Concept of Separation Panel, Report of the sixth meeting, ICAO, Montreal, December 1988.
22. Manual on Implementation of a 300 m (1000 ft) Vertical Separation Minimum between FL 290 and FL410 inclusive, ICAO, Montreal, Doc 9574, 1st edition 1992, 2nd edition 2000.
23. D.A. Anderson, RVSM safety assessment for the Australian FIRs, Airservices Australia, 21/9/99.
24. NAT SPG Mathematicians' Working Group, Risk Assessment and System Performance Monitoring for the Verification and Operation of a 300 m (1000 ft) Vertical Separation Minimum in the Minimum Navigation Performance Specifications Airspace of the North Atlantic Region, Supplement to NAT Doc 002, Draft version 2.0, 12th March 1996.
25. K. Slater, Estimates of NAT MNPS vertical collision risk for the RVSM Phase 1 operational trial, NAT SPG/34 MWG WP/9, June 1998.
26. EUROCONTROL Mathematicians Drafting Group, Mathematical supplement to the Guidance material on the implementation of a 300 m VSM in the European RVSM airspace, EUROCONTROL, Brussels, in preparation.
27. B. Flax, Estimating the rate of collisions between aircraft assigned to different flight levels on intersecting oceanic routes, RGCSP-WG/B-WP/3, St. Petersburg, May 1999.
28. B. Flax, Estimating the probability and duration of horizontal overlaps experienced by airplanes assigned to different flight levels on intersecting oceanic routes, RGCSP-WG/B-WP/2, St. Petersburg, May 1999.
29. M. Dacre, S. Owens and P. Smith, Trial risk assessment for RVSM in the London and Scottish FIRs, EUROCONTROL MDG/17-DP/4, July 2000.
30. R. Rigolizzo, Summary of statistical distributions modeled to aircraft altitude-keeping deviations and altimetry system errors and the resulting estimate of the probability of vertical overlap for NAT RVSM, NAT SPG/34-MWG IP/8, June 1998.
31. K. Slater, 1999 Estimates of NAT MNPS vertical collision risk due to large height deviations, NAT SPG/36 MWG WP/7(Revised), ICAO, Paris, May 2000.

APPENDIX A Estimating The Weighting Factor a For Distribution of Atypical Lateral Navigation Deviations

The weighting factor a within the Double Double Exponential (DDE) mixture probability distribution model for the lateral navigation deviations may be interpreted as the proportion of flying time during which the probability distribution of the lateral deviations is characterized by the scale factor a_2 (or, equivalently, the standard deviation s_2) rather than a_1. As that distribution represents atypical lateral navigation performance resulting from some sort of anomaly, a may be interpreted as the proportion of aircraft experiencing such anomalies or as the probability of an individual aircraft experiencing an anomaly resulting in its distribution of lateral deviations having the scale factor a_2.

On the assumption that ATC and/or the flight crew are able to detect lateral navigation anomalies and are reporting each occurrence thereof, the parameter a can be estimated as the proportion of flights or aircraft where an anomaly occurred. Because of the random nature of the occurrence of such anomalies, it is necessary to supplement the estimate (usually referred to as a point estimate) by a confidence interval, particularly an upper confidence limit. The confidence interval represents the uncertainty of the point estimate with regard to the true value of a.

The Aena Incident Reporting System database has been queried for any large lateral deviations. It was concluded that no such deviations were present in the database. It was realized, however, that there might exist a high likelihood of underreporting of such errors. This is supported by practical experience with monitoring lateral deviations in other airspaces. For example, a very well developed monitoring system is in operation in the North Atlantic MNPS Airspace and some large, atypical, lateral deviations are seen to occur from time to time.

Thus, it is not deemed realistic to simply put $a = 0$. To come up with some sort of conservative estimate of a, an upper confidence limit for a will be calculated and used as the estimate for a within the DDE model of the lateral deviations in the proposed RNP10 airspace in the SAT. Although this approach is considered useful and necessary, it should not be considered as a generally applicable procedure to deal with underreporting of large errors within the system. It would by far be better to ensure that such errors are properly reported.

For the subsequent analysis, the symbol p rather than a will be used for the pertinent probability to avoid confusion with the common use of the latter symbol in denoting confidence levels $1-a$.

A confidence interval for p can be determined by means of the binomial distribution for the number of aircraft X, say, experiencing a lateral navigation anomaly as described above during a certain monitoring period, i.e. in a given number of flights n, say. It holds that

$$\Pr ob\{X = k\} = \binom{n}{k} p^k (1-p)^{n-k}, \quad k = 0,1,\ldots,n \tag{A.1}$$

See e.g. Reference A.1 for a discussion on confidence intervals.

In principle, then, an integer number $A_{p,a}$ can be determined for each value of p and $a, a > 0$, such that

$$\Pr ob\{X \geq A_{p,a}\} = 1 - a \,, \tag{A.2}$$

i.e. a fraction $1-a$ of the values of the random variable X are larger than or equal to $A_{p,a}$. This means that in the same fraction of cases, the (random) interval $[0, X]$ covers the point $A_{p,a}$, i.e.

$$0 \leq A_{p,a} \leq X \tag{A.3}$$

as illustrated in Figure A.1.

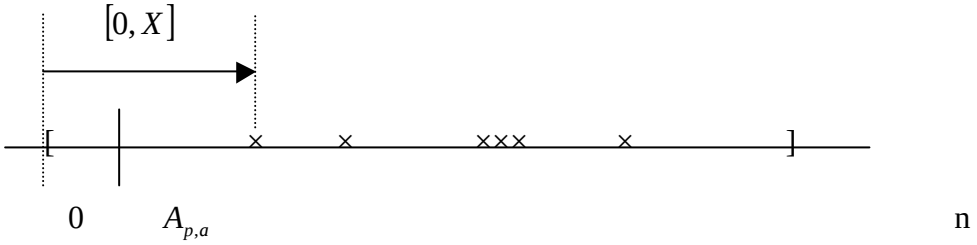

INCRUSTARINCRUSTAR

Figure A–1. The value $A_{p,a}$ Being Covered by the (Random) Interval $[0, X]$

The confidence limit for p is obtained by manipulating equation (A.2) such that it becomes

$$\Pr ob\{Y(X)_a \geq p\} = 1 - a \tag{A.4}$$

where $Y(X)_a$ is some appropriate function of the random variable X. Similarly to Figure A.1, the interval $[Y_{low}, Y(X)_a]$ where Y_{low} is the lower bound of the domain of the random variable $Y(X)_a$ will cover p in a fraction $1-a$ of cases. The actual value of the confidence limit is obtained by substituting the observed value k of the random variable X into $Y(X)_a$.

Now, if $A_{p,a}$ is written as

$$A_{p,a} = np - a_{p,a} \tag{A.5}$$

where $np = E\{X\}$, the expected value of X, and $a_{p,a} > 0$, it follows that

$$np - a_{p,a} \le X \tag{A.6}$$

or

$$p \le \frac{X + a_{p,a}}{n} \tag{A.7}$$

and this will hold in a fraction $1-a$ of the cases. The right-hand side of the inequality (A.7) may be associated with $Y(X)_a$ and thus specifies a $(1-a)\times 100\%$ upper confidence limit for the probability p.

It remains to calculate $a_{p,a}$. The mathematical details thereof will be left out. Following Reference A.2, the following approximate $(1-a)\times 100\%$ upper confidence limit p_U for the probability p is obtained where k denotes the observed value of X:

$$p_U = \frac{2k + Z_{1-a}^2 + \sqrt{\left(2k + Z_{1-a}^2\right)^2 - 4\left(k^2/n\right)\left(n + Z_{1-a}^2\right)}}{2\left(n + Z_{1-a}^2\right)} \tag{A.8}$$

Z_{1-a} is the $(1-a)$-quantile of a standard normal random variable. It holds for $a = 0.05$ that $Z_{.95} = 1.645$. The approximation concerns the fact that the binomial distribution has been approximated by a Gaussian distribution with the same mean and standard deviation.

A practical interpretation of the above and of equation (A.2) in particular is that the upper confidence limit p_U is taken as that value of the parameter p for which the observed value k of X is just equal to the a-quantile of the random variable X, see Figure A.2.

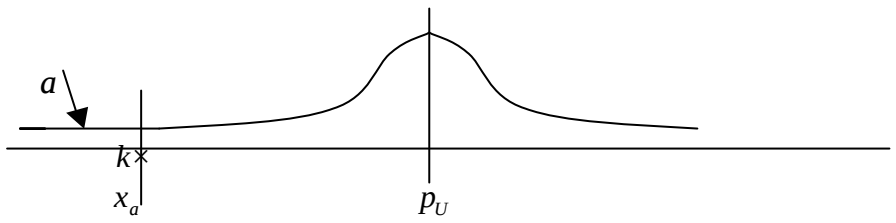

INCRUSTARINCRUSTAR

Figure A–2. Determination of the Upper Confidence Limit p_U From $k = x_a$

In the present case, there are two complicating factors. The first one is the general problem with the calculation of confidence limits for discrete distributions where it may not be possible to satisfy equation (A.2) precisely for the specified value of a. When this happens, the nearest lower value of a is taken to achieve at least the initially specified confidence level $1-a$.

The second complicating factor is specific to the current situation, i.e. that the observed value of X is zero (0) rather than any positive number. As zero is the left-hand bound of the domain of the random variable X it holds that the probability of X being greater than or equal to zero is precisely 1, regardless of the value of the parameter p.

For the benefit of deriving an upper limit for p it will, therefore, be assumed that a single large lateral deviation was observed, i.e. $X = 1$. Assuming a larger value of X would be more conservative, but is not deemed necessary because of the upper confidence bound going to be used for the probability p of an aircraft experiencing an anomaly resulting in its distribution of lateral deviations having the scale factor a_2.

The resulting upper confidence limit for p turns out to be $p_U = 2.014 \times 10^{-4}$, see Table A.1. This is based on an annual number of flights of $n = 22255$ obtained from 25791 waypoint reports for EDUMO, VORAS and GADUN for the period of time from 30th July 1999 to 25th September 2000 inclusive (423 days). Note that if actually one large error had been observed during this number of flights, the point estimate of p would have been equal to $1/22255 = 4.4934 \times 10^{-5}$. Table A.1 also shows what the probabilities are of observing zero large errors or just a single one. For comparison, the same quantities are included based on $X = 0$. It is seen that the initially specified confidence level of $1-a$ for $a = 0.05$ is not achieved for $k = 0$ and is "over-achieved" for $k = 1$.

Table A-1. Approximate $(1-a)\times 100\%$ Upper Confidence Limit p_U and Some Associated Probabilities for $a = 0.05$ Based on Equation (A.8).

	Observed number of large errors $X = k$	
	$k = 0$	$k = 1$
p_U	6.0788×10^{-5}	2.014×10^{-4}
$\Pr ob\{X = 0 \mid p = p_U\}$	0.2585	0.01130
$\Pr ob\{X = 1 \mid p = p_U\}$	0.3497	0.05068
$\Pr ob\{X \geq 1 \mid p = p_U\}$	0.7415	0.98870
$E\{X \mid p = P_U\}$	1.3528	4.4824

INCRUSTARINCRUSTARINCRUSTAR
In fact, for the specific assumed "observed" value $k = 1$ the use of a Gaussian approximation to the binomial distribution is not needed. Based on the practical interpretation illustrated in Figure A.2, the upper confidence limit p_U can be determined directly from the requirement

$$\Pr ob\{X \geq 1 \mid p = p_U\} = 1 - \Pr ob\{X = 0 \mid p = p_U\} = 1 - a \qquad \text{(A.10)}$$

i.e.

$$(1-p_U)^n = a \tag{A.11}$$

or

$$p_U = 1 - a^{1/n}. \tag{A.12}$$

This gives $p_U = 1.346\times10^{-4}$ for $a = 0.05$ and is exactly a 95% upper confidence limit for $k = 1$. Therefore, this value will be used in the Double Double Exponential probability mixture distribution for the lateral deviations.

References

A.1 D.R. Cox and D.V. Hinkley, Theoreti

A.2 I.N. Gibra, Probabil

APPENDIX B Estimating Lateral Occupancy

B.1 Methods

To estimate a system's lateral occupancy, the amount of lateral proximity time needs to be determined for each pair of aircraft in the system. In principle, this requires that for each aircraft its trajectory through the system be completely known as a function of time. In a procedural environment, the aircraft trajectories are only known at discrete time epochs, viz. at the waypoint reporting times. Linear interpolation might be used for the trajectories at intermediate time epochs.

Determining occupancy from the full time trajectories is a somewhat computationally intensive process. A computationally less demanding, approximate method described in Appendix C of Reference 10 is the "*steady state flow model*" which only uses the hourly flow rates in the system. In practice, however, the assumption of steady state traffic flows is often not met. Another method described in Reference 10 is called "*direct estimation from time at waypoint passing*". This method was developed during the 1960s for estimating occupancy in the North Atlantic Organized Track System (OTS) and is stated to have found application in other oceanic environments. It may be summarized as follows.

For a given day in the traffic sample, the flight progress information for all flights is examined and the times reported at each required point in the system are grouped by altitude. Lateral occupancy is then estimated by

$$E_y = \frac{2n_y}{n} \tag{B.1}$$

where n_y is the total number of laterally proximate pairs of aircraft and n is the total number of aircraft. The adjective "total" here refers to all the flight levels in use at the reporting points and all the pairs of parallel tracks (when there is more than a single pair of parallel tracks). It is important to note that "The points utilized should be approximately on a plane at right angles to the track system". The relation between the estimator equation (3.3) and the definition equation (3.2) may be established via the snapshot principle. In this context it means that an aircraft pair is, due to random effects, either laterally proximate during the whole flight through the system or not at all (cf. Section 2.2).

Given the cited condition on the choice of the reporting points, the determination of whether or not an aircraft pair is proximate can be carried out directly from the times at which waypoint position reports were given, i.e.

$$\left| t_i^k - t_j^{k'} \right| \le \frac{\tilde{S}_x}{\overline{|V|}} \tag{B.2}$$

where k and k' denote corresponding reporting points at two adjacent tracks and i and j are counters for the aircraft passing these points respectively, see Figure B.1. Note the square angles

between the tracks and the planes. When there is more than one set of corresponding reporting points, the proximity counts at the different points are averaged.

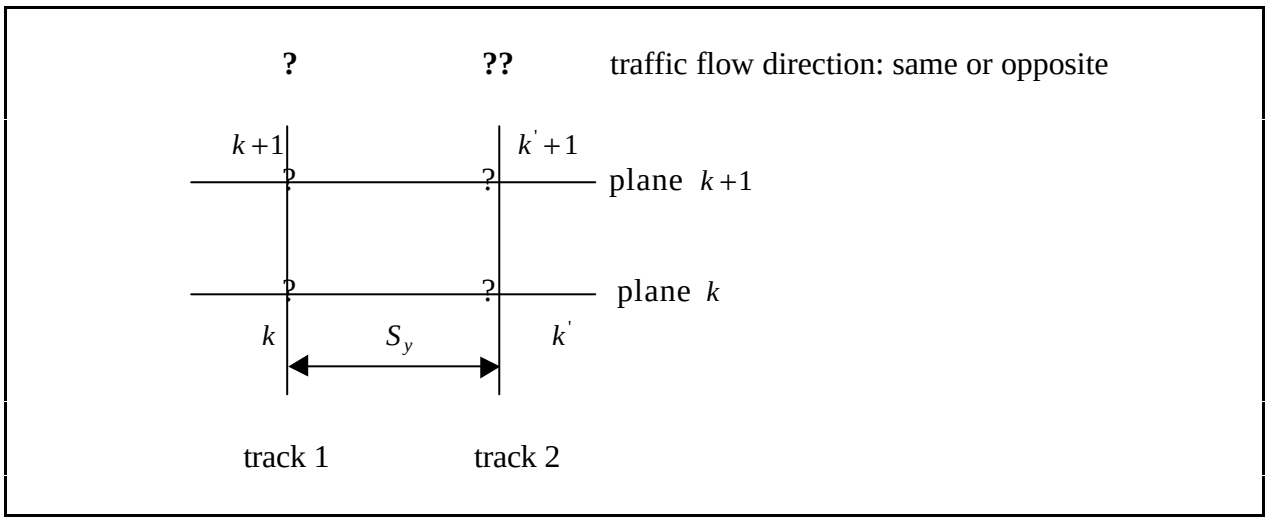

Figure B–1. Sketch of Planes With Reporting Points (Top View) Used For Estimation Of Lateral Occupancy For Two Parallel Tracks

In order to be able to use the *direct estimation from time at waypoint passing* method, the geometry of the reporting points on the different tracks needs to be examined with regard to the cited condition for applicability – that a line connecting the waypoints be perpendicular to the tracks. Figure B.2 shows a sketch of the SAT track system and the reporting points used for the estimation of lateral occupancy.

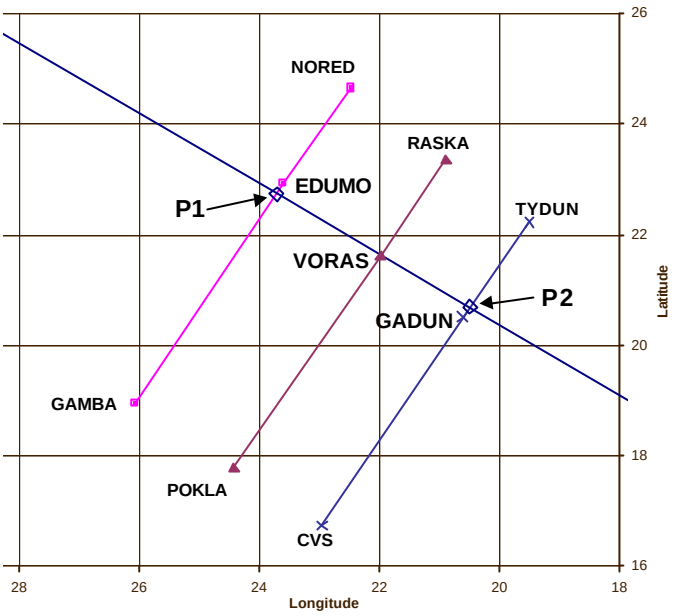

Figure B–2. Sketch Of Tracks With Reporting Points (Top View) Used For Estimation Of Perpendicular Correction Factors

The primary data set uses the waypoints EDUMO, VORAS, and GADUN; and, as indicated in the figure above, small corrections to the "locations" of EDUMO and GADUN are required to define a plane perpendicular to the tracks.

Table B-1. Waypoints Corrected to Define a Plane Perpendicular to the Tracks

	Longitude	Latitude	Range [NM]
EDUMO	23.60	22.92	
P1	23.72	22.73	12.83
GADUN	20.61	20.51	
P2	20.50	20.69	12.65

B.2 Application

Traffic flow data from the current system comprising three parallel tracks only have been used, see Figure B.3. For simplicity, the symbols a, b and c will be used to identify the existing tracks. The symbols $n_y^{ab}(same)$ and $n_y^{bc}(same)$ are used to denote the number of proximate events involving aircraft pairs on the routes a and b, and b and c respectively. Similarly n^a, n^b and n^c denote the numbers of flights on the different routes.

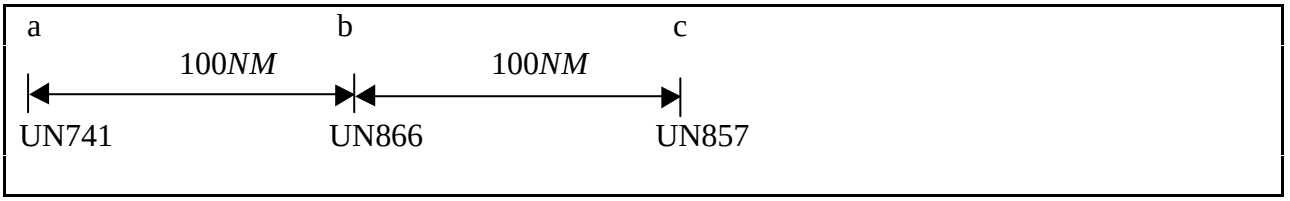

Figure B–3. Existing Track System

The same direction lateral occupancy for the existing track system is given by

$$E_y(same) = \frac{n_y^{ab}(same) + n_y^{bc}(same)}{n^a + n^b + n^c} \tag{B.3}$$

and the different parts making it up will be used to project lateral occupancy for the proposed new track system.

The proposed new system comprises four parallel tracks as shown in Figure B.4. The separation minimum is $S_y = 50NM$. Given the flight level orientation scheme in use there is only same direction traffic at the same flight level of adjacent tracks. The form of the lateral collision risk model (CRM) for this situation is given by equation (B.4),

$$N_{ay} = \left\{P_y(S_y)E_y(same) + P_y(2S_y)E_y^*(same)\right\}P_z(0)\frac{l_x}{\tilde{S}_x}\left\{\frac{\overline{|\Delta V|}}{2l_x} + \frac{\overline{|\dot{y}|}}{2l_y} + \frac{\overline{|\dot{z}|}}{2l_z}\right\}. \tag{B.4}$$

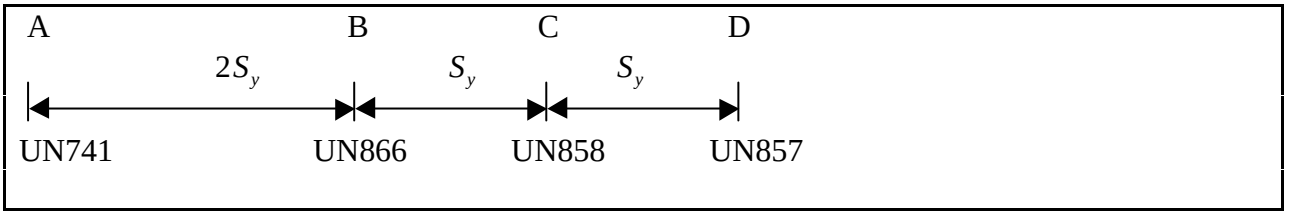

Figure B–4. Proposed Track System

The CRM has two same direction occupancy parameters, namely $E_y(same)$ for the three right most tracks B, C and D separated by S_y and $E_y^*(same)$ for the two left most tracks A and B separated by $2 \times S_y$. Similarly, the model has two probabilities of lateral overlap, $P_y(S_y)$ and $P_y(2S_y)$.

Using similar notation as for the existing system, it follows that

$$E_y^*(same) = E_y^{AB}(same) = \frac{n_y^{AB}}{n^A + n^B + n^C + n^D} \quad \text{(B.5)}$$

$$E_y(same) = E_y^{BCD}(same) = \frac{n_y^{BC} + n_y^{CD}}{n^A + n^B + n^C + n^D} \quad \text{(B.6)}$$

It is assumed that the traffic on routes a and b remains as it, but that the traffic on the existing route c is redistributed over the new routes C and D. Suppose a proportion f goes to route C and a proportion $1-f$ to route D. As the effect of traffic growth will be considered later, it follows that the amount of traffic does not change, i.e.

$$n^A + n^B + n^C + n^D = n^a + n^b + n^c \quad \text{(B.7)}$$

and also

$$n^A = n^a \quad \text{(B.8)}$$

$$n^B = n^b \quad \text{(B.9)}$$

$$n^C = f \times n^c \quad \text{(B.10)}$$

$$n^D = (1-f) \times n^c \quad \text{(B.11)}$$

It also follows that

$$E_y^*(same) = E_y^{AB}(same) = \frac{n_y^{ab}}{n^a + n^b + n^c} \quad \text{(B.12)}$$

The projection of $E_y(same) = E_y^{BCD}(same)$ may be performed by means of the steady state flow model method. This method estimates occupancy for a same direction pair of parallel routes by the formula

$$E_y^{12}(same) = \frac{4\tilde{S}_x}{V} \frac{m_1 \times m_2}{m_1 + m_2} \quad \text{(B.13)}$$

where m_1 and m_2 denote the hourly flow rates on the two routes. Application of the scale factors f and $1-f$ to the flow rates on routes C and D gives for $E_y^{BCD}(same)$

$$E_y^{BCD}(same) = \frac{4\tilde{S}_x}{V} \frac{m^b \times f \times m^c + f \times m^c \times (1-f) \times m^c}{m^A + m^B + m^C + m^D} \quad \text{(B.14)}$$

or

$$E_y^{BCD}(same) = f \times \frac{4\tilde{S}_x}{V} \frac{m^b \times m^c}{m^A + m^B + m^C + m^D} + f \times (1-f) \times \frac{4\tilde{S}_x}{V} \frac{m^c \times m^c}{m^A + m^B + m^C + m^D} \tag{B.15}$$

The first term in the right-hand side of equation (B.15) is simply equal to f times the occupancy for the existing routes b and c. Hence,

$$E_y^{BCD}(same) = f \times \frac{2 \times n_y^{bc}(same)}{n^a + n^b + n^c} + f \times (1-f) \times \frac{4\tilde{S}_x}{V} \frac{m^c \times m^c}{m^A + m^B + m^C + m^D} \tag{B.16}$$

The second term may be associated with the occupancy of a pair of parallel routes, both in stationary state, and both having the same hourly traffic flow m^c. Under the steady state assumption, this is equal to m^c/m^b times the occupancy of a pair of parallel routes with hourly traffic flow rates m^b and m^c. Thus, equation (B.16) becomes

$$E_y^{BCD}(same) = f \times \frac{2 \times n_y^{bc}(same)}{n^a + n^b + n^c} + f \times (1-f) \times \frac{m^c}{m^b} \times \frac{2 \times n_y^{bc}(same)}{n^a + n^b + n^c} \tag{B.17}$$

or

$$E_y^{BCD}(same) = \left\{ f \left(1 + (1-f) \times \frac{m^c}{m^b} \right) \right\} \times \frac{2 \times n_y^{bc}(same)}{n^a + n^b + n^c} \tag{B.18}$$

The ratio m^c/m^b of the hourly traffic flows may finally be replaced by the ratio n^c/n^b of the numbers of flights on the two tracks to give the following expression for the occupancy component $E_y^{BCD}(same)$:

$$E_y^{BCD}(same) = \left\{ f \left(1 + (1-f) \times \frac{n^c}{n^b} \right) \right\} \times \frac{2 \times n_y^{bc}(same)}{n^a + n^b + n^c} \tag{B.19}$$

APPENDIX C Estimating Crossing Track Vertical Occupancy

C1Introduction

Same direction lateral occupancy, $E_y(same)$, is discussed in Appendices A - C to Part II, Section 2, Chapter 4, of Reference C.1. The definition proper of $E_y(same)$ is

$$E_y(same) = \frac{2T_y}{H} \tag{C.1}$$

where

T_y: The total proximity time generated in the system, i.e. the total time spent by aircraft pairs on adjacent flight paths at the same flight level and within a longitudinal distance $\tilde{S}_x$ of each other;

H: The total number of flying hours generated in the system during the period considered.

Using the "direct estimation from time at waypoint passing" method, $E_y(same)$ is estimated by

$$E_y(same) = \frac{2n_y}{n} \tag{C.2}$$

where

n_y: The total number of laterally proximate aircraft pairs;

n: The total number of aircraft.

The use of equation (C.2) for the estimation of occupancy for aircraft at the same flight level of adjacent tracks is documented in e.g. Ref. C2. It is used for both same direction and opposite direction traffic.

The same relationships can be used for the estimation of vertical occupancy for aircraft on adjacent flight levels of the same track, i.e.

$$E_z(same) = \frac{2T_z}{H} \tag{C.3}$$

$$E_z(same) = \frac{2n_z}{n} \tag{C.4}$$

Vertical occupancy for aircraft on adjacent flight levels of crossing tracks may also be defined in the same way,

$$E_z(q) = \frac{2T_z(q)}{H} \tag{C.5}$$

However, the estimation of vertical occupancy for aircraft on adjacent flight levels of crossing tracks is less well-documented in literature. In analogy with equations (C.2) and (C.4), one might use the estimator

$$E_z(q) = \frac{2n_z(q)}{n} \tag{C.6}$$

where

$n_z(q)$: The total number of vertically proximate aircraft pairs on the tracks crossing under an angle of q.

The number of proximate pairs can be estimated at the crossing point of the routes. The estimator (C.6), however, does not seem to take into account that the exposure to the risk exists only around the crossing point, not during the full flight. It will be shown below on the basis of a comparison with the steady state flow model, that a correction factor should be applied for crossing traffic.

C.2 Analysis

Assume that the system is in a steady state.

The steady state flow model for aircraft at two adjacent flight levels of the same track gives the following expression for same direction vertical occupancy (Ref. C.1):

$$E_z(same) = \frac{4\tilde{S}_x}{V}\frac{m_1 m_2}{m_1 + m_2} \tag{C.7}$$

where m_1 and m_2 are the numbers of aircraft entering the respective flight levels per hour and V is the average aircraft speed. It follows from the derivation of this equation in Reference C.1 that exactly the same equation is valid for opposite direction traffic, i.e.

$$E_z(opp) = \frac{4\tilde{S}_x}{V}\frac{m_1 m_2}{m_1 + m_2} \tag{C.8}$$

The difference in the risks associated with same direction and opposite direction traffic appears when occupancy is converted into passing frequency by means of the relative speed between aircraft at adjacent flight levels. Given the traffic flow rates m_1 and m_2, the exposure to the risk as measured by the proportion of flight time is the same for same direction and opposite direction traffic.

Consider two adjacent flight levels of the crossing tracks shown in Figure C1. All quantities referring to track 1 will be labeled with a subscript 1 and all quantities for track 2 with a subscript 2. The flow densities are m_1 and m_2 aircraft per (clock) hour. The time separation between two aircraft at the same flight levels is equal to $\frac{1}{m_1}$ and $\frac{1}{m_2}$ respectively and the distance separation $\frac{V_1}{m_1}$ and $\frac{V_2}{m_2}$. It follows that

number of aircraft on track 1 with length L_1: $L_1 \frac{m_1}{V_1}$ (C.9)

number of aircraft on track 2 with length L_2: $L_2 \frac{m_2}{V_2}$ (C.10)

At any point in time, the total number of aircraft in the system is equal to

$$L_1 \frac{m_1}{V_1} + L_2 \frac{m_2}{V_2} \quad \text{(C.11)}$$

During T clock hours of observation time, the amount of flying time generated by the system is thus given by

$$T \times \left(L_1 \frac{m_1}{V_1} + L_2 \frac{m_2}{V_2} \right) \quad \text{(C.12)}$$

In the steady state model, vertical proximity time is calculated from the instantaneous aircraft density at each point of level 1 (track1) and the duration of the flight of an aircraft on level 2 (track2), multiplied by the total number of aircraft passing through the system during the observation period on level 2. The aircraft density is simply m/V.

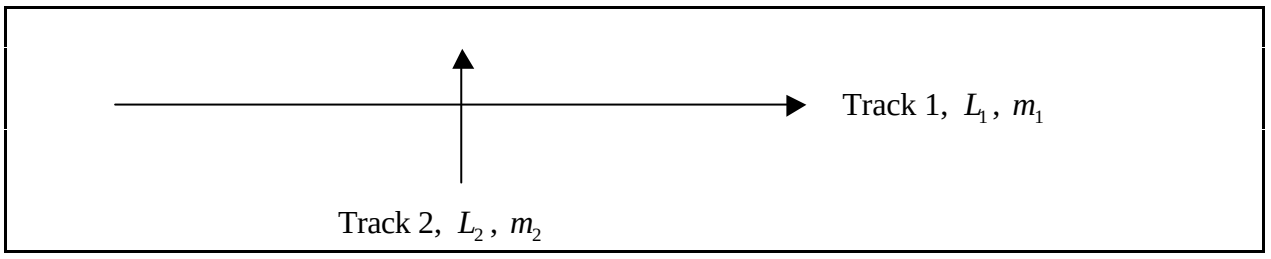

Figure C-1. Two Tracks Crossing Under a 90º Angle

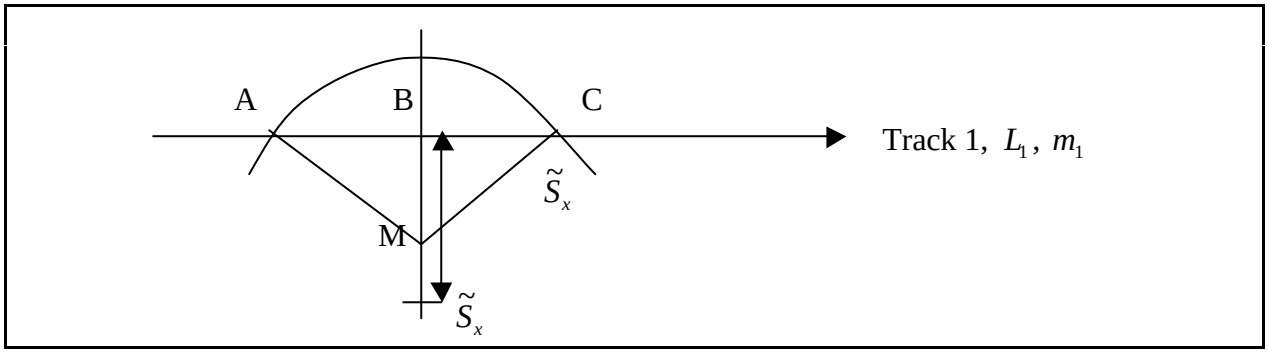

Figure C- 2. Proximate Aircraft On Track 1 For a Crossing Aircraft On Track 2

Vertical proximity begins at time "zero" when an aircraft on track 2 is at a distance $\tilde{S}_x$ from the crossing. Consider now the situation at some later epoch t, $0 < t \le t_c$, where t_c denotes the time at which the aircraft from track 2 reaches the crossing point, i.e.

$$t_c = \frac{\tilde{S}_x}{V_2} \tag{C.13}$$

See Figure C.2. In order to determine the amount of vertical proximity generated by an aircraft on track 2 when it crosses track 1, it is necessary to determine the number of aircraft of track 1 within the circle with radius $\tilde{S}_x$. This is equal to the aircraft density on track 1, i.e.

$$\frac{m_1}{V_1} \tag{C.14}$$

multiplied by the length of the segment AC. It follows that

$$BC(t)^2 = \tilde{S}_x^2 - MB(t)^2 \tag{C.15}$$

where $MB(t)$ is given by

$$MB(t) = \tilde{S}_x - V_2 \times t \tag{C.16}$$

Thus,

$$BC(t)^2 = \tilde{S}_x^2 - \left(\tilde{S}_x^2 - 2\tilde{S}_x V_2 t + V_2^2 t^2\right) \tag{C.17}$$

or

$$BC(t)^2 = 2\tilde{S}_x V_2 t - V_2^2 t^2 \tag{C.18}$$

and

$$AC(t) = 2\sqrt{2\tilde{S}_x V_2 t - V_2^2 t^2} \tag{C.19}$$

A similar expression holds for $t_c \le t \le 2 \times t_c$. Hence, the amount of proximity time generated by the aircraft on track 2 is given by

$$2 \times \frac{m_1}{V_1} \times \int_0^{t_c} AC(t)dt \tag{C.20}$$

Note that the second factor in the above expression represents the aircraft density on track 1.

The total number of aircraft on track 2 crossing track 1 during the observation clock time period T is $m_2 \times T$. Thus, the total amount of proximity time generated is

$$m_2 \times T \times 2 \times \frac{m_1}{V_1} \times \int_0^{t_c} AC(t)dt \tag{C.21}$$

or

$$T \times 2 \times \frac{m_1 m_2}{V_1} \times \int_0^{t_c} 2\sqrt{2\tilde{S}_x V_2 t - V_2^2 t^2}\, dt \tag{C.22}$$

or

$$T \times 4 \times \frac{m_1 m_2}{V_1 V_2} \times \int_0^{S_x} \sqrt{2\tilde{S}_x u - u^2}\, du \tag{C.23}$$

Using the crossing track vertical occupancy definition equation (C.5), $E_z(q)$ becomes (for $q = 90^\circ$):

$$E_z(q) = 2 \times \frac{T \times 4 \times \frac{m_1 m_2}{V_1 V_2} \times \int_0^{S_x} \sqrt{2\tilde{S}_x u - u^2}\, du}{T \times \frac{L_1 m_1 V_2 + L_2 m_2 V_1}{V_1 V_2}} \tag{C.24}$$

The integral in the numerator of equation (C.24) can be evaluated with the aid of equations 2.262 and 2.261 from Reference C.3. The result is

$$\int_0^{S_x} \sqrt{2\tilde{S}_x u - u^2}\, du = \frac{p}{4} \tilde{S}_x^2 \tag{C.25}$$

Substitution of this into equation (C.24) gives

$$E_z(q) = \frac{8p \times \tilde{S}_x^2}{4} \frac{m_1 m_2}{L_1 m_1 V_2 + L_2 m_2 V_1} \tag{C.26}$$

This equation may also be written in the form

$$E_z(q) = \left(\frac{2p \times \tilde{S}_x}{4} \frac{V(m_1 + m_2)}{L_1 m_1 V_2 + L_2 m_2 V_1} \right) \frac{4\tilde{S}_x}{V} \frac{m_1 m_2}{m_1 + m_2} \tag{C.27}$$

where V denotes the average of the aircraft speeds V_1 and V_2.

In equation (C.27), the last part gives the estimate of the vertical occupancy $E_z(same)$ for aircraft at the same flight level on the basis of the stationary flow model. On the other hand, the pertinent estimate on the basis of the "direct estimation from time at waypoint passing" method is given by equation (C.4). For crossing traffic equation (C.27) suggests to estimate its latter part by the right-hand side of equation (C.6) and to apply a correction factor given by the form in brackets. Thus, the proposed estimator for crossing track occupancy becomes:

$$E_z(q) = \left(\frac{2p \times \tilde{S}_x}{4} \frac{V(m_1 + m_2)}{L_1 m_1 V_2 + L_2 m_2 V_1} \right) \frac{2n_z(q)}{n} \tag{C.28}$$

The correction factor holds for a stationary traffic situation in the system. But the analysis above indicates that a correction factor should also be applied to the simple form of equation (C.6) for the case of non-stationary situations. Therefore, as an initial approximation, the same correction factor will be used for the general case.

To calculate a suitable value for the correction factor, estimates for its parameters have to be supplied. The speeds V_1 and V_2 may be taken as the average speed V. When the subscript 1 is assumed to refer to the main traffic Corridor, Table 2.1 of the main text shows that the track length L_1 varies between 1852 and 2253 NM. The length L_2 of the tracks crossing the Corridor may conservatively be taken as 200 NM. Assuming a traffic flow of about 60 aircraft in the Corridor per day and about 5 crossing aircraft per day gives $m_1 = 2.5$ and $m_2 = 0.21$. The correction factor then becomes approximately 0.073. Some conservatism may be built in by assuming that we have only accounted for crossing traffic in the southern half of the Corridor. The correction factor may then be rounded up to 0.15.

C.3 References

C.1 Air traffic services planning manual, first edit

C.2 L.Davies and A. Sharpe, Review

C.3 I.S. Gradshteyn and I.M. Ryzhik, Table of

INCRUSTARINCRUSTARINCRUSTARINCRUSTARINCRUSTARINCRUSTARINCRUSTARINCRUSTARINCRUSTARINCRUSTARINCRUSTARINCRUSTAR

INCRUSTAR				

INCRUSTAR**INCRUSTAR**

INCRUSTAR							

INCRUSTARINCRUSTAR